Study of Ionic Contamination in Electronic Product Assembly

Ana Margarida da Silva Ferreira Grilo

UMinho | 2021

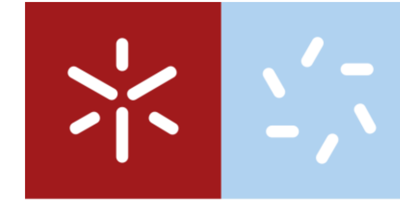

Universidade do Minho
Escola de Ciências

Ana Margarida da Silva Ferreira Grilo

Study of Ionic Contamination in Electronic Product Assembly

May 2021

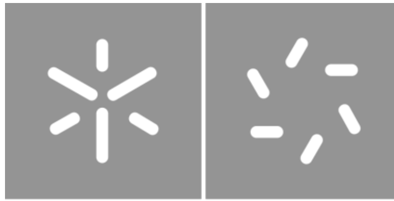

Universidade do Minho
Escola de Ciências

Ana Margarida da Silva Ferreira Grilo

Study of Ionic Contamination in Electronic Product Assembly

Master Thesis

Master's in Chemical Analysis and Characterization Techniques

Work done under the guidance of

Dr. Hugo Figueiredo

Prof. Pier Parpot

May 2021

DIREITOS DE AUTOR E CONDIÇÕES DE UTILIZAÇÃO DO TRABALHO POR TERCEIROS

Este é um trabalho académico que pode ser utilizado por terceiros desde que respeitadas as regras e boas práticas internacionalmente aceites, no que concerne aos direitos de autor e direitos conexos.

Assim, o presente trabalho pode ser utilizado nos termos previstos na licença abaixo indicada.

Caso o utilizador necessite de permissão para poder fazer um uso do trabalho em condições não previstas no licenciamento indicado, deverá contactar o autor, através do RepositóriUM da Universidade do Minho.

DE ACORDO COM A LEGISLAÇÃO EM VIGOR, NÃO É PERMITIDA A REPRODUÇÃO DE QUALQUER PARTE DESTA DISSERTAÇÃO POR UM PERÍODO DE 10 ANOS.

AGRADECIMENTOS

Esta tese de mestrado não poderia ter sido realizada sem a ajuda e encorajamento de algumas pessoas aos quais queria deixar o meu agradecimento.

Ao meu orientador de estágio da Bosch, Dr. Hugo Figueiredo, devo agradecer pela sua orientação, pela disponibilidade, pelas opiniões e sugestões, pela partilha de conhecimento e pelo acompanhamento ao longo de todo o ano.

Ao professor Pier Parpot pela disponibilidade, pelo interesse no meu trabalho e pelo auxílio que disponibilizou durante a realização deste projeto.

Aos colaboradores da Bosch Car Multimedia Portugal S.A. que, de alguma forma, contribuíram para este projeto. Em particular, aos meus colegas de trabalho do departamento CM/MFT3 pelo apoio e diversão durante todo o estágio.

A todos os docentes desde o ensino básico até ao superior que, pelos seus ensinamentos e incentivos, me encaminharam e guiaram para aquilo que hoje sou.

Aos meus amigos e colegas que me acompanharam durante todo o meu percurso académico também deixo aqui o meu agradecimento pela amizade e companheirismo.

Por último, mas acima de tudo, queria agradecer à minha família, em especial aos meus pais e ao meu irmão. Obrigada pelo incentivo, pelo apoio incondicional e pela paciência que foram especialmente bem-vindos em tempos de pandemia onde por vezes me faltava motivação para continuar. A eles dedico a minha tese!

STATEMENT OF INTEGRITY

I hereby declare having conducted this academic work with integrity. I confirm that I have not used plagiarism or any form of undue use of information or falsification of results along the process leading to its elaboration.

I further declare that I have fully acknowledged the Code of Ethical Conduct of the University of Minho.

ABSTRACT

The ever-growing demand for better PCB (printed circuit board) performance as well as component miniaturization and increasing density, are all challenges the automotive industry is facing nowadays. However, these alterations in the PCB layout alongside changes in production materials and techniques may jeopardize product reliability. One of the factors that has the ability to threaten PCB functioning is the introduction of ionic contaminants that increase the probability of electrochemical reactions and premature circuit failures. Methods have been created along the years in order to evaluate the presence of these contaminants on printed boards; one of them is the ROSE (Resistivity of Solvent Extract) test.

This thesis aimed to study the ionic contamination in electronic product assembly using the CM22 contaminometer, a ROSE test machine. Essentially, this project was divided in two studies. The first one was the study of ROSE machine response and establishment of parameters to test its performance at Bosch Car Multimedia Portugal S.A. The results revealed that although the relation between the machine response and the dissolved contamination was linear, there was some disparity in values of PCBs from the same product family. The temperature and regeneration time of the extraction bath were identified as possible influencers of this discrepancy. Further tests showed temperature is not a significant factor for this behaviour and, at lower contamination levels, the regeneration time has little impact.

The second study intended to evaluate the ionic contamination levels of printed circuit boards in 5 different stages of their production run. This research revealed that the ROSE levels of the PCBs obtained from the supplier decrease during the first steps of the process. Solder paste application, component insertion and reflow steps do not introduce much ionic residues on the board surface. Yet, the most important conclusion to this study is that the flux used for rework and selective soldering greatly increases surface contamination presence.

In conclusion, the CM22 ROSE contaminometer is suitable to monitor processes in assembly plants. It can detect contamination trends at a process line and can be used as process control tool especially in a no-clean soldering process like the one used in Bosch. For this reason, the evaluation of ionic content should be carried out in different stages of PCBA production since it can be very deceptive to do them only after reflow process as it normally done.

KEYWORDS: CM22 contaminometer, Ionic contamination, PCB assembly, ROSE test.

RESUMO

A crescente demanda por melhor desempenho de PCBs (placas de circuito impresso), bem como a miniaturização de componentes e o aumento da sua densidade, são desafios que a indústria automóvel enfrenta atualmente. No entanto, as alterações no seu design juntamente com as mudanças nos materiais e técnicas de produção podem comprometer a fiabilidade destas placas. Um dos fatores que tem a capacidade de ameaçar o funcionamento de um PCB é a introdução de contaminantes iónicos capazes de criar falhas elétricas no circuito. Vários métodos foram criados para avaliar a presença destes contaminantes em placas impressas; um deles é o teste ROSE (Resistividade do Extrato Solvente).

Esta tese teve como objetivo o estudo da contaminação iónica na montagem de produtos eletrónicos utilizando o contaminometer CM22, um dispositivo de teste ROSE. Para isto, primeiro estudou-se a resposta da máquina ROSE e estabeleceu-se parâmetros para testar o seu desempenho na Bosch Car Multimedia Portugal S.A. Os resultados revelaram que embora a relação entre a resposta do aparelho e a contaminação dissolvida seja linear, existiu alguma disparidade nos valores de placas da mesma família. A temperatura e o tempo de regeneração do banho foram identificados como possíveis influenciadores desta discrepância. Testes adicionais mostraram que a temperatura não influencia este comportamento e, em níveis de contaminação mais baixos, o tempo de regeneração tem pouco impacto.

O segundo estudo pretendia avaliar os níveis de contaminação iónica de placas de circuito impresso em 5 fases diferentes da sua montagem. Este estudo permitiu verificar que o PCB obtido do fornecedor possui um nível de ROSE que diminui ao longo dos primeiros passos do processo. As etapas de aplicação da pasta de solda, inserção dos componentes e refluxo não introduzem muitos resíduos à superfície da placa. No entanto, a conclusão mais importante deste estudo é que o fluxo usado para retrabalho e soldadura seletiva aumentam muito a contaminação na superfície das placas.

Em conclusão, o contaminometer CM22 é adequado para monitorizar os processos de fabrico. Ele pode detetar tendências de contaminação na linha de produção e pode ser usado como ferramenta de controlo de processo, especialmente num processo sem limpeza como o da Bosch. Por esse motivo, a avaliação do conteúdo iónico deve ser realizada em diferentes etapas da produção de PCBAs, dado que pode ser enganoso fazê-lo somente após o refluxo, como normalmente é.

PALAVRAS-CHAVE: Contaminação iónica, Contaminometer CM22, Montagem de PCBs, Teste ROSE.

CONTENTS

List of Figures x

List of Tables xiv

List of Abbreviations, Acronyms and Symbols xvi

CHAPTER 1 Introduction 1

1.1 Institution of Placement 1

1.1.1 Bosch Group 1

1.1.2 Bosch Group in Portugal 2

1.1.3 CM/MFT3 Department 3

1.2 Proposed Master Thesis 4

1.3 Dissertation Structure 5

CHAPTER 2 Literature Review 6

2.1 Printed Circuit Boards 6

2.1.1 Structure and Materials 7

2.1.2 Classification of PCBs 8

2.1.3 PCB Surface Finishes 10

2.2 PCB Assembly 15

2.2.1 Electronic Components 15

2.2.2 Component Mounting Technologies 16

2.2.3 Soldering Processes 17

2.2.4 BCM Assembly Line 20

2.3 Solders 25

2.3.1 Tin-Lead Alloys 26

2.3.2 Lead-Free Alloys 27

2.3.3 Solders and Oxidation 28

2.4 Soldering Flux ... 29
2.4.1 Flux Composition ... 30
2.5 Contamination on PCB Assembly ... 31
2.5.1 Types and Sources of Contamination ... 32
2.5.2 Electrochemical Migration ... 33
2.5.3 Cleanliness and Process Control Methods ... 35
CHAPTER 3 Experimental ... 38
3.1 Thesis Approach ... 38
3.2 Materials ... 40
3.2.1 PCB ... 40
3.2.2 Solder Paste ... 41
3.2.3 Solder Wires ... 41
3.2.4 Soldering Flux ... 42
3.3 Test Vehicles Assembly Processes ... 42
3.3.1 SMT Insertion ... 43
3.3.2 Rework ... 43
3.3.3 THT Insertion ... 44
3.4 ROSE Test Procedure ... 45
3.5 ROSE Studies Methodology ... 46
3.5.1 Study of Base-ROSE Levels for CM Products ... 46
3.5.2 ROSE Method Performance Tests ... 47
3.5.3 Design of Experiment (DOE) ... 48
3.5.4 Regeneration Time Tests ... 48
3.5.5 Studies of Contamination in the PCBA production process ... 49
CHAPTER 4 Results and Discussion ... 50
4.1 Study of Contaminometer Response ... 50

4.1.1 Parameter Selection 50
4.1.2 ROSE Method Performance Study 54
4.1.3 DOE Test Results 56
4.1.4 Regeneration Time Comparison Tests 61
4.2 Evaluation of Contamination Levels During PCBA Production 62
CHAPTER 5 Conclusions and Future Work 69
5.1 Conclusions 69
5.2 Future Work 71
References 72
Annex – Ionic Contamination Plots 78

LIST OF FIGURES

Figure 1 – Bosch logo evolution from **(a)** 1899's "burning magnet" (on the left) to its sucessors the "sparking armature" and 1918's "armature in a circle" (on the right) as opposed to **(b)** nowaday's modern design[2]. 1
Figure 2 – Sales revenue, associates and unit locations in Portugal, according to data from 2019[3]...... 3
Figure 3 – PCB comparison between a 1968 calculator (left) and a modern computer motherboard (right)[7]. 7
Figure 4 – Schematic representation of the PCB structure. 8
Figure 5 – Representation of a single-sided PCB[14]. 8
Figure 6 – Representation of a double-sided PCB[14]. 9
Figure 7 – Representation of a multilayer PCB[14]. 9
Figure 8 – Representation of a flex-rigid PCB[14]. 10
Figure 9 – Printed Circuit Board with OSP finish[16]. 11
Figure 10 – Scheme of an copper-azole bond formation on an OSP coated board. The chemical structures were made using Marvin JS software version 20.14.0 available online. 11
Figure 11 – Printed Circuit Board with ENIG finish[18]. 12
Figure 12 – Black pad defect on an ENIG coated PCB[20]. 13
Figure 13 – Printed Circuit Board with ImSn finish[16]. 13
Figure 14 – Tin whisker growing between pure tin-plated hook terminals of an eletromagnetic relay[21]. 14
Figure 15 – Examples of SM and TH devices[23, 24]. 15
Figure 16 – Representation of printed circuit board technologies: **(a)** THT and **(b)** SMT[25]. 16
Figure 17 – Scheme of a hand soldering procedure of a TH component[27]. 17
Figure 18 – Schematic of a board going over a solder wave[30]. 18
Figure 19 – Commonlly used reflow oven temperature profile for SnPb soldering[25]. 20
Figure 20 – Standard configuration of a SMT line in BCM[33]. 20
Figure 21 – Schematic of the stencil printing process. 21
Figure 22 – PCB resting on a bed of ICT "nails"[39]. 23
Figure 23 – Standard structure of a selective soldering machine. 23

Figure 24 – Milling machine work scheme[43] 24

Figure 25 – Melting point diagram and microstructure of the tin-lead alloys[6] 26

Figure 26 – The function of fluxing agents in soldering[6] 31

Figure 27 – Veen diagram showing the conditions for occurrence of electrochemical failure. 33

Figure 28 – Scheme of dendrite formation[67] 34

Figure 29 – Measurement principle of the ROSE method in testing (left) and regeneration (right) mode[67]. 36

Figure 30 – Scheme of the tests performed to study the ROSE method. 38

Figure 31 – Plan of the 5 stages of production where the test vehicles were collected to evaluate its surface contamination with the description of the various steps performed in each stage. 39

Figure 32 – Framework of the analysis plan of the test vehicle describing the amount of PCBs subjected to and collected from each stage of the production. 39

Figure 33 – Squeme of the rework stage plan detailing the amount of boards that passed through each step. 40

Figure 34 – Layout of the top side of the board used for sample production, the Bombardier Compact. This PCB had dimensions of 185 x 165 x 1.55 mm, an OSP surface finish, and each panel had two PCBs incorporated. 41

Figure 35 – Position of the five components (marked in blue) substitued in rework on the top side of the Bombardier Compact board. 44

Figure 36 – Top and bottom sides of the finished Bombardier Compact PCBA sample, assemblied at BCM. 45

Figure 37 – Top (left) and bottom (right) side of one of the boards analyzed. This PCB had dimensions of 185 x 160 mm, an ImSn surface finish and solder paste and components only on the top side. 47

Figure 38 – Benchmarker II test board. It has 190 x 127 mm in dimension, an ENIG surface finish. .. 47

Figure 39 – Top (left) and bottom (right) side of the Renault IVI PCBA. This PCB had dimensions of 185 x 167 mm, an OSP surface finish and is one of the boards presently produced at BCM. 49

Figure 40 – Pie chart of the main type of defects the scrap PCBs endured. 50

Figure 41 – Scatterplot of the ionic contamination (in μg/cm² NaCl eq.), measured on a ROSE contaminometer, present on scrap products collected in different stages of SMT production line, according to data from Table 11 and Table 12. Data in green refers to boards collected during insertion of solder

paste and components on the first side and data in blue on the second side of the boards. The mean contamination value for PCBs in blue is 0.54 μg/cm² NaCl eq. and in green is 0.97 μg/cm² NaCl eq. The red line refers to the historical value of the ROSE test method for finished products (1.56 μg/cm²) for reference. 52

Figure 42 – Scatterplot of the ionic contamination (in μg/cm² NaCl eq.), measured on a CM22 contaminometer, vs. temperature of the extraction bath (in °C) of one of the products collected on the SMT production line. The contamination values of this product have a mean of 1.091 ± 0.153 μg NaCl equivalent/cm². The confidence interval was calculated for a significance level of 0.01 and n-1 degrees of liberty. 53

Figure 43 – Scatter plot of ionic contamination (in μg/cm² NaCl eq.), measured on a CM22 contaminometer, Vs volume of NaCl (in μl) added to Benchmarker II boards, and their respective calibration curves. Data in blue refers to boards measured at lower temperature and data in orange to a higher temperature. The confidence intervals of the tendency lines were calculated for a significance level of 0.01 and n-2 degrees of liberty. 56

Figure 44 – DOE plots based on the results of Table 12 adjusted to a quadratic model. **(a)** Individual effect plots of temperature (in °C) and regeneration time (in minutes) of the extraction bath Vs ionic contamination (in μg/cm² NaCl eq.). **(b)** Contour plot showing ionic contamination levels (in μg/cm² NaCl eq.) on a regeneration time (in minutes) Vs temperature (in °C) surface. 60

Figure 45 – Columm graph of the mean ionic contamination (in μg/cm² NaCl eq.) of Renault IVI samples measured on a CM22 contaminometer subjected to a regeneration time of 1, 5, 8 and 10 minutes. It was analyzed nine Renault IVI samples for each condition. The confidence intervals were calculated for a significance level of 0.01 and n-1 degrees of liberty. 61

Figure 46 – Column graph of the mean ionic contamination (in μg/cm² NaCl eq.) of Bombardier Compact samples subjected to the standard PCBA assembly process without rework, analyzed on the ROSE contaminometer. Six samples were analyzed for each condition, with exception of the 2nd reflow where there were seven boards. The confidence intervals were calculated for a significance level of 0.01 and n-1 degrees of liberty. 64

Figure 47 – Column graph of the mean ionic contamination (in μg/cm² NaCl eq.) of Bombardier Compact samples in the reflow, rework and selective soldering stages. Some of the boards were subjected to two different procedures during rework stage (red and yellow columns) while others did not endure rework

(blue column). Six samples were analyzed for each condition. The confidence intervals were calculated for a significance level of 0.01 and n-1 degrees of liberty. 65

Figure 48 – Columm graph of the mean ionic contamination (in μg/cm² NaCl eq.) of Bombardier Compact samples subjected to different conditions on the rework stage, analyzed by the ROSE method. Columns in blue represent the samples cleaned after rework using a 90/10 % IPA/ethylene glycol solution (already presented in Figure 47) while columns in red represent samples who were not subjected to cleaning after rework. The confidence intervals were calculated for a significance level of 0.01 and n-1 degrees of liberty; the non-cleaned samples don't have a confidence interval as it was only analyzed one uncleaned panel for each rework. 66

Figure 49 – Graphs of ionic contamination (in μg/cm² NaCl eq.) measured along a 15-minute time on the ROSE contaminometer for Bombardier Compact samples at different stages of the manufactoring process. 79

LIST OF TABLES

Table 1 – Comparison and overview of PCB surface finishes[15, 18, 19, 22]. 14

Table 2 – Variables that can influence the size of the oxidation layer and therefore soldering efficiency[31]. 29

Table 3 – Features of the lead-free solder pastes used in this work. 41

Table 4 – Characteristics of the solder used for selective soldering the THT components. 42

Table 5 – Properties of the flux used for selective soldering the THT components. 42

Table 6 – Expressions for the calculation of PCB area[82] 46

Table 7 – DOE parameter matrix for the contaminometer's response analysis. 48

Table 8 – Area (in mm²), and individual and mean (x) values of ionic contamination (in µg/cm² NaCl eq.) of the scrap PCBs collected during their first SMT insertion organized according to the surface finish and the product family number.. 51

Table 9 – Area (in mm²), and individual and mean (x) values of ionic contamination (in µg/cm² NaCl eq.) of the scrap PCBs collected during their second SMT insertion organized according to the surface finish and the product family number. 52

Table 10 – Temperature (in °C) and individual and mean (x) contamination (in µg/cm² NaCl equivalent) of the Benchmarker II samples analyzed on the CM22 contaminometer without NaCl addition (base contamination level). These measurements were all done in diferent days. 54

Table 11 – Temperature (in °C) and individual and mean contamination (in µg/cm² NaCl equivalent) of the Benchmarker II samples added with increasing volumes of NaCl solution, tested on the CM22 contaminometer. The data is additionally distribuited according to the temperature of the extration tank. The contamination of base level is the mean of the values of Table 10. 55

Table 12 – DOE test responses (in µg/cm² NaCl equivalent) for a 2 factors, 3 levels full factorial design. 57

Table 13 – Coefficients of each term of the model obtained through the analysis of the results of Table 12 adjusted to a quadratic model. It also presents their respective standard error, t-value and p-value. 58

Table 14 – Degrees of freedom (DF), sum of squares (SS), mean square (MS), f-value and p-value of the regression and error parameters of a quadratic model based on the results of Table 12. 59

Table 15 – Area (in mm^2) and ionic contamination (in $\mu g/cm^2$ NaCl eq.) measured on the ROSE contaminometer for Bombardier Compact samples at different stages of the manufactoring process as well as the number of boards analyzed per stage. The contamination is the mean of the results obtained on the ROSE machine except for the cleaned samples where only one frame (with 2 PCBs) was measured. 63

LIST OF ABBREVIATIONS, ACRONYMS AND SYMBOLS

AE	Automotive Electronics
ANOVA	Analysis of Variance
AOI	Automatic Optical Inspection
AWA	Anti-Whisker Additive
AXI	Automatic X-Ray Inspection
BCM	Bosch Car Multimedia Portugal, S.A.
BGA	Ball Grid Array
BSH	Bosch und Siemens Hausgeräte GmbH
CAF	Conductive anodic filament
CM/MFT3	Car Multimedia/ Manufacturing Technology 3
DF	Degrees of freedom
DI	Deionized
DOE	Design of Experiment
ECM	Electrochemical Migration
ENIG	Electroless Nickel Immersion Gold
ESD	Electrostatic discharge
FCT	Functional Testing
FMEA	Failure Mode Effects Analysis
FR	Flame Retardant
HASL	Hot Air Solder Leveling
IC	Ion Chromatography OR Integrated circuit
ICT	In-Circuit Test
IMC	Intermetallic compound
ImSn	Immersion Tin
IPA	Isopropyl alcohol / 2-propanol
IPC	Association Connecting Electronics Industries
MS	Mean squares
OSP	Organic Solderability Preservative
PCB	Printed Circuit Board

PCBA	Printed Circuit Board Assembly
PEEK	Polyether ether ketone
PTFE	Polytetrafluoroethylene
PWB	Printed Wiring Board
QFP	Quad Flat Pack
R	Correlation coefficient
R&D	Research and Development
R^2	Coefficient of determination
RoHS	Restriction of Hazardous Substances
ROSE	Resistivity of Solvent Extract
SAC	Sn-Ag-Cu
SIR	Surface Insulation Resistance
SMD	Surface Mount Device
SMT	Surface Mount Technology
SPI	Solder Paste Inspection
SS	Sum of squares
T	Temperature
THD	Through-Hole Device
THT	Through-Hole Technology
$T_{liquidus}$	Temperature above liquidus
t_{reg}	Regeneration time
VOC	Volatile organic compound
vol%	Volume fraction (V/V) in percentage
WEEE	Waste Electrical and Electronic Equipment
WOA	Weak organic acid
wt%	Weight fraction (m/m) in percentage
α	Significance level
σ	Standard deviation
$\bar{x}$	Mean

CHAPTER 1 INTRODUCTION

1.1 INSTITUTION OF PLACEMENT

1.1.1 Bosch Group

On November 15, 1886, Robert Bosch (1861-1942) founded a company by the name of "Workshop for Precision Mechanics and Electrical Engineering" in Stuttgart. At the outset, he focused on constructing and installing all types of electrical equipment, including telephone installations and remote electrical water-level indicators. Bosch achieved his first economic success a year later when asked by a costumer to build a magneto ignition device for a stationary engine based on an existing design. The purpose of the mechanism was to generate the electric spark needed to cause the explosion of the air-fuel mixture in the engine. Even though only ten years later, he was the first to adapt the magneto ignition device to a vehicle engine, which would prove to be a key step for the development of the company[1].

The magneto ignition mechanism was the first step to introduce Bosch's company into its largest and oldest business sector – the automotive. This is the same device that represents the company on its official logo[2], shown in Figure 1.

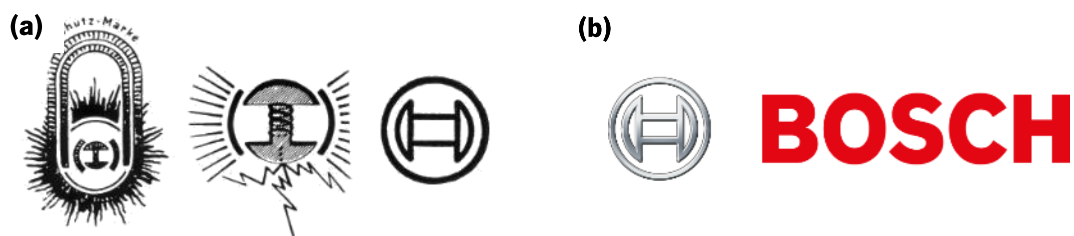

Figure 1 – Bosch logo evolution from **(a)** 1899's "burning magnet" (on the left) to its sucessors the "sparking armature" and 1918's "armature in a circle" (on the right) as opposed to **(b)** nowaday's modern design[2].

Now by the name of Robert Bosch GmbH, or just Bosch, this previously small yet innovative enterprise evolved to become a multinational engineering and technology company headquartered in Gerlingen, Germany. The Bosch Group's strategic objective is to create solutions for a connected life, aspiring to improve the quality of life worldwide with innovative and exciting products and services[3].

Bosch has production units in 3 continents and more than 400.000 workers, which contributed to generate a turnover of 77.7 billion euros in 2019. The Bosch Group comprises Robert Bosch GmbH and

its roughly 440 subsidiary and regional companies in approximately 60 countries. Including sales and service partners, Bosch's global manufacturing, engineering, and sales network covers nearly every country. Its operations are divided into four business sectors: Mobility Solutions, Industrial Technology, Consumer Goods, and Energy and Building Technology. The Mobility Solution sector represents 60 % of its total sales and the remaining 40 % is attributed to the other three sectors[3].

1.1.2 Bosch Group in Portugal

Present in Portugal since 1911, Bosch is one of the most recognized companies in the country, exporting over 95 % of its production to international markets. The company has three production centers: Bosch Thermotechnology in Aveiro, Bosch Car Multimedia Portugal in Braga and Bosch Security Systems in Ovar that focus on the development and production of hot water solutions; automotive sensors and multimedia; and security and communication systems, respectively. Bosch has also a national central office and a BSH sales office located in Lisbon and employs about 6250 employees over the country (according to data from 2019). It is one of the largest industrial employers in Portugal and generated, in 2019, 1.6 billion euros in internal sales[4]. Figure 2 shows the dimensions of the company in Portugal.

The Braga unit particularly is the main plant in the Bosch Car Multimedia (BCM) division, and the largest Bosch Company in Portugal. It was founded in 1990 when Blaupunkt, a Bosch Group company, took over the production and marketing of the previously manufactured Grundig car radios. In 2009, the Car Multimedia (CM) division was restructured and the Blaupunkt brand sold. Since then, the factory was renamed Bosch Car Multimedia Portugal, S.A and it specialized in the manufacturing and development of electronic equipment, mainly car radios and navigation systems for the automotive industry[4].

Nowadays, it is one of the biggest private employers in the region with over 3500 associates, the largest car radio plant in Europe, and one of the top national exporters. In 2012, as a result of a demand for increasingly advanced technologies, Bosch and University of Minho signed what would become the largest innovation partnership in Portugal and one of the largest partnerships between a company and an university in Europe[4].

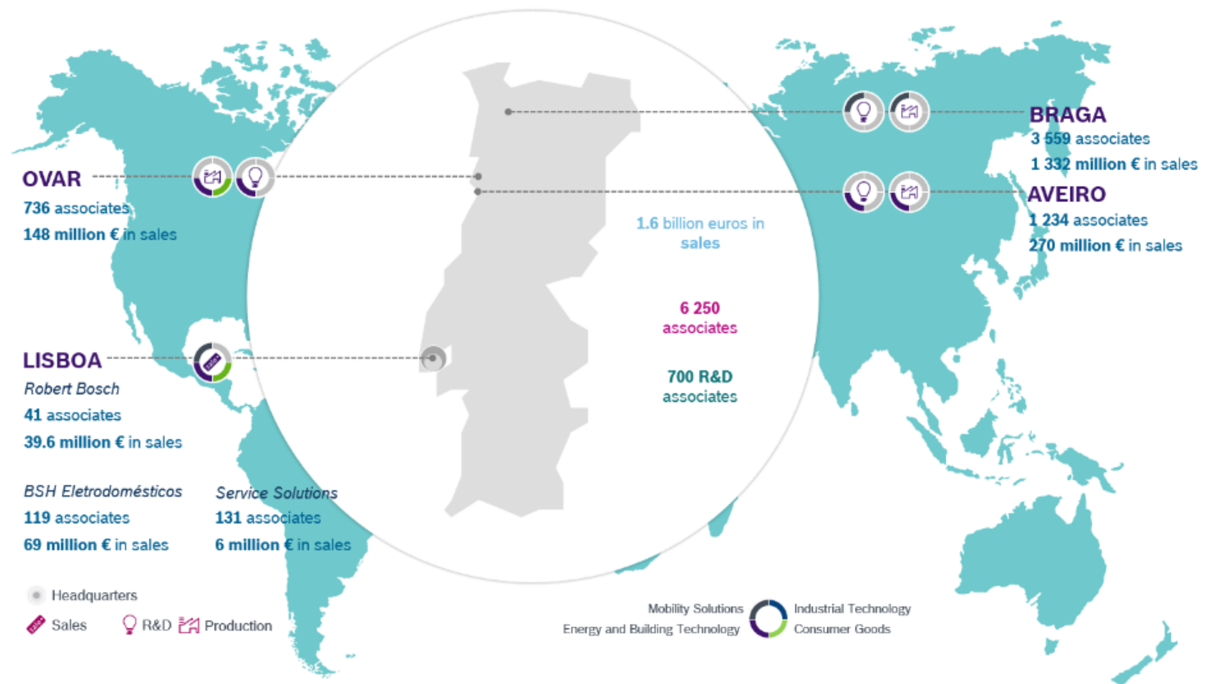

Figure 2 – Sales revenue, associates and unit locations in Portugal, according to data from 2019[3].

1.1.3 CM/MFT3 Department

The Car Multimedia/ Manufacturing Technology 3 or CM/MFT3 department, where the current dissertation was developed, is a CM division that belongs to a centralized organization in Hildesheim, Germany. This department is worldwide accountable in the area of PCB assembly and interconnection technologies and its responsibilities include:

- Process development, release and standardization of the process technology.
- Setup process and technology roadmaps together with development business units.
- Definition of process quality standards for each process, considering Bosch and external benchmark results.
- Setup Standard Process Control Plans and FMEA definition for all processes.
- Definition of "best practice" costs for each process, considering local influences[3].

1.2 PROPOSED MASTER THESIS

The electronics industry emerged in the 20th century and since then has become one of the largest global industries. It covers a wide range of products in areas like communication, transportation, military defense, health, space research and many others. The functionality and practicality of electronic devices has made modern society extremely dependent on them.

One of the most competitive markets is the automotive manufacturing. Better product performance, lower manufacturing costs and faster production processes are some of the goals the automotive industry has been working over the past decades. PCBs are becoming progressively more complex, mainly because of the demand for smaller systems. Due to these advancements, nowadays it is possible to have a great number of features on a board of the size of a hand or even smaller.

However, miniaturization increases the probability of performance failures and raises many problems to the production units. The constant miniaturization of components, reduction in path, board sizes and distance between components as well as the rise in package density can compromise the reliability of these printed circuit boards. In addition, changing from Sn-Pb solders to Pb-free solders resulted in lower wetting and higher melting points. In order to adapt the product to these layout and solder changes, manufacturers must use different materials and techniques that may introduce new and potentially harmful contaminants to the product.

Among all contamination sources that can affect PCBs, the most worrisome is the contamination caused by ionic species as a result of soldering fluxes, etching, cleaning, plating chemistries, etc. These species can dissociate and migrate on the surface of the board, which can cause short-circuits. Therefore, monitoring and controlling these species is vital to assure the reliability of PCBs.

The proposed Bosch Car Multimedia project is to study the ionic contamination in electronic product assembly through an ionic contamination technique called the resistivity of solvent extract (ROSE) test. Thus, this thesis has two main objectives:

- Study the ROSE response and establish parameters to test its performance at BCM.
- Evaluate the ionic contamination levels of printed circuit boards in the various phases of its production run.

1.3 Dissertation Structure

The presented dissertation is divided into five key sections. The current section, CHAPTER 1, presents a guide concerning the company where this thesis was elaborated, its history and field of operation, as well as the intent of the developed project.

CHAPTER 2 revises the literature of interest for this work, describing essential concepts linked to printed circuit boards' assembly. It also explains essential techniques for the understanding of the next chapters of this dissertation.

Furthermore, in CHAPTER 3, the materials and methods used during this research at Bosch Car Multimedia Portugal are presented.

CHAPTER 4 comprises the presentation and discussion of experimental results obtained through the methodology explained in the prior chapter.

In the last chapter, namely CHAPTER 5, the main conclusions of the project and future work suggestions are given.

CHAPTER 2 LITERATURE REVIEW

2.1 PRINTED CIRCUIT BOARDS

Printed circuit boards or PCBs, also called printed wiring boards (PWBs) and etched wiring boards, have long been the foundation of electrical engineering. These rugged, inexpensive and highly reliable boards provide mechanical support and connect electronic components in electronic devices. They require greater layout effort and higher initial cost than other technologies, but they are much cheaper, faster and consistent in high-volume production[5].

Like many other great inventions in history, the printed circuit board was built on a foundation of achievements throughout history. Their history can be traced back to the early 1900s. In 1925, Charles Ducas submitted a patent that involved creating an electrical path directly on an insulated surface. The idea was later developed in Austria when Dr. Paul Eisler began making the first real operational printed circuit boards for a radio in 1943. In 1956, the US Patent Office granted a patent for the "Processing of Assembling Electrical Circuits" to a group of scientists in the US Army. Some of the major PCB advancements were made under the leadership of the American army due to their need for new weaponry and communication systems[5, 6].

Over time, PCBs have evolved as a tool for optimizing the manufacturing of electronics. Once bulky and inefficient designs assembled by hand soon gave way to microscopic components that required the precision and efficiency of machinery. One prime example would be modern computers. Many computer manufacturers are using PCBs as motherboards instead of three or four additional expansion cards, needed to operate a computer earlier. In the past, it was quite common to have a separate video card, sound card, modem, and sometimes game port[7]. Nowadays, with the use of PCBs, they can all be integrated on a single motherboard. Take for instance the two circuit boards shown in Figure 3. One is a board for a calculator made in the 1960s, while the other is a typical high-density motherboard used in present day computers. Through the advancements of modern technology, everything on that calculator's PCB can now fit into a single chip on today's designs.

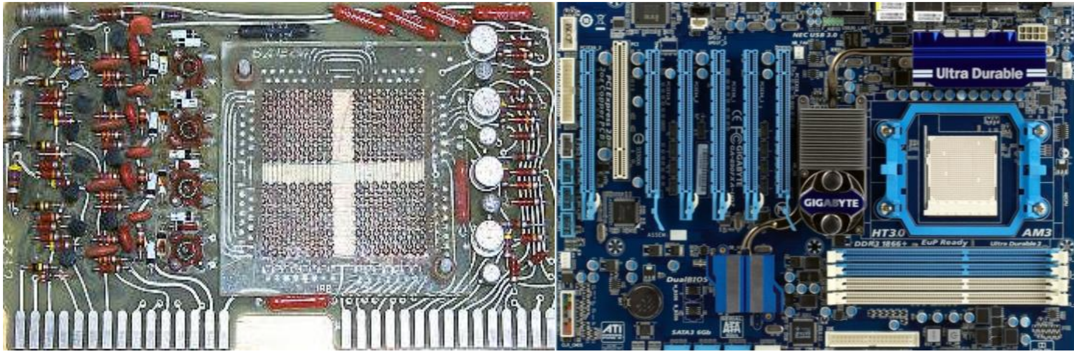

Figure 3 – PCB comparison between a 1968 calculator (left) and a modern computer motherboard (right)[7].

2.1.1 Structure and Materials

An unprocessed board is constituted of a conductive material arranged to create patterns (tracks) on layers of an insulating dielectric substrate (base). FR-4 (FR meaning Flame Retardant), by far the most used base material for printed circuits, is made of woven fiberglass cloths impregnated with an epoxy resin or epoxy resin blend. The outstanding electrical, mechanical, and thermal properties of FR-4 have made it an excellent material for a wide range of applications including computers and peripherals, servers and storage networks, telecommunications, aerospace, industrial controls, and automotive applications. Other commonly used materials have been FR-2 and PTFE (polytetrafluoroethylene)[8, 9].

The conductive layer is almost invariably copper foil, adhesive bonded under heat and pressure to the substrate. There are areas of exposed copper on the PCB surface, known as pads, which are located in specific positions where the components are mounted[8]. Depending on the purpose of its use, the boards can have more complex designs with several conductive and insulating layers. In order to provide an interlayer communication, most PCBs are equipped with a technology called via which consists in copper cylinders that electrically and thermally join traces and pads on different layers of a PCB. High-density PCBs may have copper holes that either connect different layers of the PCB (blind and buried vias) or the top and bottom layers (through holes)[9, 10].

Applied to the board after all copper processing has been completed, the solder mask, also known as solder resist, is a thin, tough coating of insulating material. Holes are left in the resist where pads are to be soldered. It serves to protect copper from being soldered and therefore prevent the risk of short circuits between tracks and pads during and after soldering. It is sometimes used as an anti-corrosion coating and to provide a dark, uniform background for components identification and inspection[11].

Figure 4 illustrates a graphic representation of a PCB, including its layers, base material, electrical structure and solder mask.

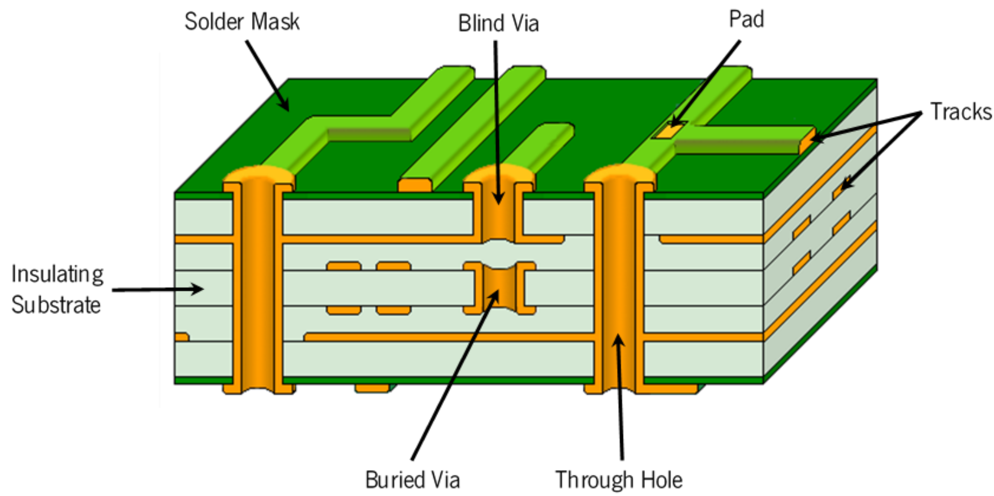

Figure 4 – Schematic representation of the PCB structure.

2.1.2 Classification of PCBs

PCB's numerous applications are possible partially because each board has their own manufacturing specifications, material types and usages. Manufacturers choose what PCB type to use in a particular product based on their needs. Different board types are distinguished based on the number of layers and type of components.

Single-sided PCB has just one layer of substrate containing electronic components and circuits on one of the sides. As displayed in Figure 5, one side of the substrate is covered with a thin layer of copper and, usually, a protective solder mask is placed on top of the copper layer. This type of board shows better performance for low cost and bulk manufacturing applications like calculators, radios and printers[12, 13].

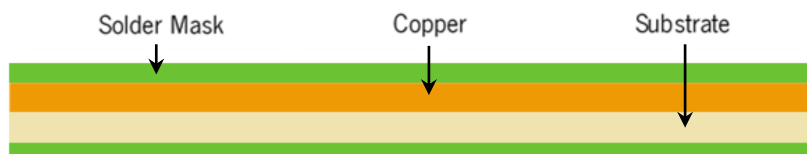

Figure 5 – Representation of a single-sided PCB[14].

The **double-sided PCB** is much more common than the single-sided. Both sides of the substrate have metal conductive layers, and components are attached to both sides as well. Holes on the board allow circuits on one side to be connected to others on the other side (Figure 6). Double-sided boards connect the circuits on each side using one of two types of components: through-hole devices (THD) and surface mount devices (SMD). Through-Hole Technology (THT) involves inserting tiny wires, known as leads, through the holes (seen in Figure 4) and soldering each end to the appropriate component or circuit. Unlike through-hole technology, Surface Mount Technology (SMT) does not use wires. Instead, chip type components without lead wires get soldered directly onto the PCB through the pads[9, 12]. The most important advantages of these double-sided boards are its compact circuit and relatively lower cost. This type of PCB is mostly used in industrial controls, UPS systems, HVAC applications, phones, amplifiers and power monitoring systems[13].

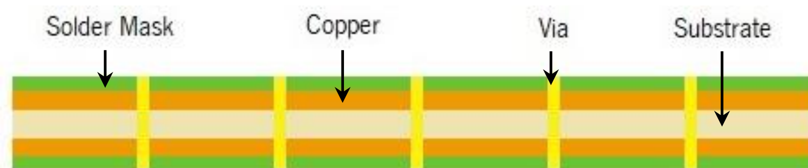

Figure 6 – Representation of a double-sided PCB[14].

Multilayer PCB is based on the technology used on the double-sided board. It has several layers of copper separated by insulating material. As with double-sided boards, components on multilayer boards can be connected to each other through holes or vias on the board, as can be perceived in Figure 7. The multilayer design saves even more space than a double-sided design[12]. This type PCB designing is very complex and used for very complicated and large electrical task in very low space and compact circuit like GPS technology, satellite system, medical equipment, file server and data storage[13, 15].

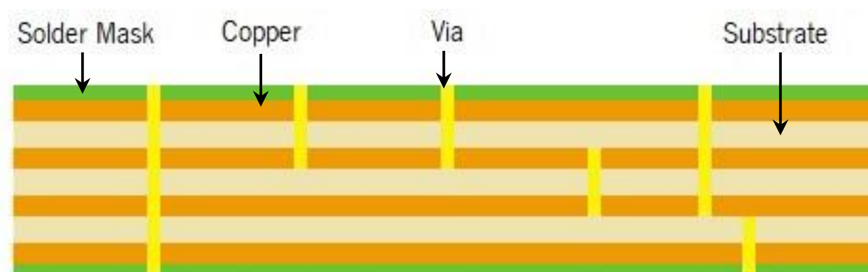

Figure 7 – Representation of a multilayer PCB[14].

In addition to having various numbers of layers and sides, PCBs can also come in different rigidities. Most consumers typically think of a **rigid PCB** when they picture a circuit board. Rigid PCBs use a solid,

inflexible substrate material such as fiberglass-reinforced thermosetting resins, that limit the bending of the board contrarily to the **flexible PCB**, also known as flex circuit. This type of PCB uses a flexible plastic material like polymide, PEEK (polyether ether ketone) or transparent conductive polyester film, allowing the board to fit into different shapes and to twist during its use without damaging the circuits on the board. This is very complex type of PCB and, like rigid PCBs, it can contain different ranges of layers. Finally, displayed in Figure 8, the **flex-rigid board** consists of multiple layers of flexible PCB attached to a number of rigid PCB layers[12, 13].

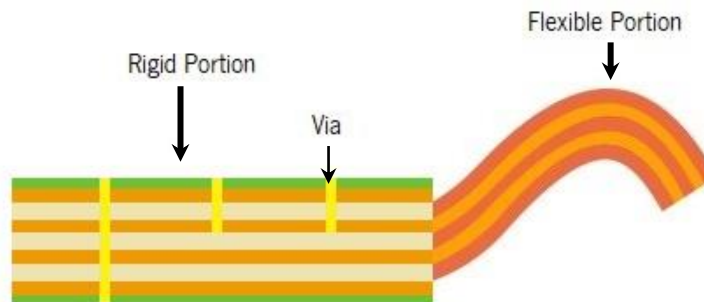

Figure 8 – Representation of a flex-rigid PCB[14].

2.1.3 PCB Surface Finishes

After applying solder mask to the board, a significant amount of metal area is left exposed to the environment. If left unprotected, the copper will oxidize and deteriorate, making the circuit board unusable. The surface finish forms a critical interface between the component and the PCB. It has two essential functions, to protect the exposed copper circuitry and to provide a solderable surface when assembling the components to the printed circuit board. The final surface finish must meet several functional criteria, including solderability, environmental, electrical, physical, and durability demands. Perhaps no other step in the PCB manufacturing process has undergone more changes in the era of surface mount manufacturing than the final finish chemical process[15].

Hot Air Solder Leveling (HASL) was once the best method for delivering consistent assembly results. It consisted of the immersion of a circuit board into molten solder constituted of a tin-lead solder alloy. In modern day, however, the elimination of lead (Pb) from PCBs due to the RoHS and WEEE European directives has rendered this standard surface finish increasingly obsolete[15]. The higher melting temperature of lead-free alloys and therefore, the additional thermal stress caused to the PCB, triggered

a slow replacement of HASL for other finishes more capable of adapting to these changes. Listed below are the three surface finishes used nowadays in Bosch Car Multimedia (BCM).

Organic Solderability Preservative (OSP) is one of the preferred final finishes in the post-HASL era. OSP preserves the copper surface from oxidation by applying a very thin protective layer (0.2 to 0.5 μm) of organic compounds over the exposed copper. An OSP coated board is portrayed in Figure 9.

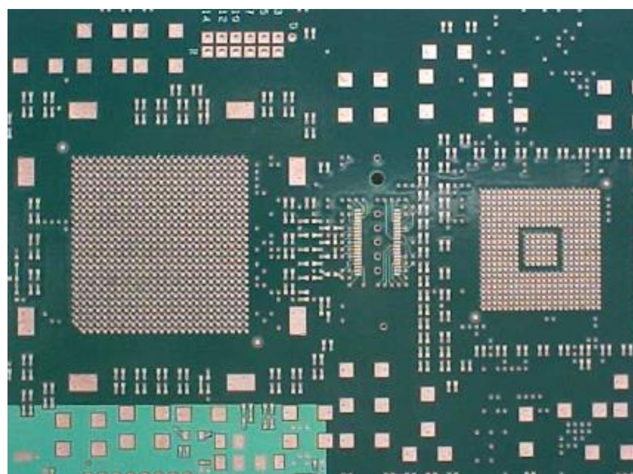

Figure 9 – Printed Circuit Board with OSP finish[16].

In brief, a large organic molecule, typically an azole, is dissolved into a solution of water and organic acid. The circuit board is exposed to the solution, and the OSP molecule is attached to the PCB's exposed copper surfaces. A chemical bond is formed between copper and a nitrogen group[15], as depicted in Figure 10. Progress to-date has allowed the selection of derivatives of 2-phenylimidazole and benzimidazole as chemical reagents used in OSP coatings[17].

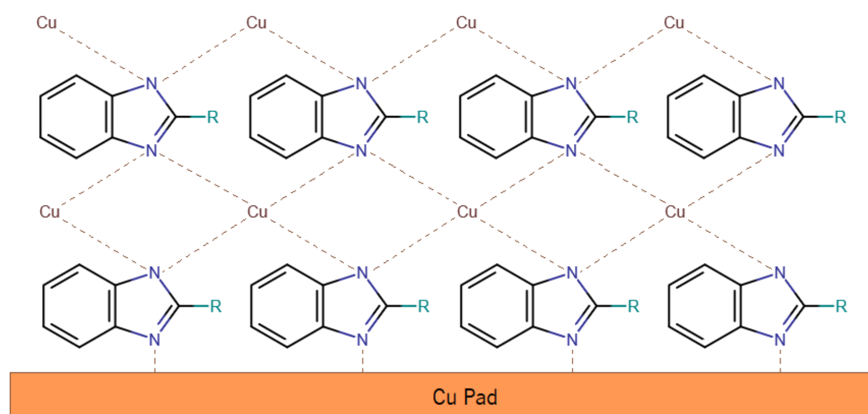

Figure 10 – Scheme of an copper-azole bond formation on an OSP coated board. The chemical structures were made using Marvin JS software version 20.14.0 available online.

This finish is environmentally friendly in comparison to other common lead-free finishes, which suffer from either being more toxic or substantially higher energy consumption[18]. OSP is the cheapest and simplest of all major surface finish options, so it enjoys wide use throughout the world. Its use is limited, however, due to poor contact functionality for electrical tests and deterioration after multiple thermal operations, so it is not preferred for multiple soldering processes[19].

Electroless Nickel Immersion Gold or **ENIG**, represented in Figure 11, is a two-layer coating of gold and nickel over catalyzed copper. Nickel is the barrier between copper and the surface to which the components are soldered while gold protects nickel during storage and provides low contact resistance required for thin gold deposits. ENIG is now arguably the most used finish in the PCB industry[18].

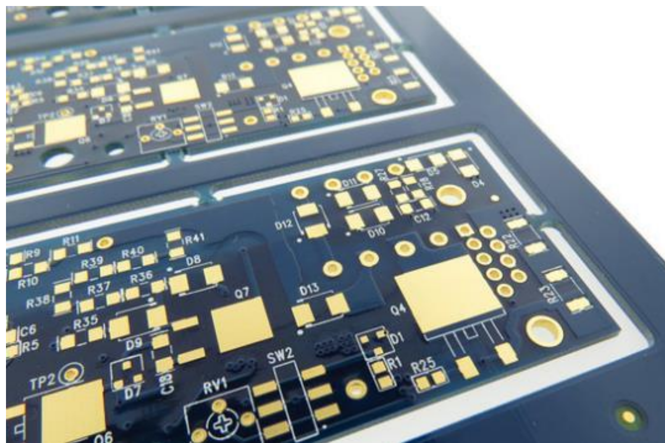

Figure 11 – Printed Circuit Board with ENIG finish[18].

Chemically, gold is the ideal element for external coating of PCBs. It does not form an oxide, so it is unaffected by temperature and storage conditions that might reduce the shelf life of other finishes. In addition, this metal dissolves nearly instantaneously into solder, promoting higher wettability. However, gold embrittles solder joints when present in excess and dissolves very quickly into copper as well. To prevent the mixing of gold with copper, a layer of electroless nickel is deposited between them through chemical reduction using sodium hypophosphite. Normally, 3 to 5 μm of nickel is used in this finish, with a thin gold coating of 0.05 to 0.15 μm to prevent nickel oxidation[15].

This is the most expensive of the three finishes and it is often used because there is some technical restriction on the other two more accessible finishes. Despite being an ideal surface finish, ENIG coated PCBs can suffer a major drawback, named black pad. In simple terms, a black pad, as the one exhibited in Figure 12, refers to a deficient connection that occurs between the solder and nickel interface. All reports and analysis point to the conditions of the nickel bath as the main cause of this flaw, with the

primary issue being excess of phosphorus, a byproduct of the dissolution of nickel. The affected joints are easily broken in this case, and the corroded "black" nickel is exposed, providing basis for the term "black pad"[15, 20].

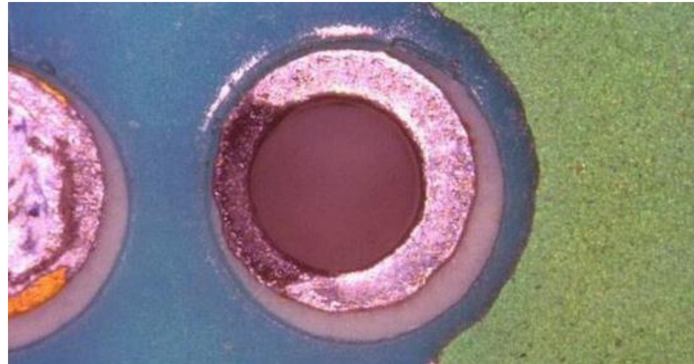

Figure 12 – Black pad defect on an ENIG coated PCB[20].

Lastly, **Immersion Tin (ImSn)** is a thin coating of pure tin, typically 0.6 to 1.2 μm thick. This metal is applied by immersing the PCB in liquid tin, which protects the underlying copper from oxidation and provides a dense, uniform coating with highly solderable surface. Tin boards, like the one in Figure 13, are used primarily for solderability and have very good compliant pin connector functionality[15].

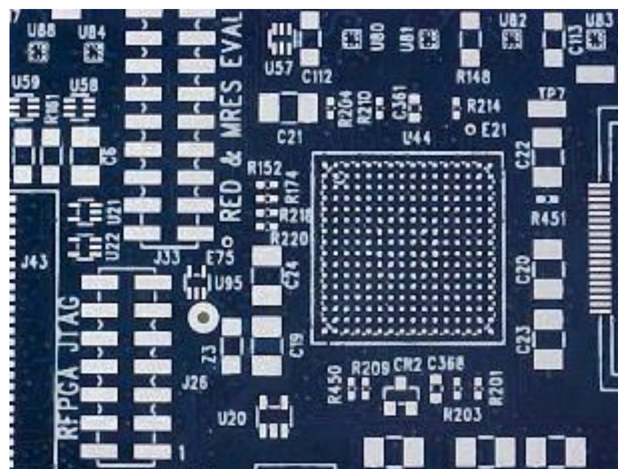

Figure 13 – Printed Circuit Board with ImSn finish[16].

Copper and tin have a strong affinity for one another so the diffusion of one metal into the other will occur inevitably. Therefore, it creates an intermetallic form that directly affects the shelf life of the deposit and the performance of the finish. Alongside this, this finish is restricted in some regions due to environmental concerns over the use of its bath ingredient thiourea, a known carcinogen[15, 18].

One naturally occurring characteristic of tin in direct contact with copper is the formation of tin whiskers. Tin whiskers are thin, electrically conductive, crystalline structures of tin that can grow up to 10

mm from surfaces where this metal is used as a final finish[21], as can be observed in Figure 14. Numerous electronic system failures have been attributed to short circuits caused by tin whiskers that bridge closely-spaced circuit elements maintained at different electrical potentials[21]. Although the precise mechanism for whisker formation remains unknown, this structures can be suppressed by doping the tin deposit with an anti-whisker additive (AWA) which alters the grain structure to create defined structures with uniform distribution resulting in less stress[22]. This defect can be confused with a more familiar phenomenon known as "dendrites" commonly formed by electrochemical migration processes, a theme that will be described on later chapters.

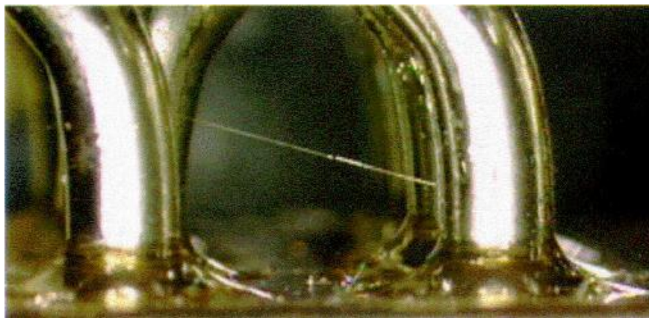

Figure 14 – Tin whisker growing between pure tin-plated hook terminals of an eletromagnetic relay[21].

A summary of BCM's three surface finishes is displayed on Table 1, comparing characteristics like thickness, shelf life, price as well as their advantages and disadvantages.

Table 1 – Comparison and overview of PCB surface finishes[15, 18, 19, 22].

	OSP	ENIG	ImSn
Typical thickness	0.2 – 0.5 μm	3 – 5 μm Nickel + 0.05 – 0.15 μm Gold	0.6 – 1.2 μm
Shelf life	6 months	12 months	6 months
Price	Low	High	Moderate
Strengths	Simple process; Environmentally friendlier; Re-workable; High productivity at fabrication.	High corrosion resistance; Good for THT; Excellent solderability.	Well suited for pin insertion applications; Good solderability; Re-workable.
Problems	Poor for THT; Degradation with multiple reflow; Difficult to inspect; Sensitive to handle.	Black-pad formation; Possibly aggressive to soldermask; Complex process; Not re-workable.	Sensitive to handle; Whisker potential; Solder mask attack; Use of thiourea.

2.2 PCB Assembly

The PCB serves as the electrical interconnection device between different electronic components that are essential to the functioning of the electronic products ever-present in today's society. Components from a few hundred to some thousands can be assembled on a single PCB. A PCB populated with these components is called a printed circuit board assembly (PCBA). There are two basic steps in the assembly of a printed circuit board: first is the placement of the components and second is their soldering to the substrate.

2.2.1 Electronic Components

Electronic components are structures that, when mounted on the surface of the PCB and connected to each other, form an electrical circuit. These components can be categorized by the type of mounting technology used on their assembly: surface mount devices (SMDs) or through-hole devices (THTs), as shown in Figure 15.

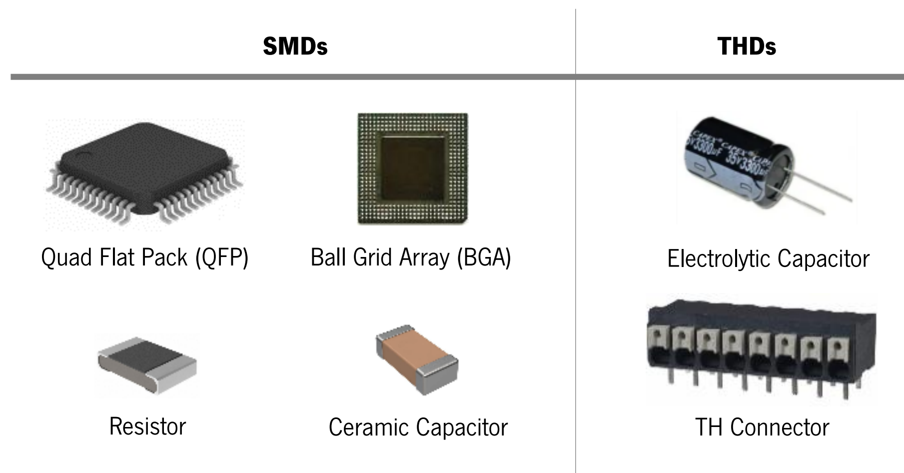

Figure 15 – Examples of SM and TH devices[23, 24].

They can also be classified into two types according to their function: active components like transistors, diodes, ICs (integrated circuits); and passive components like capacitors, resistors, inductors. Passive components can store or maintain energy either in the form of current or voltage while the active ones rely on a source of energy and are able to control the electron flow through them[23].

2.2.2 Component Mounting Technologies

The PCB must go through a process of assembling electronic components in order to reach its final configuration. PCB assembly technologies can be categorized into two main groups already mentioned in chapter 2.1.2: Through-Hole Technology (THT) and Surface Mount Technology (SMT) that are defined by the type of components used (THDs and SMDs respectively). Figure 16 illustrates the principles of these technologies. There is also, what can be considered a third type of assembly process, which is a combination of SMDs and THDs on the same board (Mixed Technology). SMT is used in around 90 % of board assemblies, but through hole still accounts for the remainder and is unlikely to disappear completely[11].

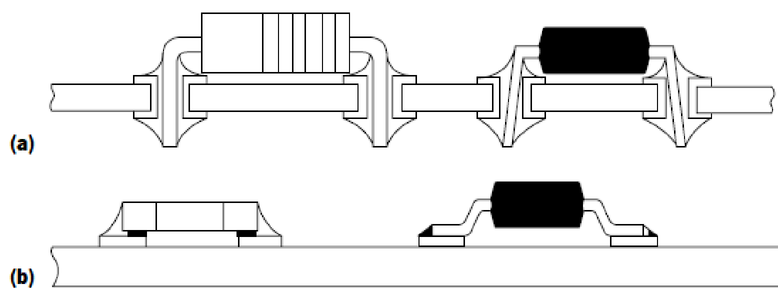

Figure 16 – Representation of printed circuit board technologies: **(a)** THT and **(b)** SMT[25].

For products where overall board size is not a major concern, **Through-Hole Technology (THT)** is applied. The components are inserted into holes drilled through the PCB and then the connections are soldered on the underside of the PCB, between the component lead and the PCB pad (Figure 16a). THDs are usually soldered by selective and wave soldering processes[25] (explained in the next subchapter).

Through-hole technology is used because it is the only format available for some components, particularly large devices, all of which require additional mechanical support that is offered by through-hole interconnections. Even though this assembly process is reliable, the relatively large devices and the requirement for holes on the board limit component density, restricting product functionality and further miniaturization[26].

Surface Mount Technology (SMT) refers to assemblies with components directly soldered to pads on the surface of circuit boards (Figure 16b), thus allowing the placement of components on both sides of the PCB. In this process, a solder material is applied onto paths and components are mounted and soldered in their assigned location[25, 26].

The deposition of flat leaded or leadless components and electronic packages on the surface of printed circuit boards, as opposed to the conventional THT, allows a higher degree of automation, higher circuitry density, smaller volume, lower cost, and better performance[25]. Large holes could be replaced by small vias for signal conduction between sides and internal layers. Finer traces and reduced component heights also contribute to increased circuit board miniaturization and functionality[26].

2.2.3 Soldering Processes

Soldering is one of the oldest techniques of joining two pieces of metal together. In this joining technique, a material filler called solder is fused between the gap of the two materials to be joined, solidifying and therefore creating a mechanical and electrical joint between two materials. A cleaning agent, the flux, is added to, when heated or activated, eliminate oxides and contaminants on the surface of the board, allowing the formation of a proper solder joint. Nowadays, reflow and wave soldering are the chosen techniques for large scale PCBA manufacturing, due to their ability to solder entire circuit boards simultaneously (or sequentially in the case of wave soldering)[6].

Hand soldering is a process in which components are individually soldered to a PCB. In this soldering technique, an iron provides the heat necessary to instantly molten a solder wire (Figure 17), at a temperature around 360 °C for lead-free solders.

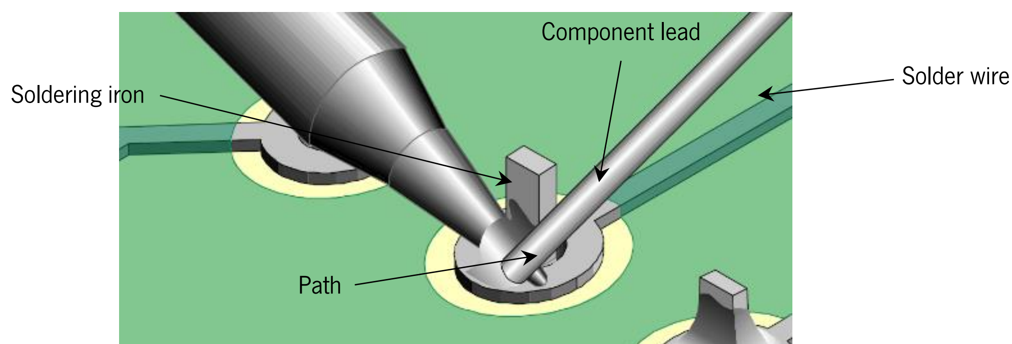

Figure 17 – Scheme of a hand soldering procedure of a TH component[27].

First, the tip of the iron is applied to the junction of the lead and the path to be soldered and a heat bridge is formed by touching the solder wire to the junction. Most of the solder alloys used for this process have a core of liquid flux so, when heated, the solder starts to be melted, and the flux activated. The flux moves away from the heat and ahead of the solder over all the metal surfaces uncovered by the surface finish while the liquid solder moves towards the heat covering the heated metal. The flux is pushed along

by the solder as it performs its cleaning job. While it moves in front of the solder, it also floats away the lose contaminants. The flux will end up pooled around the edges of the pad as the soldering operation is completed[9, 28]. Nowadays, this technique is mostly used for rework purposes, to retouch components that were poorly soldered in the assembly line.

Wave soldering is commonly used in the soldering of through-hole and mixed circuit boards but can also be used in surface mount PCB assemblies. The PCB, with the components already inserted, travels over the wave via a conveyor belt. This belt carries the board through three sections: fluxing, preheating, and lastly wave soldering. Firstly, flux is applied to the surface of the board by spray or foam, and an air knife removes any excess. Afterwards, the preheat stage, necessary to avoid PCB's thermal shock when subjected to the solder wave. Heating the board up to around 100 °C also allows flux activation and removes possible solvents and moisture present on the board[26, 29].

In the next step, a solder wave is created by pumping molten alloy upward through a nozzle, where it exits and then falls back into the bath. The solder bath temperature is 260 °C for most solder materials. The conveyor carries the printed circuit board so that is passes over the surface of the wave. The bottom side of the circuit board contacts the wave, allowing the molten solder to wet the exposed pads as well as to flow upward through the holes by capillary action (Figure 18). In the case of SMDs, the components are secured in position with adhesive before being treated through the molten solder wave. The speed of the conveyor and the take-off angle, the angle at which the circuit board approaches the wave, are critical parameters for minimizing wave-soldering defects. An additional zone, a cleaning zone, can be used depending on the type of flux used[26, 29].

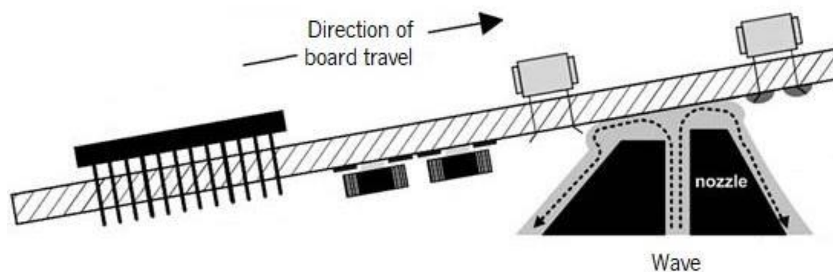

Figure 18 – Schematic of a board going over a solder wave[30].

A variation of wave soldering is the so-called **selective soldering**. Instead of using a long wave to accommodate the dimensions of an entire circuit board, it is used a small fountain of molten solder. A metal mask under the PCB protects the non-solderable areas. The reduced geometry allows for the soldering of individual components or several components on only selected areas of the circuit board. A

manual operation is used to apply flux and preheat the circuit board prior to the actual soldering process. This particular soldering method is used when soldering certain components may damage other more sensitive components and the board due to heat[26].

In **reflow soldering**, generally both solder and flux are already in place before the joints are heated in the form of a solder paste. Thus, for a board surface populated entirely with SMDs, this is the primarily used soldering process. To prepare a board for this process, solder, generally in the form of solder paste, is applied to the circuit board followed by the attachment of components on top of the solder and the insertion of the board into a conveyorized reflow oven. The oven is set to raise the circuit board and component temperatures gradually. Flux in the solder paste is activated with the increase of temperature and strips metal surfaces of oxides which inhibit solder joint formation. Finally, enough heat is provided, allowing the solder to reflow (common expression for the re-melting of the solder alloy). When built and implemented properly, the reflow process results in a controlled and predictable heating and cooling cycle and reproducible solder-joint formation[6, 30].

Commonly used reflow methods employ infrared reflow, vapor phase reflow, in-line-conduction reflow and forced convection reflow[25]; the latter being the one used in BCM. In convection reflow process, a heated gas is forced into the oven process chamber in order to heat the PCBs. Usually, it is an inert gas such as nitrogen (N_2) to remove the oxygen from the oven chamber and avoid oxidation during the process. The gas used in this type of method can also be air, as solder pastes with high flux content are more solderable in air[31]. Nonetheless, nowadays nitrogen is preferred over air atmosphere, as in the case of BCM.

The oven is divided in several heating zones whose temperatures can be altered independently in order to form thermal profiles adjusted to fulfill the soldering parameters. The time and temperature of the reflow take into account factors like the activation of the flux of solder paste, thermal resistance of the components and melting temperature of the solder paste so that the process does not damage the circuit board nor the electronic components. During the reflow process, the thermal profile typically has four stages: preheat, soak, reflow and cooling[25, 32], as represented in Figure 19.

Firstly, in the preheating zone, solvents evaporate, and solder paste begins to dry as the temperature increases at a maximum rate of 3 °C/s. This stage is followed by the soak zone that aims to remove all solder paste volatiles and activate the flux. Also, the lower heating rate in the soak stage allows sufficient time for homogeneous temperature distribution between components with different thermal masses, in

order to prepare for the subsequent stage. Next in the reflow zone, the temperature rises at a rate of approximately 2 °C to a temperature above the melting point (the temperature above liquidus, or $T_{liquidus}$). The peak temperature for the reflow zone is at least 25 °C above $T_{liquidus}$ to guarantee the lead-free solder particles melting, as well as to ensure reliable solder joints throughout the whole range of components of the PCBA. Finally, the cooling zone ideally has a ramp down between 4 and 6 °C/s, to cool down quickly, but avoiding thermal stress[25, 32].

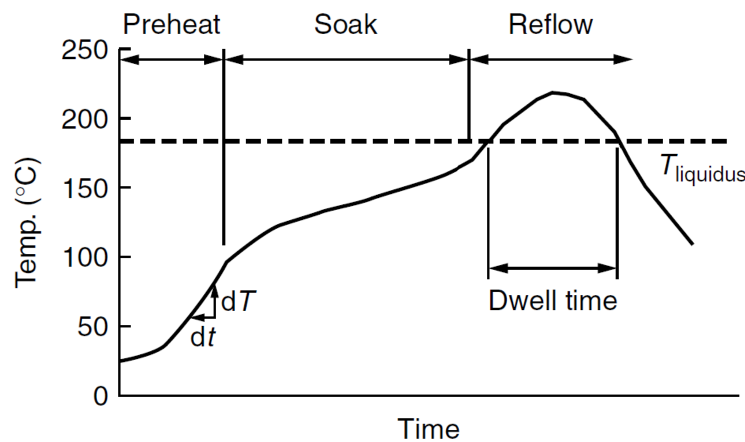

Figure 19 – Commonlly used reflow oven temperature profile for SnPb soldering[25].

2.2.4 BCM Assembly Line

PCB assembly processes are determined by the location of the components (on one or both sides of the PCB), and the type of parts used in the assembly (THDs, SMDs or both). Depending on the type and the class of production, several assembly stages are required to assemble a PCBA. BCM boards are mostly assembled by SMT with THT being used in assemblies of larger components. The basic assembly process sequence for surface mount technology is solder paste printing, “pick-and-place” the components and reflow the solder. In Figure 20, it is possible to perceive the layout of a SMT line operating at Bosch Car Multimedia.

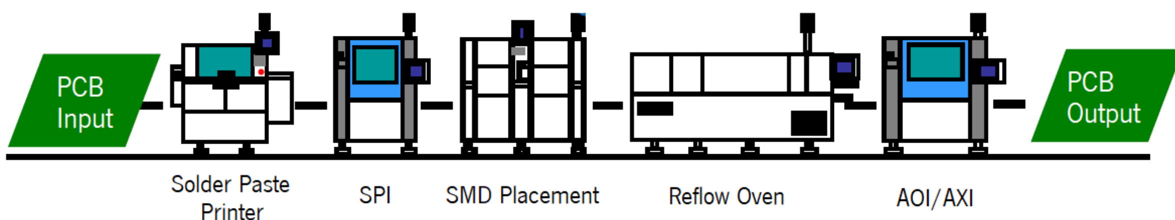

Figure 20 – Standard configuration of a SMT line in BCM[33].

This automatic process begins with the loading of the PCB from the container where it is kept to the PCB loader. The PCB then passes to the laser-marking machine where a barcode is marked on the board allowing its traceability. The laser marking of the board can be done online or offline. It changes the solder mask color creating readable information like PCB number, PCB lot, production date, etc. The board passes on a traceability system where the barcode is stored in the computer system[34].

The first process in SMT assembly is the application of solder paste on the substrate, where solder paste must be deposited for electrical connections. Nowadays, the most common method for solder paste application is the **screen (stencil) printing**, which is ideally suited for high production volumes of similar assemblies with a large number of surface mounted components. The stencil is a thin metal foil that has patterns of the apertures matching the copper pads existent on the PCB for placement of solder paste and components[14, 29]. It is normally made of stainless steel with thickness between 100 and 175 µm (commonly 125 µm). The stencil is attached to a metal frame by an open wire mesh in which solder paste must flow through. It is then placed on top of the PCB with the patterns registered properly. The solder paste is deposited onto one side of the stencil and a squeegee drags solder paste across it. The PCB is then detached from the stencil, with solder paste deposited on top of the corresponding pads[25, 29]. The stencil printing process is schematically illustrated in Figure 21.

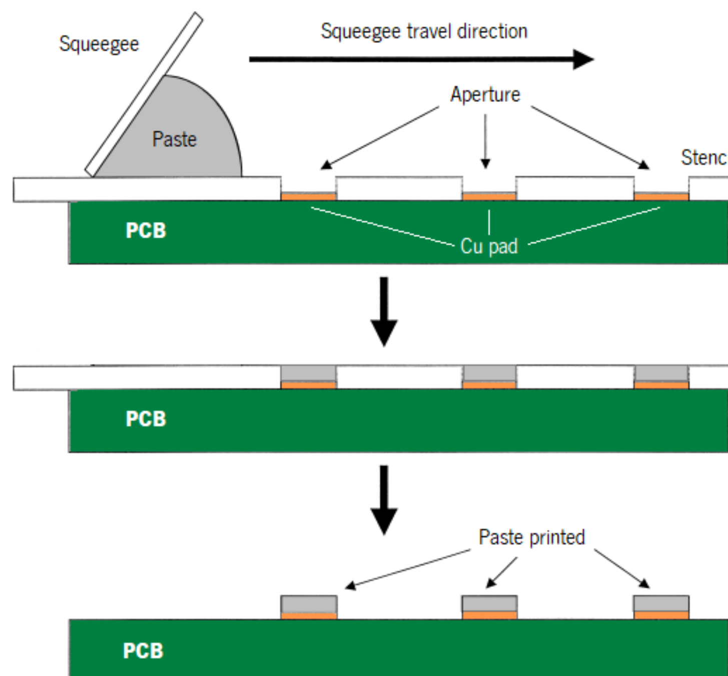

Figure 21 – Schematic of the stencil printing process.

After solder paste application, the board is conveyed to a **Solder Paste Inspection (SPI)** machine, capable of measuring and analyzing the areas, volumes, heights, widths bridges, shapes deformations and offsets from the paste deposited using 3D cameras. All these parameters are previously defined and, if they are not fulfilled, the board has to be rejected since it is forbidden to correct printing defects[35]. Following the SPI is the **component placement** process, also known as "pick-and-place", where size-specific vacuum nozzles pick each component from its packaging, orient them correctly and place them in the programed location at high speed. The process must be done with high accuracy and precision in order to minimize possible defects in the finished product[25, 34]. After component placement, the board moves into the **reflow oven** where all the solder connections are formed between the components and the PCB pads by heating the assembly to a sufficient temperature as explained in subchapter 2.2.3.

Lastly, the final inspections are performed. The **Automated Optical Inspection (AOI)** is a technology that uses cameras to scan the PCBA surface, capturing images, which are then processed and compared with a standard, allowing the detection of defects in component placement and solder joints. However, AOI cannot check the solder joints underneath the components or in areas with reduced visibility due to high density of components[36]. Optionally, the running of an **Automatic X-Ray Inspection (AXI)**, allows the inspection of this kind of joints. The technology behind AXI is similar to AOI, with the difference that it uses x-rays to form the image instead of 3D optical cameras[37]. The operator is responsible to interpret the results of both AOI and AXI and approve or deny the PCB for the next stage.

After SMT insertion, the **In-Circuit Test (ICT)** is a powerful tool for printed circuit board testing. This method uses a "bed of nails", visible in Figure 22, that connects to circuit nodes on a board and measures the performance of the components regardless of the other components connected to them. The nodes are physically represented by the soldered leads of the components, or by special test pads connected by copper tracks to component terminations. The nails or spring loaded probes in the interface are wired back to driver and receiver circuits inside the ICT equipment that translates the electrical signal[38].

As most faults on a board arise out of the manufacturing process and usually consist of short circuits, open circuits or wrongly placed components, this form of testing catches most of the problems on a board. ICT is not designed to check the functionality of the PCBA, however, this test guarantees the circuit does function, though not necessarily to its full specification[3]. The full evaluation of PCBA functionality is

done in the final assembly of CM in several FCT (Functional Testing) stations. There, more specific parameters of electrical and even software performance are tested.

Figure 22 – PCB resting on a bed of ICT “nails”[39].

The last components to be mounted are the THDs and, in BCM, they are soldered on the THT assembly line by either multi-wave or mini-wave selective soldering. The later technique was the one used to mount the THDs of the board assembled in this project.

The **selective soldering** machine consists of an inline fluxer, preheating and soldering modules. The machine is programmed with the coordinates for the TH components which are positioned on the board manually. After the PCBA is placed onto the conveyor line, it is moved to the first step of the process, flux application, where this fluid is applied by a jet fluxer that sprays it on the paths. The next step is the preheating stage where the board is gradually heated from the bottom either by infra-red short-wave radiators or hot air to activate the flux. Afterwards, the PCBA enters the soldering module that consists of a dual solder pot and top side convection heating. The electromagnetic solder bump provides a consistent solder wave that is applied to the THDs pins through a solder nozzle[40]. The board exits the machine and is then inspected by machine operators. The sequence of the selective soldering machine modules can be perceived in Figure 23.

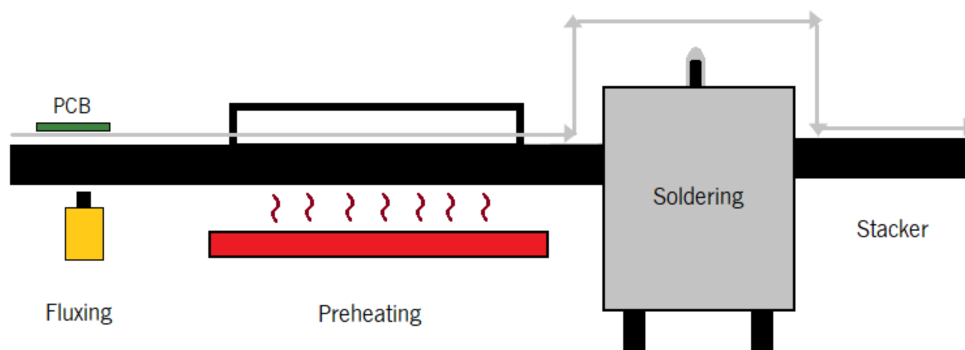

Figure 23 – Standard structure of a selective soldering machine.

If the components on the boards appear unsuccessfully soldered during inspection, the PCBA may be subjected to **rework**. Rework is done manually on an offline stand and it can be performed either SMT or THT insertion, depending on which and how many components were poorly soldered. In BCM, only PCBAs with maximum ten unsuccessfully soldered components are allowed for rework[3].

In order to remove the defective component, the solder that secures it must be re-melted with the help of a hot thermal tweezer or sometimes using a hot air pistol. In BCM, the reworked component is soldered by hand soldering using a soldering iron and a specific solder wire consisting of compatible solder alloy and a core of liquid flux. In some cases, additional flux maybe be added before the solder wire to allow a better adherence of the solder to the pad. Finally, the newly formed solder joint is cleaned with an alcohol-based solution to assure no flux remains on the PCBA[41, 42].

Typically, one of the last steps of the BCM circuit board assembly is the **depaneling** or **milling**. To increase the throughput of the PCB production, printed circuit boards are often designed to be connected to an extension of the board and even sometimes to each other via connection tabs in order to form clusters. These clusters are so called "panels" and they have to be separated during the production process into single parts, or to be "depaneled"[43]. The depaneling process, illustrated in Figure 24, is necessary so that the final PCBA can be installed on the device. Depending on the product, the panel may be depaneled right after SMT process, after ICT, after Selective Soldering of THT components, or even right before the final assembly of the PCBA into its enclosure[44].

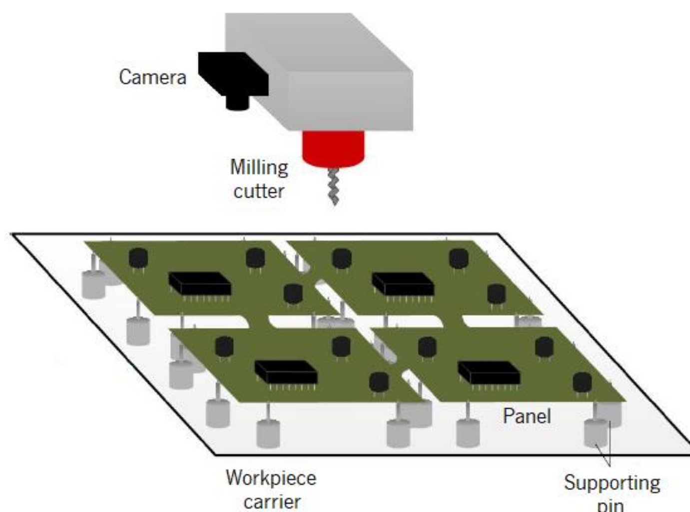

Figure 24 – Milling machine work scheme[43]

In this process, the layout of the panel and the positions of the connection tabs are inserted into a computer. The panel is positioned on supporting pins so that they can hold all separated items after being cut. The automated depaneling is carried out usually using straight or spiral tooth high speed steel milling cutters. The dust formed during milling is aspirated to avoid the presence of dirt in the PCBA[43, 45].

The PCB assembly initiates with the SMT insertion, but the order of all other assembly processes depends on the type of product made. After all this done, the final PCBA goes to an installation phase, where it is mounted in order to form the automotive support for which it was created.

2.3 SOLDERS

Soldering is defined as the process in which two or more metals are joined with the help of a melting filler material, known as solder. This solder, besides proving to be a reliable mechanical connection, is also responsible for conducting the electrical signal between the two metals. Generally composed of an alloy of metals, it must have a lower melting point than the surfaces to be soldered so that they do not melt during the soldering process. Once molten, the solder must wet the component lead and the pad, an action named ‘wetting’. Upon solidification, the resultant solder joint should provide bond strength to survive differences in thermal expansion rates of the associated component assembly[46].

In the soldering process, there are interfacial reactions between two different materials. When the solder touches the pad, two reactions take place in the interface in between solder and base material. First is the dissolution of the base material into the molten solder followed by the formation of an interfacial reaction product. An intermetallic compound (IMC) is the intermediate phase that serves as the boundary of solder and the surface of the metals with which it is in contact[47].

The IMC is a crystalline intermediate alloy phase composed of some or all the contacting metal constituents. The thin and uniform layers of IMCs represent structural bonds (metallic, ionic and covalent), between the solder and parent metals, that hold them together. For this reason, it is important that at least one of the alloy metals must be compatible with the surfaces metal. It is a hard and brittle material with a high melting-point that is electrically conducting or even semiconducting[46, 48]. The reaction between solder and substrate is of crucial importance for both the process of soldering, and for the resultant soldered joint.

For electronics production, solder is available in both wire and paste. While solder wire is normally used in hand or wave soldering, solder pastes are key materials for reflow soldering. This ‘grey paste’ is a suspension of metal alloy particles (around 90 % by weight) in a flux-containing printing vehicle (the remaining 10 %), in which the shape and size of the alloy particles and the flow properties (‘rheology’) of the flux vehicle are matched to the method used for paste application[49]. Solder pastes are classified as type 1 to 8, by the ICP J-STD-005A standard, according to its solder powder size (spheres diameter in μm). The finer the particles, the easier their passage through the printing screen or syringe, the greater the definition of the print and higher the percentage of oxide for a given oxide layer thickness[50].

2.3.1 Tin-Lead Alloys

Alloys composed of lead and tin have been widely used in the electronics industry because of its low melting temperature as well as its good wettability, mechanical and electrical properties, and relative low cost. Lead melts at 327 °C whereas tin melts at 232 °C. Tin-lead alloys form a so-called eutectic system: both alloy partners, added to one another, lower the melting point of the resultant mixture. The two descending melting point curves meet at the eutectic composition of 63 % tin/ 37 % lead, which melts at the eutectic temperature of 183 °C. They also set completely solid at that temperature when cooled down from the molten state. To either side of the eutectic, the alloys have no sharp melting point, but a melting range, which gets wider as the composition moves away from the eutectic[9, 48, 51] (Figure 25).

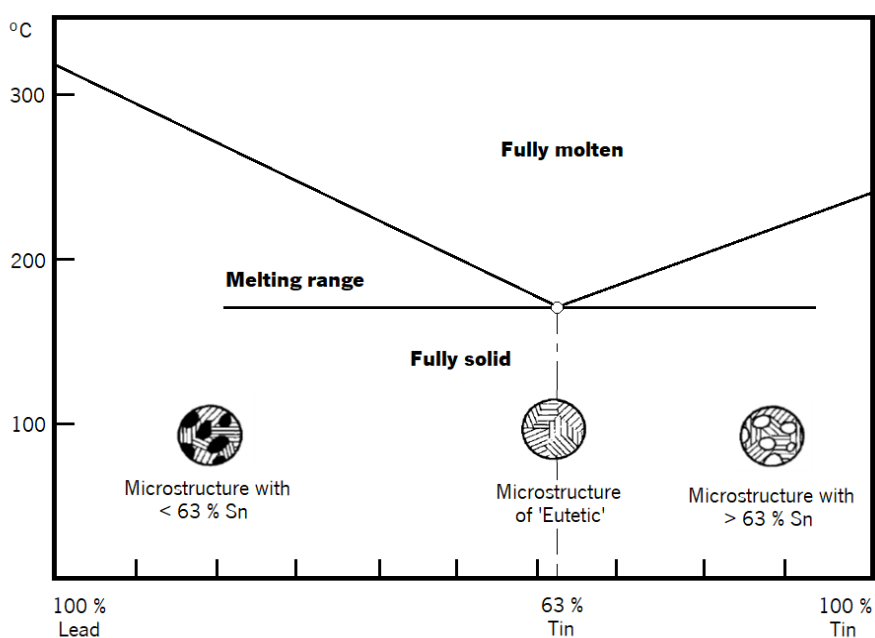

Figure 25 – Melting point diagram and microstructure of the tin-lead alloys[6].

This melting behavior is reflected in the microstructure of the solidified alloys: seen under the microscope, the eutectic itself forms a finely interlaced pattern of thin layers of tin and lead. On the tin side of the eutectic, small crystals of nearly pure tin are embedded in its microstructure; lead-rich crystals are embedded on the lead side. On heating, the eutectic always melts at the eutectic temperature, called the solidus, but the tin or lead-rich crystals do not melt until the temperature has reached the top end of the melting range, called the liquidus[6]. This behavior can be observed in Figure 25.

2.3.2 Lead-Free Alloys

Despite the vast abilities, lead had long been recognized as a highly toxic material that can cause health or environmental hazard; hence, the increasing amount of lead from electronic waste had come to pose as a threat to the environment and public health. Therefore, following the implementation of the new European environmental directives, Restriction of the Use of Certain Hazardous Substances (RoHS) and Waste Electrical and Electronic Equipment (WEEE), poisonous substances like lead, mercury and cadmium are currently banned from electronic and electrical products[52, 53].

For this reason, the demand for new lead-free alloys is a priority concern and several alloys were and still are currently being tested. Common materials in Pb-free solders are Sn, Cu, Ag, Zn, Bi, In, and Sb with other electronic materials such as Au, Co, Pt, Pd, Fe, and Al being occasionally introduced to the solder for alloying effects. Of the many lead-free solder series proposed in the last decade or so, SnAgCu or SAC alloys have emerged as one of the most promising[54].

Typical SAC alloys are composed of 3–4 % silver, 0.5–0.7 % copper, and at least 95 % tin. Differently from the eutectic tin-lead solder, the most used SAC alloy is the near eutectic SAC 305 (96.5 wt% Sn, 3 wt% Ag, and 0.5 wt% Cu). Cheaper alternatives with less silver are used in some applications, such as SAC 105 and SAC 0307, at the expense of a somewhat higher melting point[55]. SAC solders have melting points between 217 and 225 °C, roughly 35 °C higher than conventional tin-lead solders. Higher temperatures cause more stress on components and the entire manufacturing process. It also means an increase in the time it takes to make products, since more time is required to heat and cool the products during the course of their manufacture. Besides this, the increase in energy consumption may additionally pose as a problem for the electronics industry[51].

Currently, in BCM, the two most established lead-free SAC alloys are in use. SAC 405 is used in the SMD soldering process, while alternatively SAC 305 is the implemented alloy for wave and selective soldering.

2.3.3 Solders and Oxidation

Immediately after manufacturing, a thin and stable native oxide layer is rapidly formed once exposed to the environment. Metal surfaces need 'cleaning' because once a layer of these compounds forms on the surface of the metal, it causes passivity of the metal surface. The surface then becomes solder-repellent, which leads to poor wettability and poor soldering of joints on the PCB[55].

Oxidation occurs in the presence of air, and any oxidized coating will grow thicker with reflow temperatures above 200 °C. Pb-free systems, in which alloys are high in tin, and copper surfaces result in the formation of SnO (mainly), SnO_2 and CuO_2 oxides. Oxidation is affected by temperature, surface area, flux content, metal content and condition, and oxygen levels around the solder joint[31].

The size of the powder particles can worsen the oxide layer. Solder particles smaller than 20 μm have a high oxidation level. This is because as the solder powder size decreases, the surface area to volume ratio of the powder increases. The higher surface area of smaller solder powder types causes the rate of reaction to be higher than the larger solder powder types. Therefore, these types of solder powder are more susceptible to oxidation when exposed to air. In order to minimize the oxide content, the inclusion of particles smaller than 20 μm must be as low as possible[49].

Pared with surface area, metal content also has a significant role on the reflow performance of the solder paste. Some metals are more solderable than others. For instance, it is much easier to solder to a board that has a tin/lead coating on it as compared to a bare copper board. In addition to this, double sided reflow can be more difficult when reflowing the second side as the PCB has already been heated once, which may have created surface oxidation[31].

A summary of the influence of the mentioned and other unmentioned variables on the size of the oxide layer can be found in Table 2.

Table 2 – Variables that can influence the size of the oxidation layer and therefore soldering efficiency[31].

VARIABLE	VARIABLE TREND →	REFLOW RESULT
Temperature	Higher	Worse
Air velocity	Higher	Worse
Oxygen content	Lower	Better
Exposed content	More	Worse
Metal content	Non-tinned	Worse
Flux activity	Less	Worse

2.4 SOLDERING FLUX

Any non-metallic surface layer on the substrate, such as an oxide or sulfide or any contamination whatever, even if thin, prevents the formation of the intermetallic compound, and by implication prevents soldering. So effective soldering requires metal surfaces clean of surface oxide layers using a technique called fluxing, which involves the application of a reducing agent to the metal surface. While solder provides the bonding material, the purpose of flux is to enable formation of metal joints by ensuring that the metal surfaces are 'clean' of oxides at the time the metal joint is formed. Besides preventing oxidation of the metal surfaces, fluxes must dissolve the metal salts formed during the reaction with the metal oxides, protect the surface from reoxidation, promote thermal transfer to the area of the solder joint and enhance wetting of the solder on the base metal[56].

Fluxes can be provided in many ways. For surface mounting, it is delivered in a mixture with pure solder spheres, known as solder paste or solder cream. In wave soldering, a liquid flux is sprayed or otherwise applied to the secondary side of the board before the pre-heat and soldering steps. In hand-soldering, the flux can be an integral part of the solder wire, which has lumens within the wire filled with flux. As the solder melts, the flux is released to do its job[57].

2.4.1 Flux Composition

Due to the high competitiveness of the automotive market, flux chemistry is usually covered by patents. Nonetheless, its fundamental elements are known. Soldering flux formulations contain four basic types of ingredients: vehicle, solvent, activators and additives.

Of these chemicals, the vehicle and the activators are the ones involved in the fluxing function. The **vehicle** is a solid or nonvolatile liquid that coats the surface to be soldered, dissolves the metal salts formed in the reaction of the activators with the surface metal oxides, and, ideally, provides a heat transfer medium between the solder and the base metals. Among the major base materials used are rosins, resins, glycols, polyglycols, polyglycol surfactants, polyethers and glycerin[56].

The **solvent** acts as a carrier system for the solder paste. It evaporates during the pre-heat and soldering process. Alcohols, glycols, glycol ethers and water are common solvents used. It is very important to choose the right solvent or solvents blends because they affect work life and profile requirements[56, 58].

Soldering fluxes often contain small amounts of **additives** that provide specific characteristics to the flux formulation. Solder paste formulations require the presence of additives to provide good viscosity or flow characteristics, low slump during the preheat step, and good tack characteristics for holding the component in place until reflow occurs. Other example are surfactants added to enhance wetting properties. Additives may also be included to lower the interfacial surface tension between the molten solder and the PCB as it exits the solder wave, decreasing the chance for solder bridges to form[56].

Activators are not always necessary but, when applied, their purpose is to enhance the removal of metal oxides and contaminates from metal surfaces during reflow (Figure 26). They also prevent the highly reactive molten metal from reacting with the atmosphere until the metal re-solidifies. They may be reactive at room temperature, but their activity is enhanced at elevated temperatures. Among the common activators found in flux formulations are amine hydrochlorides and halide-free acids such as dicarboxylic acids (e.g. adipic or succinic) and other organic acids (e.g. citric, malic or abietic). Activators containing halide and amine give excellent soldering yields, however, they may cause reliability problems if not properly removed. For this reason, the PCBAs may be subjected to an additional process after soldering, the cleaning process, also known as de-fluxing, in cases where the flux used is an highly active one[56].

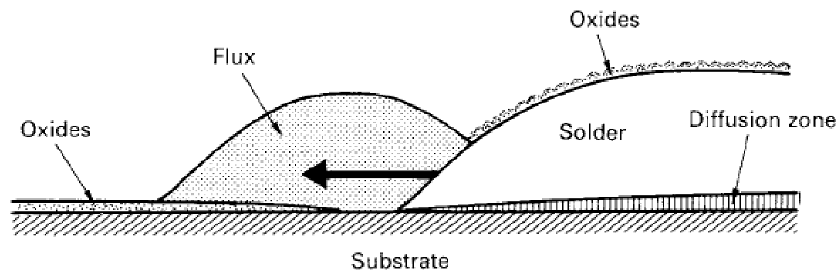

Figure 26 – The function of fluxing agents in soldering[6].

In the present day, two flux categories are in widespread use for PCB assembly: water-clean and no-clean. The former contains the most aggressive fluxing agents and leaves a residue that must be removed from the PCA, otherwise, corrosion will set in. No-clean flux, as the name implies, leaves a benign residue that is meant to be left on the circuit board and that can serve as a shield from moisture and atmospheric contaminants. Both can be effective oxide strippers for soldering but the choice between this flux categories has a profound effect on the process and may also affect subsequent process steps or long-term reliability. Although the trend of the industry is gradually shifting towards the no-clean process, a considerable part of the industry still applies cleaning to soldered PCBAs[57].

2.5 CONTAMINATION ON PCB ASSEMBLY

Understanding the mechanics and chemistry of contamination has become necessary for improving quality and reliability and reducing costs of electronic assemblies even more so at present days where smaller electronic devices are in increasing demand. Miniaturization requires a higher electronic density of the PCB, implying changes in soldering materials and components. Changes like the decrease of pad size, fine pitches or the use of package-on-package components increase the fragility of solder joints. Furthermore, changing from Sn-Pb solders to lead-free solders resulted in lower wetting and higher processing temperatures. All these conditions can contribute to introduce more contamination factors that need to be studied and controlled[59, 60].

2.5.1 Types and Sources of Contamination

Nearly every operation that a printed circuit undergoes from the time it reaches the assembly plant to the time it leaves can introduce contamination, either by being subject to, at best, fingerprints or glove marks or, at worse, a large number of aggressive contaminants. The origin of contamination on the printed circuit boards can usually be attributed to the manufacturing processes or to the operating environment. The latter is difficult to predict due to the widespread application of electronics, nevertheless, it can be controlled to a significant extent by proper encapsulation. The key factor for long-term reliability therefore becomes cleanliness levels obtained during the PCB manufacturing and assembling processes[60].

The board fabrication process, especially the drilling or plating of the layers, along with environmental exposure, can leave residues such as particulate residues, oils, salts and dust, thus manufacturers must ensure no contaminants were left over from previous steps in the production process. Copper etching liquid, water-soluble soldering chemistry and other kinds of aggressive chemistry from PCB assembly processes can also leave behind residues that change the board's conductivity when not cleaned properly. However, the most contaminating process used for PCB fabrication is the application of solder, mainly because of fluxing[59–61].

Contamination can have ionic (organic or inorganic salts), and nonionic origins (organic, hydroscopic substances as polyethylene-glycol from fluxes, fibers from clothes, hair, dust). Of all contamination sources that can affect PCBAs, the most worrisome is the contamination caused by ionic species. An ionic residue can become conductive when exposed to moisture and move on the board provoking short circuits. A PCBA can also have nonionic contamination however as nonionic residues do not have conductive properties, they can usually remain on the board after production and assembly. For that reason, most manufacturers focus on ionic contamination when examining a board's cleanliness[61, 62].

2.5.2 Electrochemical Migration

Achieving high reliability is the vital issue in today's electronic assemblies. As the electronic density on PCBAs increases and the space between conductive surfaces decreases, the elimination of ionic contaminants becomes crucial for PCB's reliability. Ionic residues are corrosion accelerating factors as most of them are hygroscopic and therefore cause water adsorption to the surface. When an electric current is applied, electrochemical reactions such as electrolysis may occur, involving water molecules and other species as conductive metals[60, 63]. In Figure 27, the variables that induce electrochemical failure are represented.

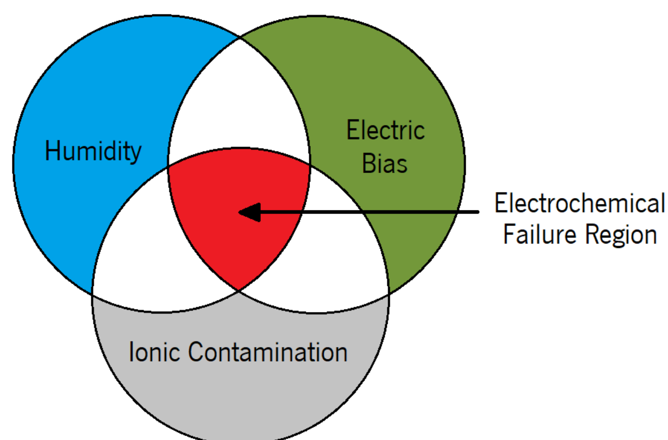

Figure 27 – Veen diagram showing the conditions for occurrence of electrochemical failure.

Electrochemical migration (ECM), a typical form of corrosion found in electronic systems, is defined as the growth of conductive metal filaments on a printed circuit board through an electrolytic solution under the influence of a voltage bias. In general, higher moisture, voltage gradient and temperature, as well as narrower spacing, cause faster migration rates and greater damage caused by electrical shorts[64].

The ECM phenomena happens when an electric field is applied, and a voltage is established between two neighbor terminals or paths in a humid environment. These terminals begin to behave like two electrodes, anode and cathode. The process is initiated at the positively charged conductor, the anode, where metal oxidation occurs. This enables the metal ions to migrate to the cathode through the isolation region. When they reach the negatively charged conductor, the ions are reduced to metal and deposited there, forming filaments. The metal filaments, by the name of dendrites, can extend from the cathode to the anode and eventually trigger a short circuit[65, 66]. A visual rendition of this mechanism can be found in Figure 28.

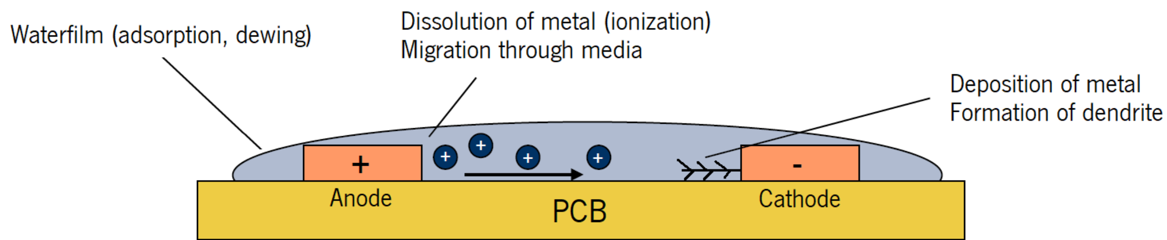

Figure 28 – Scheme of dendrite formation[67].

As water electrolysis occurs, a pH gradient forms on the board surface. At the anode, as concentration of H^+ growths, the pH decreases thus increasing the metal ions solubility and, conversely, at the cathode, the medium becomes more alkaline[66]. Silver is the metal most susceptible to migration since it is highly soluble in cationic form and requires lower activation energy to initiate the migration process. Other metals on a PCBA such as Sn, Pb, and Cu are also susceptible to ECM as they are easily oxidized. Still, some of these conductive metals, such as Au, Pt and Pd only oxidize in the presence of contaminants with greater oxidizing power, such as bromide, chloride or iodide[68].

The chemical reactions for anode metal dissolution and water decomposition are described below[65]:

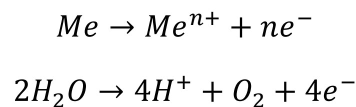

$$Me \rightarrow Me^{n+} + ne^-$$

$$2H_2O \rightarrow 4H^+ + O_2 + 4e^-$$

The chemical reactions for cathode metal deposition and water decomposition are described below[65]:

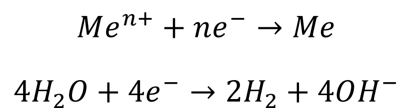

$$Me^{n+} + ne^- \rightarrow Me$$

$$4H_2O + 4e^- \rightarrow 2H_2 + 4OH^-$$

Dendrite growth is one form of ECM, but other structures called conductive anodic filaments (CAFs) can also be formed in this phenomenon. CAFs, like dendrites, are filaments formed as metal leads which become ionized and begin to migrate. However, contrary to dendrites, CAFs grow from the anode to the cathode within the PCB and not on the surface. CAFs composition also differs from dendrites, being constituted by metallic salts instead of neutral metal atoms. The formation of CAFs or dendrites is a significant failure mode in electrical and electronic systems, particularly in microelectronic components on PCB and electronic packages[69, 70].

2.5.3 Cleanliness and Process Control Methods

To ensure that ionic residues do not reduce the lifespan of the PCBA, the boards' cleanliness must be regularly evaluated during the manufacturing process. Resistivity of solvent extract (ROSE) test and ion chromatography (IC) are the most used methods for measuring the level of ionic contamination and evaluating the cleanliness of the PCBs. Moreover, surface insulation resistance (SIR) test is being established as a fundamental technique for cleanliness evaluation since it accelerates failure mechanisms in the presence of contaminants, predicting the reliability of PCBAs and the interaction between materials (namely solder pastes/ fluxes)[71, 72]. The IPC has standardized these three techniques as essential test methods as can be consulted in IPC-TM-650 2.3.25, 2.3.28 and 2.6.3.7.

Developed in the 1970s, the **Resistivity of Solvent Extract (ROSE)** test was the first method available to determine ionic contamination levels. It still is in use today, in a modernized version. It is typically employed as a quality control tool in the manufacturing of PCBAs and its primary aim is to check for remaining, easily soluble residues from products that have undergone a cleaning process. When conducted by a capable and experienced technician, ROSE testing can effectively analyze and detect any failures or unintended ionic residues resulting from the various manufacturing processes[73].

Ion extraction techniques can be either manual, dynamic or static and the procedures for performing these tests are detailed in the IPC Test Methods Manual, under IPC-TM-650 2.3.25. In this thesis, the extraction method used was the static one and Figure 29 is a representation of its mode of operation. This extraction technique measures ionic residues, or ions, by immersing PCBs into a tank filled with an isopropanol/deionized water solution and dissolving and extracting their ionic content. The resistance of the solution is measured by applying an electric current in a conductivity cell. After each measurement, the extraction solution passes through an ion exchange column where it is regenerated using a resin capable of capturing ions[74, 75].

In general, salts with a high ionization potential give a rapid rise in conductance as the concentration increases. Others with weaker ionization potential like organic acids give weaker responses. ROSE test does not discriminate the type of ions present, so all results are expressed as sodium chloride equivalent ($\mu g/cm^2$ NaCl eq.). This test treats all ionic effects on conductance as if all ions were originated by NaCl dissolution[76].

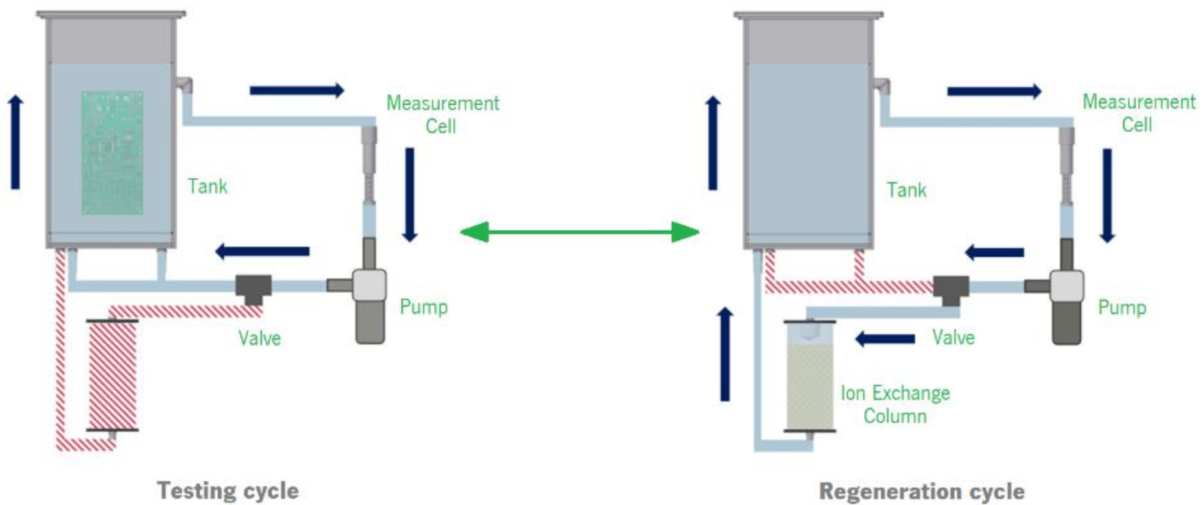

Figure 29 – Measurement principle of the ROSE method in testing (left) and regeneration (right) mode[67].

Since ion contamination is one of the main factors of PCBA failure, PCB buyers demand process audits to the supplier and regular ionic contamination inspections. PCB manufacturers do intensive rinsing processes after final finishing to ensure that the reactive process chemicals are thoroughly removed. Following IPC-6012DA, bare PCBs for automotive applications must leave the manufacturer with a maximum ionic contamination value of 0.75 µg/cm² NaCl-equivalent[77].

As seen before, the boards' assembly causes the biggest source of ionic contamination by the combination of many different materials as well as by the multiple different processes. The acceptance criteria of ROSE test method for cleaned PCBAs was 1.56 µg/cm² NaCl-equivalent in former years. The 1.56 value was decided by US authorities to implement in standards as reliability threshold. This one- fits-all limit, however, became obsolete over time as studies show there are no guaranteed value that excludes any ECM failure[77, 78].

This is especially true when measuring uncleaned boards. As Bosch is following a no-clean philosophy for nearly all products, no water or solvent based cleaning and rinsing steps are applied at the end of the assembly on the electronic unit (except for very few specific molding and bonding applications). Given that all those contaminants may remain on the PCBA due to the no-clean approach, no international accepted and single value for ROSE-testing is available and it is up to each producer to define their limit[77-79].

The ROSE method is quick and very easy to conduct, and these characteristics contribute to its importance in process control. Weaknesses of this method include its inability to determine the exact

ionic species of the contaminants and the localized ionic contamination level for a certain portion of the board[64]. For this last reason, it can only be used as a process control method and, with no other supporting objective evidence, cannot be considered an acceptable basis for qualifying a manufacturing process[79].

Alternatively, **Ion Chromatography (IC)** is the most common tool for precision testing and process base lining. This method separates, identifies, and quantifies specific ionic species present on an electronic device. This is a more vigorous analytical method than ROSE test as it enables a trained scientist to determine the exact source of ionic contamination[72].

IC and ROSE are both chemical analytical methods designed to determine what chemical ions are present and in what amounts. The question often remains on what effect those ionic materials have on electrical performance and what is the best way to demonstrate acceptable or unacceptable electrical performance. The **Surface Insulation Resistance (SIR)** test determines the corrosive effects of fluxes, the effect of conformal coatings, and cleaning materials. SIR testing also characterizes the material's resistance for avoiding short circuits[80].

SIR testing consists of an electrical test that measures the resistance between two surface conductors, separated by a dielectric material, in response to an electrical bias in a humid environment. The presence of contamination lowers the insulation resistance of the material between the conductors[71]. This test takes a minimum of 72 hours and can detect the presence of ionic contamination, but cannot pinpoint the type of contamination, or its degree. As a result, SIR test is mostly used as a R&D tool as it is not attractive for today's high-mix, high-speed, and high-volume production lines unless used as spot-check backup method for use with faster in-line quality control testing procedures[81].

Studies show that neither of these tests alone can guarantee a trustworthy acceptance/failure cleanliness system. SIR test conditions are too aggressive and mostly do not represent the actual conditions PCBAs are submitted to during service life. Ionic evaluation tests give us a general value of contamination but cannot provide information regarding localized concentration levels. Besides this, high contamination does not necessarily mean dendrite formation considering that research works have demonstrated that some assemblies with more than 3 μg NaCl-equivalent/cm^2 did not display ECM[78]. Consequently, ROSE tests should be complemented with techniques like IC to determine the nature of the ionic contaminants and SIR to verify the impact of these contaminants on the reliability of the PCBA.

CHAPTER 3 **EXPERIMENTAL**

This chapter describes the methodologies implemented for the development of this dissertation. Throughout the section, it will be presented the materials used and the experimental procedures adopted for sample preparation, as well as a detailed description of the characterization methods performed to the PCB and PCBA samples. All the work for this study, from the samples production to the data analysis, was conducted in Bosch Car Multimedia Portugal, located in Braga.

3.1 THESIS APPROACH

Before initiating the objectives of this project per se, scrapped PCBs were analyzed in order to establish ROSE base-levels for general CM products. Only then the consistency of the ROSE machine's response was evaluated, using a standard addition method. It was important to study this because, even though this technique was already studied in other Bosch units, this is not an established method for cleanliness assessment at BCM and other CM divisions. Posteriorly, two seemingly influential factors of the machine's response were chosen, and a design of experiment (DOE) was conducted. Figure 30 illustrates the steps taken to understand the ROSE method.

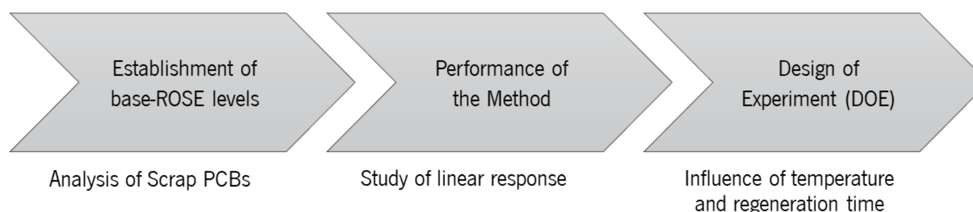

Figure 30 – Scheme of the tests performed to study the ROSE method.

The main purpose of this thesis was to study the progression of ionic contamination along the production of PCBAs using the ROSE technique. For this intent, a product family currently being manufactured at BCM was selected and its production plan examined. Five different stages of production were chosen, and the test vehicles were collected. These phases included the bare board after laser marking, SMT insertion of the bottom and top sides of the panels, rework and the finished PCBA after selective soldering the THDs. Figure 31 shows all the stages where the PCBs were collected as well as the steps necessary to perform each stage.

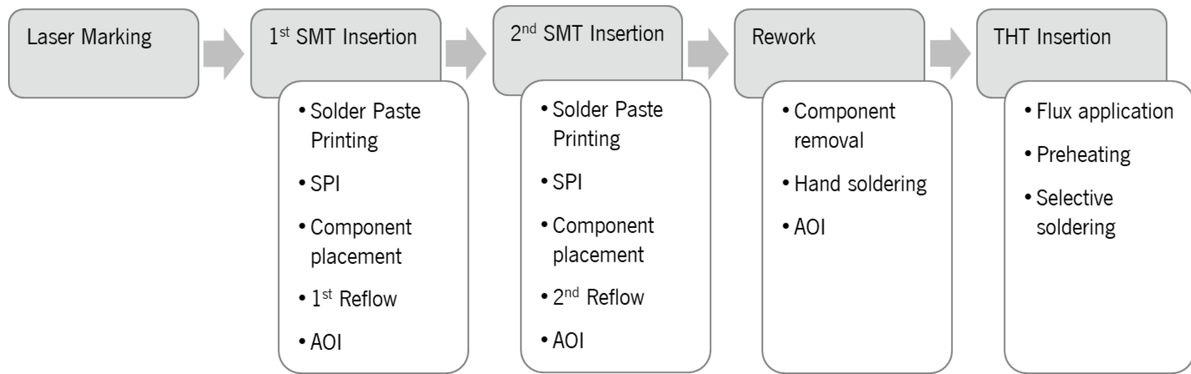

Figure 31 – Plan of the 5 stages of production where the test vehicles were collected to evaluate its surface contamination with the description of the various steps performed in each stage.

In this study, twelve boards were collected in the beginning right after laser marking. Other twelve PCBs were collected from the first SMT insertion after solder paste reflow and AOI inspection of the bottom side of the board and fourteen PCBs were collected after the second SMT insertion. The PCBAs followed a normal production run up until the 2nd reflow and AOI inspection, after which six of the boards were sent directly to selective soldering stage and forty to an offline rework station. This last panels were subjected to two different rework practices, after which, six boards from each method were delivered to the final stage, selective soldering. Boards that arrived at the last stage of the assembly process had to be submitted to an ICT and milling stage. A total of 84 boards were later analyzed for their ionic content using the ROSE test contaminometer. Figure 32 shows the plan described for this last part of the thesis.

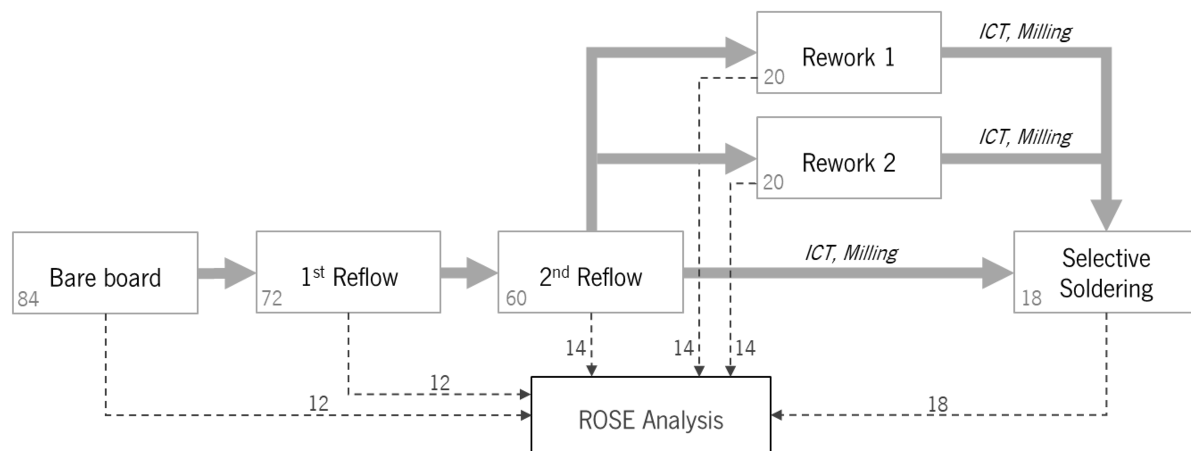

Figure 32 – Framework of the analysis plan of the test vehicle describing the amount of PCBs subjected to and collected from each stage of the production.

Five components per PCB were reworked using two different practices. Twenty boards were amended using only cored solder wire (rework 1) and other twenty were reworked by adding an extra flux before soldering with the cored wire (rework 2). This allowed us to have a better understanding of the

surface contamination the rework process adds to the board compared to boards that do not need any rework. Additionally, in order to comprehend the role of post-rework cleaning, two PCBs for each practice were not cleaned after being reworked. From the eighteen of the cleaned boards, only six were sent through the ICT and milling machines so that they could have their TH component soldered in the selective soldering stage. Figure 33 sums up schematically what was explained.

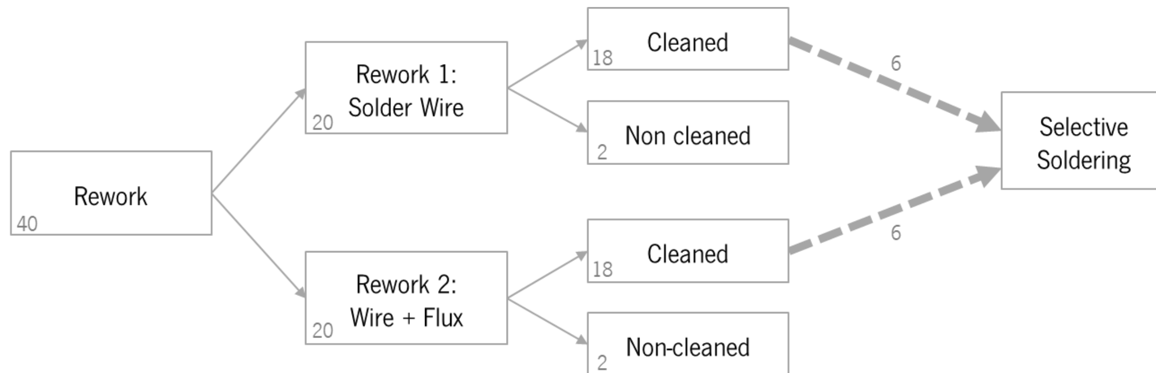

Figure 33 – Squeme of the rework stage plan detailing the amount of boards that passed through each step.

It is important to notify that each panel of the product chosen for this study contains two PCBs so, when analyzing one panel on the ROSE contaminometer, we were testing the contamination of two boards instead of just one. We only analyze the contamination of an individual PCB after it reached the selective soldering stage, following milling, where the boards were released from their frame.

3.2 Materials

3.2.1 PCB

The PCB chosen for this project was the Bombardier Compact supplied by Dynamic Electronics Co, Ltd. The PCB design, composed by a FR-4 base, Cu layers, solder mask layers and an OSP surface finish, is displayed in Figure 34. The layout of the board was designed at BCM to mount on Bombardier vehicles. This product is one of the current PCBs being assembled at the BCM production plant.

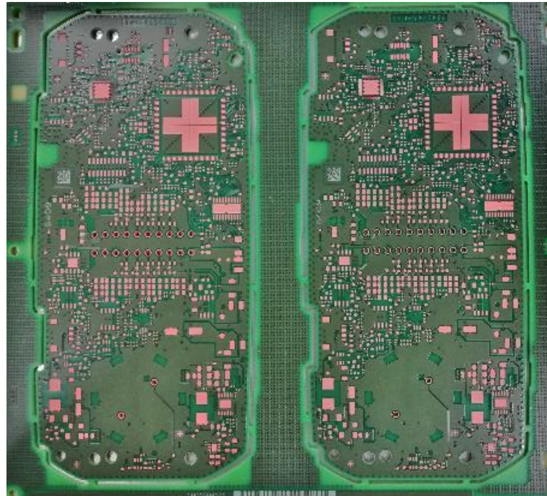

Figure 34 – Layout of the top side of the board used for sample production, the Bombardier Compact. This PCB had dimensions of 185 x 165 x 1.55 mm, an OSP surface finish, and each panel had two PCBs incorporated.

3.2.2 Solder Paste

A no-clean lead-free solder paste was used for the PCBs and PCBAs, the type 3 SAC 405 produced by Heraeus Group (F620 series). This solder paste is the one presently being used in the SMT insertion line. Table 3 describes some of the properties of the mentioned solder paste.

Table 3 – Features of the lead-free solder pastes used in this work.

SOLDER PASTE	SOLDER ALLOY	GRAIN TYPE	POWDER SIZE (µm)	METAL CONTENT (%)	MELTING POINT (°C)	ATMOSPHERE
Heraeus F620	SAC 405	3	25 – 45	88,0 ± 0,5	217 – 219	Air or N_2

3.2.3 Solder Wires

The rework of the Bombardier board required the use of a SAC 305 Multicore C511 no-clean cored solder wire supplied by Henkel-Loctite while SAC 305 Telecore HF-850 solder wire produced by Alpha was used for selective soldering. Both wires traits are presented below in Table 4.

Table 4 – Characteristics of the solder used for selective soldering the THT components.

SOLDER	SOLDER ALLOY	FLUX CONTENT (%)	HALIDE CONTENT (%)	ACID VALUE (mg KOH/g)	MELTING POINT (ºC)
Multicore C511	SAC 305	2.7	1.1	164 – 176	217
Telecore HF-850	SAC 305	2.2	-	180 – 200	217

3.2.4 Soldering Flux

For Bombardier Compact assembly, the same flux was used for both rework and selective soldering, the Cobar 94-QMB distributed by Cobar Europe BV. The properties of this low-VOC wave soldering flux are described in Table 5.

Table 5 – Properties of the flux used for selective soldering the THT components.

FLUX	DENSITY (kg/dm³)	SOLIDS CONTENT (% w/w)	WATER CONTENT (% w/w)	VOC CONTENT (% w/w)	ACID VALUE (mg KOH)
Cobar 94-QMB	0.847	2.48	21.00	76.00	15.94

3.3 Test Vehicles Assembly Processes

In order to study the progression of ionic contamination along PCBA production, it was essential to monitor the production of a PCB regularly assembled in this factory. For this study, the Bombardier Compact samples were produced in a BCM lead-free production line just as this product typically would be, with the same type of materials, components, procedure and soldering parameters.

The processes mentioned in this subchapter were already explained in 2.2.4. All the machine configurations were defined within the allowed limits established by BCM Process Rules for Production. The products were kept and transported along all these processes in metallic ESD containers.

3.3.1 SMT Insertion

The SMDs of the Bombardier Compact board were assembled on a standard BCM SMT line. Firstly, laser marking was done on an online machine (ASYS Insignum 4000), where 2D barcodes were printed on the test boards for traceability.

Solder paste printing was performed on EKRA Serio 5000 machine. An electropolished stainless steel stencil (supplied by Christian Koenen GmbH), with 125 µm thickness was used and Solder Paste Inspection (SPI) was carried out on a Koh Young aSPIre3 machine.

Next, the placement of the SMDs was accomplished in Panasonic NPM-W2 machines. Reflow process was performed in a Rehm VisionXP nitro 3500 (Typ 734) oven using 10 heating zones and 4 cooling zones. To evaluate the effectiveness of the assembly process, an Automated Optical Inspection (AOI) was then performed in a Mirtec MV-9DL.

3.3.2 Rework

The substitution of certain components by rework was completed on an offline station by a qualified operator. Five components per module, shown in Figure 35, were replaced using two rework procedures mentioned in subchapter 2.2.4. To achieve this, the worker operated with a Metcal hand soldering kit containing a MX-H1-AV iron, a MX-PTZ thermal tweezer and a tipsaver workstand to clean the iron. The temperature setting on the manual soldering iron was around 350 °C. After soldering, a 90 % IPA / 10 % ethylene glycol solution was applied on the joint using a brush. A Linx EVO optical microscope was used as an auxiliary tool for visual aid. Finally, the PCBs were then inspected in a Viscom S6056 AOI machine.

After SMT insertion and rework, the 18 PCBs that needed a THD insertion had to pass through an ICT machine in order to assure that there is no design or component placing errors. This test was done using an offline Tri Innovations TR5001.

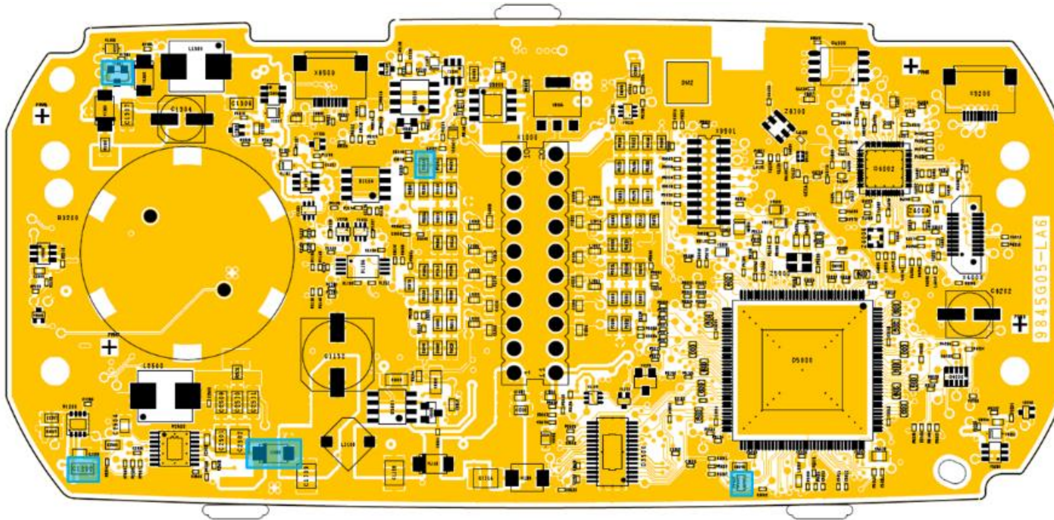

Figure 35 – Position of the five components (marked in blue) substitued in rework on the top side of the Bombardier Compact board.

3.3.3 THT Insertion

For this specific product, the panel milling is done before selective soldering the THDs. This was accomplished on a separated milling machine, which consists of the Grohmann HOC-202B depanelling machine, where the modules were released from the frame, stored in ESD plastic bags individually and placed on an UTZ RAKO container.

The THDs of the Bombardier Compact board were assembled in a different BCM section on a standard THT line. The frameless PCBs were inserted in groups of six on a Myselective 6745 selective soldering system supplied by Vitronics Soltec and subjected to a solder wave at a temperature of 300 °C. The finished PCBA is displayed in Figure 36.

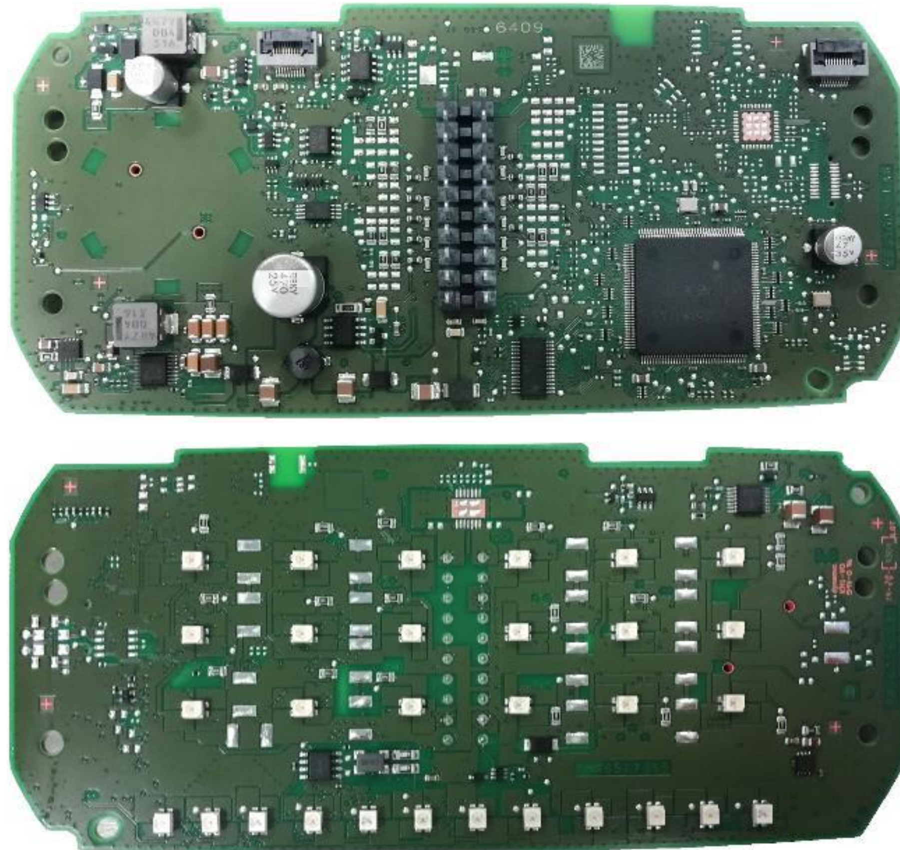

Figure 36 – Top and bottom sides of the finished Bombardier Compact PCBA sample, assemblied at BCM.

3.4 ROSE TEST PROCEDURE

ROSE tests were performed at CM/MFT3 laboratory, in Bosch Car Multimedia (Braga), on a CM22 contaminometer supplied by GEN3 Systems Limited. The operation of the equipment and the analysis procedure used was established beforehand by Bosch's internal document AnP/QMM8 based on IPC-TM-650 2.3.25.

Prior to testing, the tank of the contaminometer must be properly filled with the solvent mixture (50/50 vol% IPA/DI-water). After switching on the device, some procedures must be completed daily before performing the measurements. First, it is necessary to measure the temperature of the extraction bath and compare it with the one displayed on the software; then, the density of the bath is measured, and the volume of the tank is readjusted if necessary. Finally, the equipment is tested by adding 2 ml of a 0.1 wt% NaCl solution to the tank.

For the sample analysis, the area of the PCBs needs to be inserted onto the CMxxSE software. They were calculated by measuring either manually or by AutoCAD software (in the case of frameless PCBs), and then applying the area modificators figured in Table 6. The test time for each sample was 15 minutes, with 5 minutes blank measurements in between sample analysis to regenerate the extraction bath and ensure there was no residues left from previous samples.

Table 6 – Expressions for the calculation of PCB area[82].

PCB	ADDITIONAL AREA (%)	EFFECTIVE AREA
PCB bare board	-	Length PCB × Width PCB
SMD population, one-sided	15	Length PCB × Width PCB × 1.15
SMD population, two-sided	30	Length PCB × Width PCB × 1.3
SMD population, one-sided, single THT-Elkos	25	Length PCB × Width PCB × 1.25
SMD population, two-sided, single THT-Elkos	40	Length PCB × Width PCB × 1.4
SMD population, one-sided, single THT-Elkos, connector	35	Length PCB × Width PCB × 1.35
SMD population, two-sided, single THT-Elkos, connector	50	Length PCB × Width PCB × 1.5

3.5 ROSE STUDIES METHODOLOGY

3.5.1 Study of Base-ROSE Levels for CM Products

Before analyzing the test vehicle, it was important to determine the standard ROSE values for custom CM PCBs. For this, over 100 scrap PBCs were analyzed on their ionic content on the CM22 contaminometer. These PCBs were collected in various stages of SMT production line after suffering some sort of fabrication error and being scrapped. Most of these errors were due to poorly printed paste, misplaced components, soldering sorts, among other errors. One of the products analyzed is shown below in Figure 37.

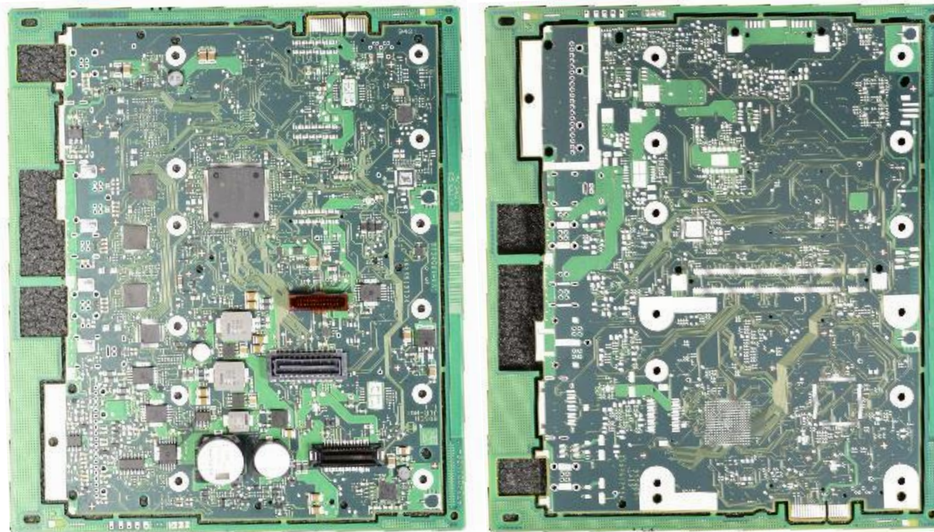

Figure 37 – Top (left) and bottom (right) side of one of the boards analyzed. This PCB had dimensions of 185 x 160 mm, an ImSn surface finish and solder paste and components only on the top side.

3.5.2 ROSE Method Performance Tests

In order to further develop this study, it was essential to evaluate the linearity region of the ROSE test. For this, a standard addition method was developed using Benchmarker II test boards (Figure 38). The Benchmarker II used in these tests are very simplistic with no complex design elements. They were designed for solder paste performance studies and are not intended for production.

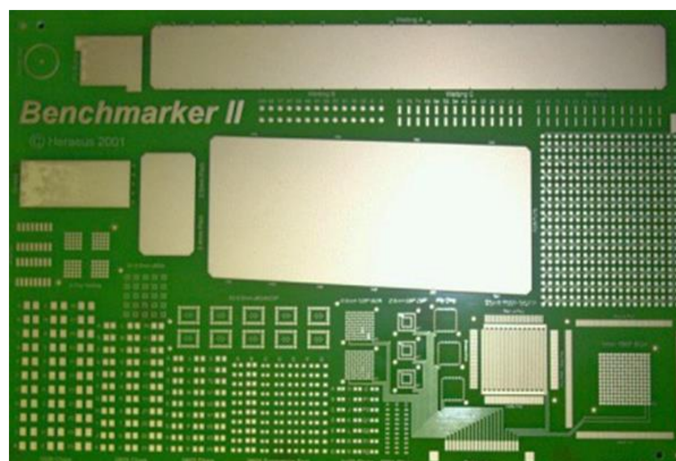

Figure 38 – Benchmarker II test board. It has 190 x 127 mm in dimension, an ENIG surface finish.

From a sodium chloride stock solution, with a concentration of 2510 ± 15 ppm, 5 different volumes between 48 to 965 μl were added to the boards surface using an Eppendorf micropipette. So that to

define the Benchmarker II ionic content, 5 bare boards were analyzed without NaCl addition. All the boards were dried for two hours on a stationary oven at a temperature of 50 °C. Additionally, two temperature ranges of the extraction bath were used (20 to 22 °C and 23 to 25 °C), forming two standard addition lines, to monitor the effect of the temperature of the extraction bath.

3.5.3 Design of Experiment (DOE)

The ROSE analyses earlier done suggested there were two factors that may influence the response of the machine: the temperature and the regeneration time of the contaminometer extraction bath. These were the factors considered for this DOE. Each factor was tested in three levels; the temperatures studied were: 24, 25.5 and 27 °C, and the times of regeneration were: 1, 5 and 10 minutes. Table 7 summarizes the DOE matrix.

Table 7 – DOE parameter matrix for the contaminometer's response analysis.

FACTORS		LEVELS			RESPONSE
		-1	0	1	
A	Temperature – T (°C)	24.0	25.5	27.0	µg/cm² NaCl equivalent
B	Regeneration Time – t_{reg} (min)	1	5	10	

These factors were studied by direct addition of 100.0 ± 0.2 µl of a 2510 ± 15 ppm NaCl solution to the ROSE contaminometer tank, establishing a fictional PCB area of 2500 mm². NaCl was added directly to the extraction bath in order to verify the linear response of the device in a controlled manner, in order to eliminate the background variation caused by the contamination of the boards.

3.5.4 Regeneration Time Tests

Additional tests were done to study the influence of the regeneration time alone on the contaminometer readings. A product used in prior CM/MFT3 studies was used this time, the Renault IVI board (exhibited in Figure 39).

Figure 39 – Top (left) and bottom (right) side of the Renault IVI PCBA. This PCB had dimensions of 185 x 167 mm, an OSP surface finish and is one of the boards presently produced at BCM.

Thirty-six boards were analysed on the CM22 contaminometer and were subjected to a 15-minute analysis and a regeneration time of either 1, 5, 8 or 10 minutes (nine samples per condition). It is important to mention that the Renault IVI boards were assembled in mid-2019 for a department project and had been keeped inside a container since then, so they may not be in the same conditions of a newly assembled PCBA. However, this difference did not interfere with the analysis since all the batch was in the same storage conditions.

3.5.5 Studies of Contamination in the PCBA production process

The main goal of this dissertation was to understand what stages of PCBA production increase ionic contamination on the surface of the boards using an ionic contamination technique called the ROSE test. For this intent, the Bombardier Compact, currently manufactured at BCM, was selected and its production plan (explained in detail in section 3.3) examined. Five different stages of production were chosen to analyze the panels' ionic content. The boards were collected after laser marking, SMT insertion of the bottom and top sides of the panels, rework and, at last, after selective soldering of the THDs.

All boards were analyzed on the CM22 contaminometer according to the procedure of section 3.4, established by Bosch-AE. Most of the areas inserted in the contaminometer software were calculated manually apart from the area of the frameless selective soldering samples, that was calculated using AutoCAD program.

CHAPTER 4 RESULTS AND DISCUSSION

This chapter presents and discusses all the results obtained throughout the development of the experimental work. It is divided in two parts, the first one is related to the study of ROSE test and the experimental parameters of the CM22 ROSE test contaminometer, while the second part is focused on the characterization of ionic contamination during Bombardier Compact production and on the influence of the different production processes on ionic surface contamination.

4.1 STUDY OF CONTAMINOMETER RESPONSE

4.1.1 Parameter Selection

Before the DOE realization, a study of ROSE base levels for CM products was conducted. These series of analysis were done in order to establish mean ionic contamination levels for general CM boards produced here at BCM. For this, defective PCBs from the SMT line were collected and analyzed on the CM22 contaminometer. Figure 40 displays the principal defects of the more than 100 scrapped PCBs collected during the assembly of components on either the first side or second side of the boards.

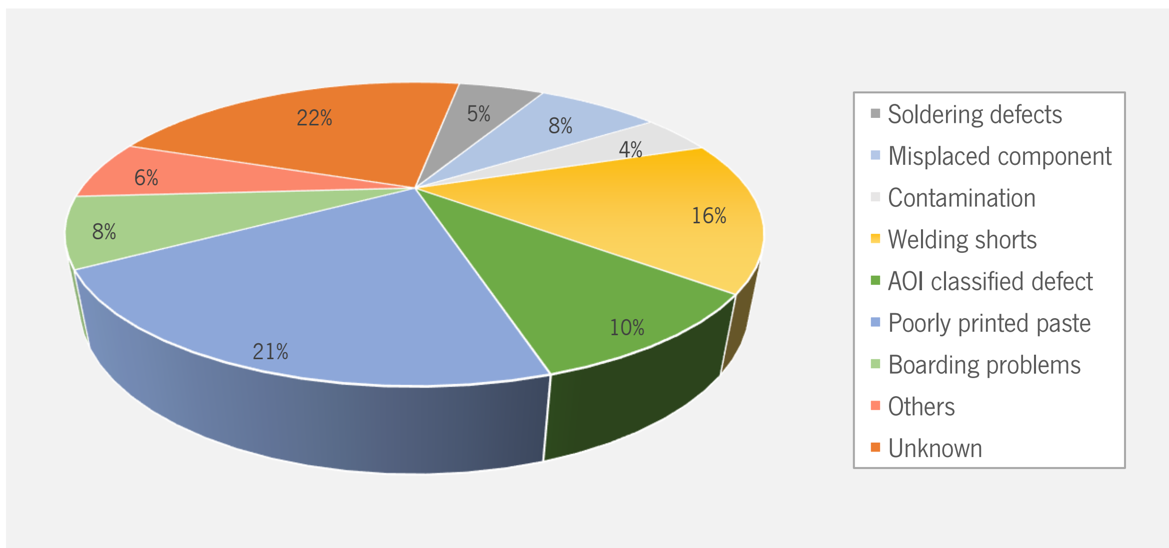

Figure 40 – Pie chart of the main type of defects the scrap PCBs endured.

The SMT insertion is automatic but not infallible, as it can be seen in Figure 40. A large part of the boards collected (around 21 %) experienced paste printing errors, either for excess or insufficient paste or off-center paste. Other frequent errors happen during reflow namely soldering shorts, non-conform soldered components and other defects detected posteriorly on AOI. The remaining 22 % of the boards suffered unspecified assembly errors.

These boards were later analyzed on a ROSE test machine. Table 8 and Table 9 summarized the contamination results of the panels collected on their first and second SMT insertion, respectively. Defective boards of the second SMT insertion were in less quantity since, as they have more components, the operator sends them to the rework station to fix the error (in the case of products liable to rework).

The PCBs were organized according to their respective family of products. The product family number shown in both tables is only a reference to allow a better organization of the data of this thesis. This just means that PCBs with the same family number share the same dimensions, components and layout.

Table 8 – Area (in mm^2), and individual and mean ($\bar{x}$) values of ionic contamination (in µg/cm^2 NaCl eq.) of the scrap PCBs collected during their first SMT insertion organized according to the surface finish and the product family number.

<table>
<tr><th>SURFACE FINISH</th><th>PRODUCT FAMILY NO.</th><th colspan="6">MEASURED VALUES (µg/cm^2 NaCl eq.)</th><th>$\bar{x}$ (µg/cm^2 NaCl eq.)</th><th>AREA (mm^2)</th></tr>
<tr><td rowspan="9">OSP</td><td>1</td><td>0.639</td><td>0.770</td><td>0.733</td><td>0.710</td><td>0.681</td><td>0.920</td><td>0.742</td><td>28721</td></tr>
<tr><td>2</td><td>0.487</td><td></td><td></td><td></td><td></td><td></td><td>0.487</td><td>33528</td></tr>
<tr><td>3</td><td>0.390</td><td>0.485</td><td></td><td></td><td></td><td></td><td>0.438</td><td>35190</td></tr>
<tr><td>4</td><td>0.626</td><td></td><td></td><td></td><td></td><td></td><td>0.626</td><td>43792</td></tr>
<tr><td>5</td><td>0.632</td><td></td><td></td><td></td><td></td><td></td><td>0.632</td><td rowspan="2">31395</td></tr>
<tr><td>6</td><td>0.616</td><td></td><td></td><td></td><td></td><td></td><td>0.616</td></tr>
<tr><td>7</td><td>0.606</td><td>0.563</td><td></td><td></td><td></td><td></td><td>0.585</td><td rowspan="3">37231</td></tr>
<tr><td>8</td><td>0.635</td><td></td><td></td><td></td><td></td><td></td><td>0.635</td></tr>
<tr><td>9</td><td>0.584</td><td>0.544</td><td>0.542</td><td></td><td></td><td></td><td>0.557</td></tr>
<tr><td rowspan="6">ImSn</td><td>10</td><td>0.415</td><td></td><td></td><td></td><td></td><td></td><td>0.415</td><td>51060</td></tr>
<tr><td>11</td><td>0.876</td><td></td><td></td><td></td><td></td><td></td><td>0.876</td><td>34040</td></tr>
<tr><td rowspan="2">12</td><td>0.583</td><td>0.587</td><td>0.690</td><td>0.696</td><td>0.769</td><td>0.607</td><td rowspan="2">0.594</td><td rowspan="2">34040</td></tr>
<tr><td>0.562</td><td>0.432</td><td>0.508</td><td>0.473</td><td>0.564</td><td>0.655</td></tr>
<tr><td>13</td><td>0.376</td><td>0.352</td><td>0.336</td><td>0.382</td><td></td><td></td><td>0.362</td><td>31913</td></tr>
<tr><td>14</td><td>0.439</td><td>0.425</td><td>0.339</td><td>0.290</td><td>0.426</td><td></td><td>0.384</td><td>34040</td></tr>
<tr><td rowspan="4">ENIG</td><td>15</td><td>0.369</td><td>0.406</td><td></td><td></td><td></td><td></td><td>0.388</td><td>33402</td></tr>
<tr><td rowspan="2">16</td><td>0.328</td><td>0.466</td><td>0.275</td><td>0.347</td><td>0.399</td><td>0.536</td><td rowspan="2">0.413</td><td rowspan="2">33508</td></tr>
<tr><td>0.370</td><td>0.517</td><td>0.454</td><td>0.491</td><td>0.469</td><td>0.298</td></tr>
<tr><td>17</td><td>0.570</td><td>0.423</td><td>0.400</td><td></td><td></td><td></td><td>0.464</td><td>34040</td></tr>
</table>

Table 9 – Area (in mm²), and individual and mean ($\bar{x}$) values of ionic contamination (in µg/cm² NaCl eq.) of the scrap PCBs collected during their second SMT insertion organized according to the surface finish and the product family number.

SURFACE FINISH	PRODUCT FAMILY NO.	MEASURED VALUES (µg/cm² NaCl eq.)						$\bar{x}$ (µg/cm² NaCl eq.)	AREA (mm²)
OSP	18	1.145	1.188	1.076	1.084			1.123	40164
	19	1.304	0.923	0.976	0.989	1.15	1.121	1.304	
		1.107	1.159						
	20	1.198	1.017	1.092	1.399	1.198	1.314	1.108	
	21	0.927	0.873					0.900	39780
	22	0.84	0.754	0.934	0.991	0.922		0.888	
	23	0.727	0.816					0.772	40164
	24	0.995	0.864	0.646				0.835	
	25	0.883	0.841	0.761	0.986	1.057	0.966	0.916	
ImSn	26	0.910	0.961	1.014				0.962	38480

The PCBs were also organized according to their respective surface finish, yet the data collected did not show any obvious variation between boards with different finishes. Moreover, these data show a considerable increase in contamination from boards with solder paste and components on one side to boards with both sides covered with paste and components. Figure 41 presents the values of these two tables in the form of a graph.

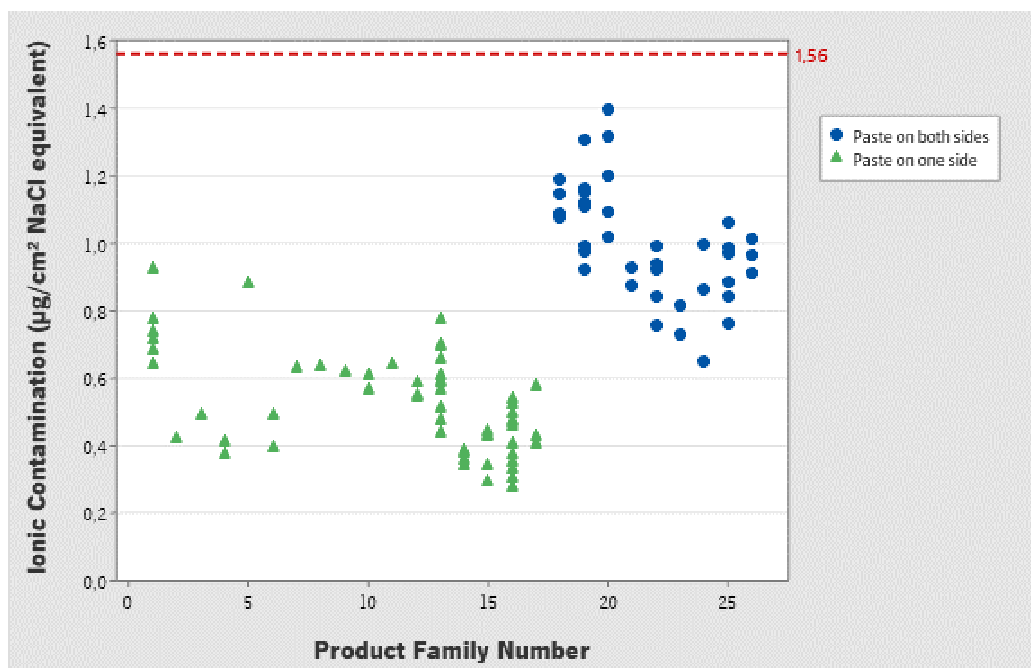

Figure 41 – Scatterplot of the ionic contamination (in µg/cm² NaCl eq.), measured on a ROSE contaminometer, present on scrap products collected in different stages of SMT production line, according to data from Table 11 and Table 12. Data in green refers to boards collected during insertion of solder paste and components on the first side and data in blue on the second side of the boards. The mean contamination value for PCBs in blue is 0.54 µg/cm² NaCl eq. and in green is 0.97 µg/cm² NaCl eq. The red line refers to the historical value of the ROSE test method for finished products (1.56 µg/cm²) for reference.

Figure 41 shows that the contamination roughly doubles between boards populated on only one side and on both sides, which was an expected result as a great part of components and solder paste are added to the board on the second reflow. All the PCBs studied have a contamination below 1.56 μg/cm² NaCl equivalent which, despite outdated, was still used as a reference in this study.

As can be seen through this data, boards from the same family have a noticeable dispersion in contamination values. One of the suspected reasons for this was the temperature of the extraction solution as, in some products, it was observed an increase in contamination in certain bath temperatures. An example of this behavior is shown below in Figure 42 on one of the discarded products analyzed for this study. In this graph we can see that the contamination values tend to increase as temperature rises between about 23 and 25.5 °C. This assumption is strengthened by the fact that temperature trends had been observed in other Bosch studies.

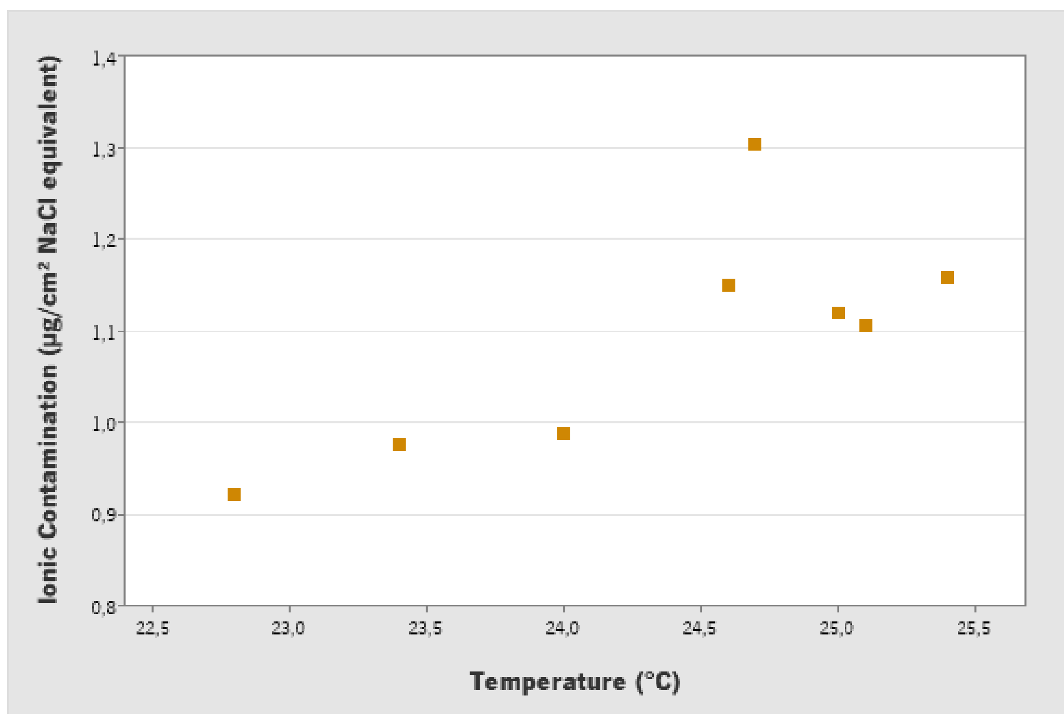

Figure 42 – Scatterplot of the ionic contamination (in μg/cm² NaCl eq.), measured on a CM22 contaminometer, vs. temperature of the extraction bath (in °C) of one of the products collected on the SMT production line. The contamination values of this product have a mean of 1.091 ± 0.153 μg NaCl equivalent/cm². The confidence interval was calculated for a significance level of 0.01 and n-1 degrees of liberty.

Another proposed reason is that the 5 minutes given for regenerating the tank solution (established by a Bosch-AE division) could be insufficient for a proper renewal. This means the tank does not fully regenerate its extraction solution and, therefore, accumulates ionic content from prior analysis. As a

result, the base contamination of the bath is contributing (externally to the sample) to a higher final contamination value of the board under test.

It is important to highlight that the scrapped boards were thrown away for different reasons, as explained before. This means that even PCBs with the same design may not have the characteristics of a completely identical sample population, and this could be the reason for such sparse values. Despite that these variables mentioned were still considered for the DOE.

4.1.2 ROSE Method Performance Study

The next step was evaluating if the ROSE machine obtains a linear response to a crescent surface contamination. This was accomplished by adding increasing volumes of NaCl solution to Benchmarker II boards. Additionally, two temperature ranges were used, forming this way two standard addition lines. Table 10 displays the values of contamination of the 5 bare boards analyzed without adding extra contamination. Table 11 presents the rest of the results of the calibration curves, defined according to a standard addition method.

Table 10 – Temperature (in °C) and individual and mean ($\bar{x}$) contamination (in μg/cm² NaCl equivalent) of the Benchmarker II samples analyzed on the CM22 contaminometer without NaCl addition (base contamination level). These measurements were all done in diferent days.

SAMPLE	T (°C)	RESPONSE (μg/cm² NaCl eq.)	$\bar{x}$ (μg/cm² NaCl eq.)
1	23.0	0.281	
2	22.3	0.279	
3	23.3	0.349	0.278
4	23.2	0.245	
5	22.6	0.237	

Table 11 – Temperature (in °C) and individual and mean contamination (in µg/cm² NaCl equivalent) of the Benchmarker II samples added with increasing volumes of NaCl solution, tested on the CM22 contaminometer. The data is additionally distribuited according to the temperature of the extration tank. The contamination of base level is the mean of the values of Table 10.

SOLUTION	VOLUME (µl)	20–22 °C SAMPLES		23–25 °C SAMPLES	
		T (°C)	RESPONSE (µg/cm² NaCl eq.)	T (°C)	RESPONSE (µg/cm² NaCl eq.)
Base level	0.0	-	0.278	-	0.278
1	48.0	20.2	0.435	23.4	0.468
2	96.5	21.0	0.724	23.9	0.717
3	289.0	21.8	1.635	24.2	1.795
4	579.0	21.6	2.947	24.1	3.114
5	965.0	22.4	4.410	24.6	4.982

It was important to clearly identify the initial contamination value in order to establish the base of the calibration curves. The tested batch of Benchmarker II boards presented in Table 10 have a mean ionic contamination of 0.278 µg/cm² NaCl eq. and a standard deviation of 0.044 µg/cm² NaCl eq. which represents around 16 % of the board's mean contamination.

Figure 43 illustrates the regression lines obtained for the data of the two temperature ranges through the results of Table 11. The lines obtained have a great fit to the data, achieving both high correlation coefficients (R) and having very similar slopes. A two-tailed t-test with a significance level of 0.01 was done to compare the slopes of the regression lines and this way determine if there is a significant difference between these two groups. Using the values of Table 11 and defining a null hypothesis (H_0) where the slopes are equal, we could conclude the data from the two temperature ranges does not differ significantly. This means that the two methods are equivalent and there is no evidence that the temperature of the extraction bath interferes with the ROSE machine response. However, this data is not enough to dismiss the temperature as a factor that has influence on ROSE data.

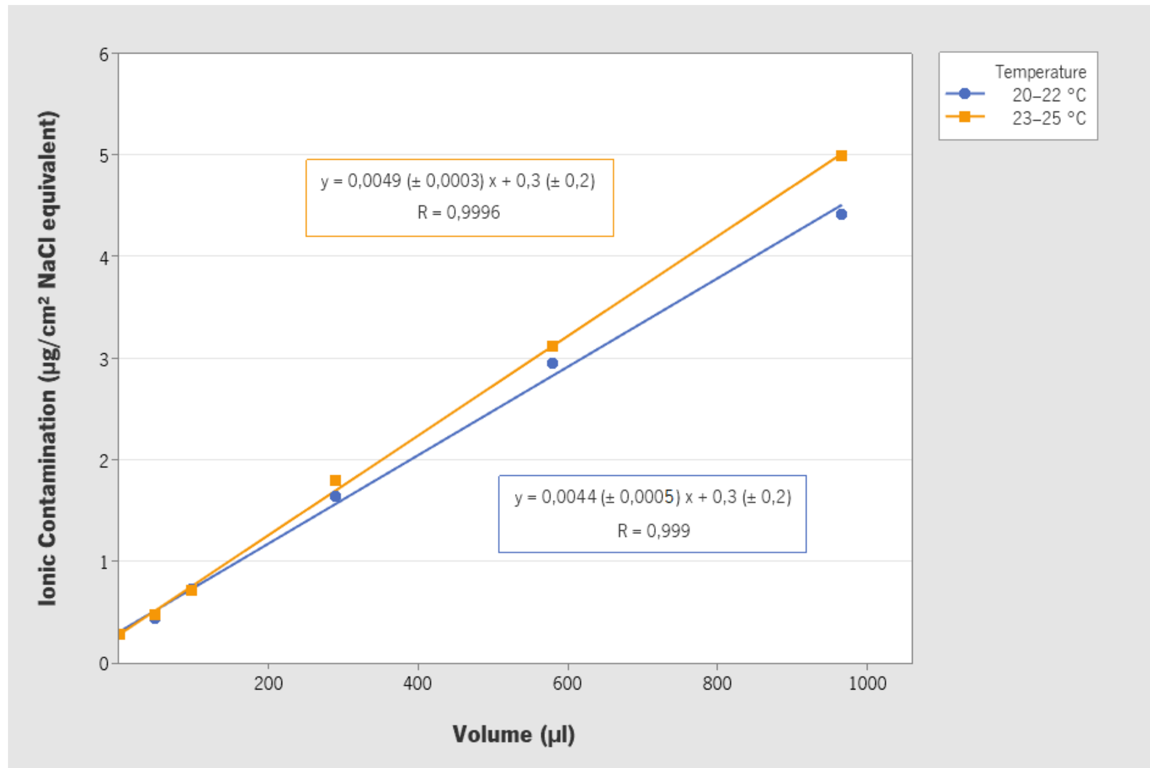

Figure 43 – Scatter plot of ionic contamination (in µg/cm² NaCl eq.), measured on a CM22 contaminometer, Vs volume of NaCl (in µl) added to Benchmarker II boards, and their respective calibration curves. Data in blue refers to boards measured at lower temperature and data in orange to a higher temperature. The confidence intervals of the tendency lines were calculated for a significance level of 0.01 and n-2 degrees of liberty.

4.1.3 DOE Test Results

Next, it was important to confirm if there was any factor that may influence the contaminometer readings, so a DOE was developed. A design of experiment (DOE) is a statistical method used to quantify the effects of process input parameters on the process output parameter (response variable). This experiment studied the factors mentioned before: temperature and regeneration time of the extraction bath. The model chosen for this DOE was a full factorial design with replicates (2 factors, 3 levels). The results of this test are presented in Table 12. All the statistical data in this DOE was analyzed using Minitab software version 19.2020.1 for a full quadratic model with a significance level (α) of 0.01.

Table 12 – DOE test responses (in µg/cm² NaCl equivalent) for a 2 factors, 3 levels full factorial design.

RUN ORDER	T (°C)	t_{reg} (min)	RESPONSE (µg/cm² NaCl eq.)
1	24.0	1	7.208
2		5	6.444
3		10	6.364
4		10	6.351
5	25.5	1	6.808
6		5	6.727
7		5	6.323
8		5	6.622
9		10	6.276
10	27.0	1	7.030
11		1	6.472
12		5	6.571
13		10	6.769

Minitab, the program used for the analysis of this DOE, uses the analysis of variance (ANOVA) procedure to calculate variance components and the regression analysis to estimate the relation between variables. Table 13 and Table 14 provide information about the statistical analysis of this model and Figure 44 depicts the results as effect and contour plots.

These results follow a quadratic model, which delivers a R^2 (coefficient of determination) of 0.685. This is not a very desirable fit of the statistical model to the data as it indicates that the model accounts for 69 % of the total variation of the results and there is a good part of the variation of the data not explained by the model. This R^2 value could suggest that the regression model has a missing factor leading to poor precision.

Table 13 reveals the coefficients of the terms of the quadratic model alongside their respective standard error. Minitab uses the t-value, which is the ratio between the coefficient and its standard error, to calculate the p-value. The p-value is the probability of rejecting the null hypothesis when it is in fact true. The null hypothesis affirms that a given parameter has no significant contribution for the measured response. The lower the p-value, the more significant that effect is. The significance level of 0.01 indicates a 1 % risk of concluding that a dependency exists when there is no real association.

Table 13 – Coefficients of each term of the model obtained through the analysis of the results of Table 12 adjusted to a quadratic model. It also presents their respective standard error, t-value and p-value.

	COEFICIENTS	STD. ERROR	t-VALUE	P-VALUE
(Intercept)	6.596	0.107	60.586	8.76E-11
Linear terms				
T	0.005	0.077	0.062	0.953
t_{reg}	-0.219	0.077	-2.848	0.025
Quadratic terms				
T*T	0.103	0.129	0.800	0.450
t_{reg}*t_{reg}	0.138	0.129	1.067	0.321
Interaction terms				
T*t_{reg}	0.206	0.090	2.275	0.057

Through the information provided by Table 13, we can see that the only factor that seems to significantly influence contamination levels is the regeneration time, as it has a p-value close to the established significance level. This means that the variation caused by the samples with different regeneration time does differ significantly from the variation due to the experimental error. The two-factor interaction between the temperature and the regeneration time also has a low p-value, which may indicate that the relationship between temperature and ionic contamination depends on the regeneration time, and vice versa. The temperature alone does not seem to have a direct effect on ROSE response.

The variance analysis of the quadratic model is presented on Table 14. It shows the parameters related to the quadratic regression and error of the model. The degrees of freedom (DF) for a term reveal how much information that term uses and are determined by the number of observations in the sample. For the Analysis of Variance table, Minitab separates the sums of squares (SS) into different components that describe the variation due to different sources. The mean squares (MS) are the ratio between their respective SS and the degrees of liberty and measure how much variation a term or a model explain.

The F-value for the regression is the test statistic used to determine whether any term in the model is associated with the response. A sufficiently large F-value is an indicator of statistical significance. The program uses this value to calculate the p-value, which is used to decide about the statistical significance of the test. To determine whether the model explains variation in the response, the p-value must be compared with the selected significance level to assess the null hypothesis. The null hypothesis affirms that the difference between two variances is not significant.

Table 14 – Degrees of freedom (DF), sum of squares (SS), mean square (MS), f-value and p-value of the regression and error parameters of a quadratic model based on the results of Table 12.

	DF	SS	MS	F-VALUE	P-VALUE
Regression	5	0.673	0.135	3.05	0.089
Residual Error	7	0.309	0.044		
Lack-of-fit	3	0.066	0.022	0.36	0.787
Pure error	4	0.244	0.061		
Total	12	0.982			

As seem before through the coefficient of determination, the model does not completely explain the variation in the response. There are two different explanations for why our data might not fall right on the estimated regression line. One possibility is that the regression model does not describe the trend in the data well enough. That is, the model may exhibit "lack of fit". The second possibility is that, as is often the case, there is just random variation in the data. This realization suggests that we should decompose the error into two components (shown in Table 14), one part due to lack of fit of the model and the second part just due to random error. If most of the error is due to lack of fit, and not just random error, it suggests that the model in not usable, and a new approach is needed.

To determine whether the model correctly specifies the relationship between the response and the predictors, the p-value for the lack-of-fit test to has to be compared to the significance level. In this case, the null hypothesis is that the model correctly specifies the relationship between the response and the predictors. The p-value obtained for the lack-of-fit is superior to the significance level, which leads to the acceptance of the null hypothesis. So, it can be concluded that the variation of the data is due to random error and not to the lack of fit of the model.

The effects of regeneration time can also be observed in both graphs of Figure 44. In Figure 44a, we can see that the contamination remains relatively constant as the temperature inside the solution tank rises. On the other hand, there is a clear decrease in contamination from samples subjected to 1-minute regeneration to samples subjected to 5 minutes and to 10 minutes of regeneration. This does seem to suggest that a 5-minute or 10-minute renewal is better than that observed for 1 minute as the contamination left on the tank from previous tests was more efficiently removed. The same observations can also be made as we analyze Figure 44b. This graph indicates a clear gradient of contamination along regeneration times that is not as visible along temperature.

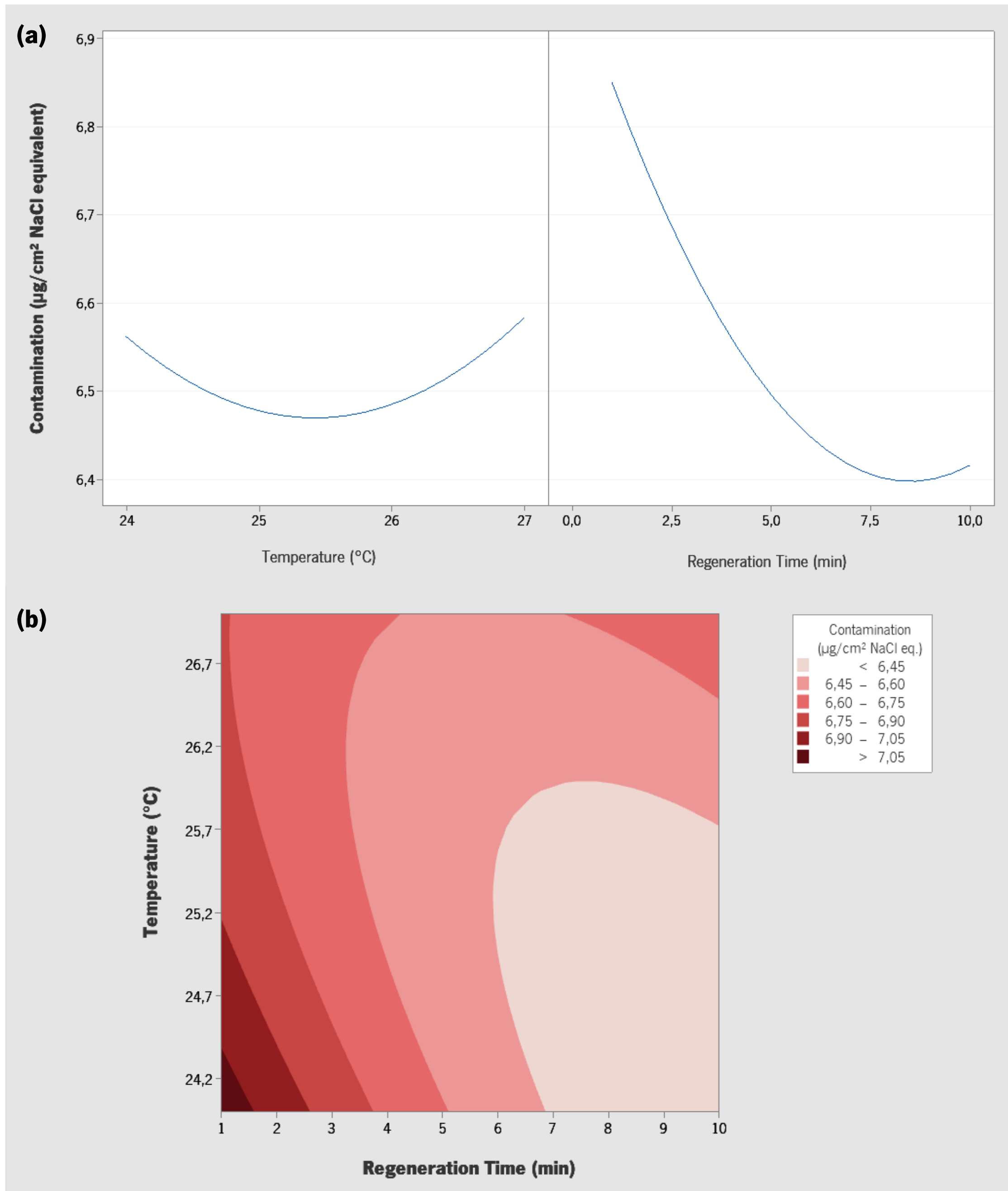

Figure 44 – DOE plots based on the results of Table 12 adjusted to a quadratic model. **(a)** Individual effect plots of temperature (in °C) and regeneration time (in minutes) of the extraction bath Vs ionic contamination (in µg/cm² NaCl eq.). **(b)** Contour plot showing ionic contamination levels (in µg/cm² NaCl eq.) on a regeneration time (in minutes) Vs temperature (in °C) surface.

One other interesting result of this DOE was the fact that Figure 44a presents its lowest peak of contamination around 7,5- and 9-minute regeneration. This might indicate a time of renewal around these values is the optimal set for testing, as there seem to be less interference from former analysis at least in this contamination range. As this is a high value for ionic contamination on a PCB, we cannot conclude that the effect of regeneration time is equivalent in a lower, more typical contamination scenario (which

is around 2 μg/cm² NaCl eq.). So, it is important to further study the contaminometer functioning in order to make sure these factors affect its response.

4.1.4 Regeneration Time Comparison Tests

Considering the results of the previous DOE, a study of the influence of regeneration time on the ROSE values measured was later carried out. Different from the DOE, this study was conducted on a Renault IVI board. Thirty-six sample boards were analyzed on the ROSE contaminometer for their ionic content after being subjected to either 1, 5, 8 and 10 minutes for regeneration of the solution inside the tank. Figure 45 sums up the results acquired.

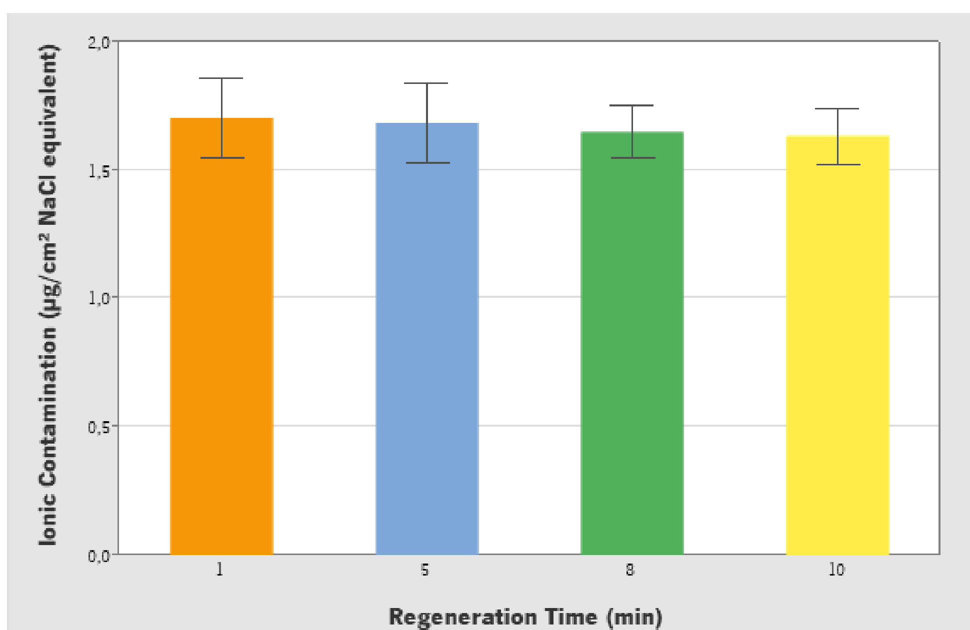

Figure 45 – Columm graph of the mean ionic contamination (in μg/cm² NaCl eq.) of Renault IVI samples measured on a CM22 contaminometer subjected to a regeneration time of 1, 5, 8 and 10 minutes. It was analyzed nine Renault IVI samples for each condition. The confidence intervals were calculated for a significance level of 0.01 and n-1 degrees of liberty.

The contamination levels in this test were much lower than those on the DOE and were equivalent to the contamination levels found in a PCBA manufactured at BCM. The values in Figure 45 are very close to each other, having a very slight decrease in contamination as we increase the regeneration time. This result suggests that there is no significant difference in between the groups of samples analyzed.

However, there is an evident decrease in variance from the left columns to the right ones. Therefore, although not significantly different, the values appear be more precise when the ROSE machine has at least 8 minutes to regenerate its solution.

Taking into account these results as well as the DOE results, 5 minutes was chosen as regeneration time of the extraction solution. The readings obtained for the samples submitted to this condition seem to have a satisfactory precision without having to spend much time amid sample analysis, which could be a bottleneck for the implementation of this method in the production line. As PCBAs coming from production line have ionic contamination readings below 2 $\mu g/cm^2$ NaCl eq., a 5-minute regeneration is efficient enough for this range of contamination. Considering all these aspects, the following ROSE evaluations were done accordingly to the procedure norm established by Bosch-AE.

4.2 Evaluation of Contamination Levels During PCBA Production

ROSE tests were performed to measure the level of ionic contamination of the Bombardier Compact test vehicle along the production cycle. Samples at different stages of the manufacturing process were analyzed to predict at which stages an increase in ion contamination occurs in the test boards. Table 15 presents the mean ionic contamination values obtained for the samples assembled at the production stages, as well as the respective areas inserted in the contaminometer software. All ionic contamination graphs for each Bombardier board are listed in annex. Figure 46 presents the results of the samples subjected to the standard assembly process without rework in the form of a column graph.

As we go deeper into the assembly process, the area of the product increases progressively (as seen in Table 15). This is because the components inserted in the PCB broaden its surface area, increasing the surface where contaminating ions may be located. The selective soldering process for this product is done after milling, so the two PCBs in the same panel are released from the frame. That is the reason for the abrupt reduction in surface area in this stage of the assembly run.

Table 15 – Area (in mm²) and ionic contamination (in µg/cm² NaCl eq.) measured on the ROSE contaminometer for Bombardier Compact samples at different stages of the manufactoring process as well as the number of boards analyzed per stage. The contamination is the mean of the results obtained on the ROSE machine except for the cleaned samples where only one frame (with 2 PCBs) was measured.

ASSEMBLY STAGE		AREA (mm²)	SAMPLE SIZE	IONIC CONTAMINATION (µg/cm² NaCl eq.)
BARE BOARD		30525	12	0.874
1ST REFLOW		35104	12	0.448
2ND REFLOW		39683	14	0.500
REWORK 1	CLEANED	39683	12	0.598
	NON-CLEANED		2	0.715
REWORK 2	CLEANED		12	0.742
	NON-CLEANED		2	1.017
SELECTIVE SOLDERING	WITHOUT REWORK	15261	6	1.223
	REWORK 1			1.410
	REWORK 2			1.663

Through the data collected with the CM22 contaminometer, it can be noticed that the unpopulated PCB is above the obsolete limit of 0.75 µg NaCl equivalent/cm² established by IPC-6012DA. Additionally, Figure 46 shows the biggest dispersion on the ionic content of these bare samples. AE-released PCB suppliers do intensive rinsing processes after final finishing so that reactive process chemicals are thoroughly removed. These ionic contamination values may be due to the surface finish of the Bombardier Compact boards. Out of all final finishes used at BCM, OSP is the most challenged by the higher temperatures of Pb-free processing. It is the only non-metallic finish and by nature the least thermally robust and, therefore, the most unpredictable in terms of surface contamination.

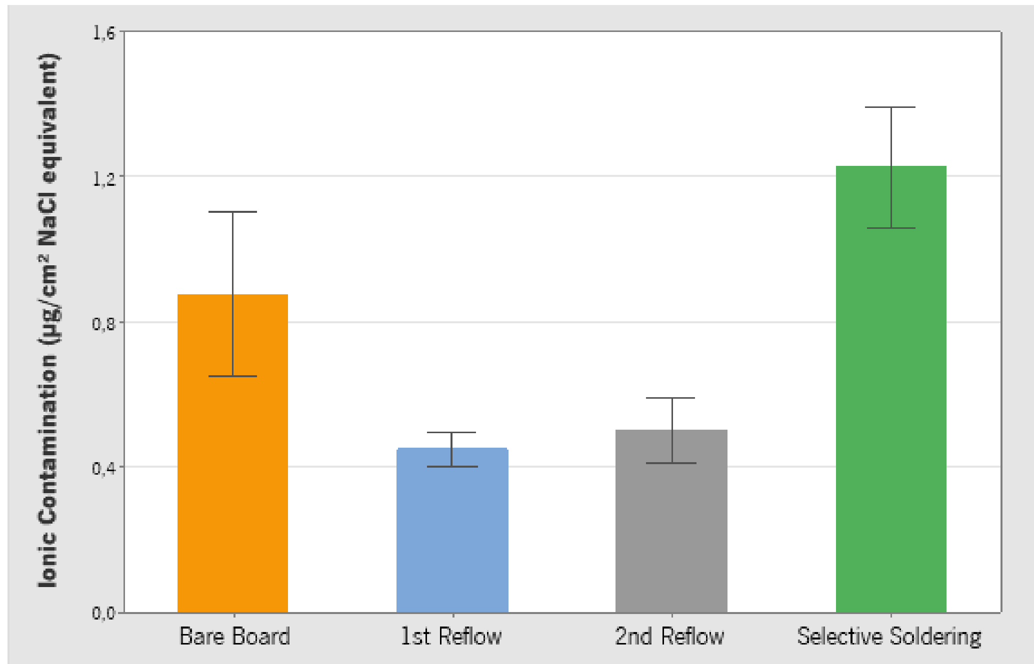

Figure 46 – Column graph of the mean ionic contamination (in µg/cm² NaCl eq.) of Bombardier Compact samples subjected to the standard PCBA assembly process without rework, analyzed on the ROSE contaminometer. Six samples were analyzed for each condition, with exception of the 2nd reflow where there were seven boards. The confidence intervals were calculated for a significance level of 0.01 and n-1 degrees of liberty.

Adding to that, other Bosch studies assert that PCBs in state of delivery yield in an ionic contamination level that is mainly originated by photo-initiators from the solder mask and that this level of contamination is reduced as the assembly undergoes the first reflow. In this research, by the 1st reflow process a significant drop in NaCl equivalent is in fact apparent, as seen in Table 15 and Figure 46. This might suggest the high temperatures to which the boards are subjected during reflow may cause volatilization and decomposition of photo-initiators and other compounds on the boards surface which could result in a significant decrease in ROSE values between the bare board and the PCBA of the 1st reflow. Additionally, the application of solder paste and placement of the components to the pads can retain ionic species, preventing them from being dissolved in the extraction process. Lastly, if the deactivation of the flux occurs, the ionic residues can be uptake by the resin, which acts as a protective layer where the ionic residues are covered and prevented from later release.

Figure 46 reveals a further 12 % surge in ionic content, from the 1st to the 2nd reflow. In this stage, the second side components are added to the top side of the Bombardier Compact board. The components added on this side take up more space and, hence, require much more solder paste.

Arguably the most interesting data of this thesis was the study of the contribution of rework and selective soldering to ROSE levels, since contamination assessment is defined as the ROSE levels after 2nd reflow. So, the last steps of the assembly stage are the least explored regarding ionic contamination.

A sizeable but expected surge in contamination happens between reflow and rework stages, as exhibited in Figure 47. The rework stage permitted us to compare two hand soldering procedures done in BCM. On one side, rework only using solder wire with flux on its core (rework 1). On the other side, rework 2 was done by adding extra flux before applying the cored solder wire to the space in between the component lead and the copper pad. This last one is reserved for components who need a better adherence of the solder to the pad.

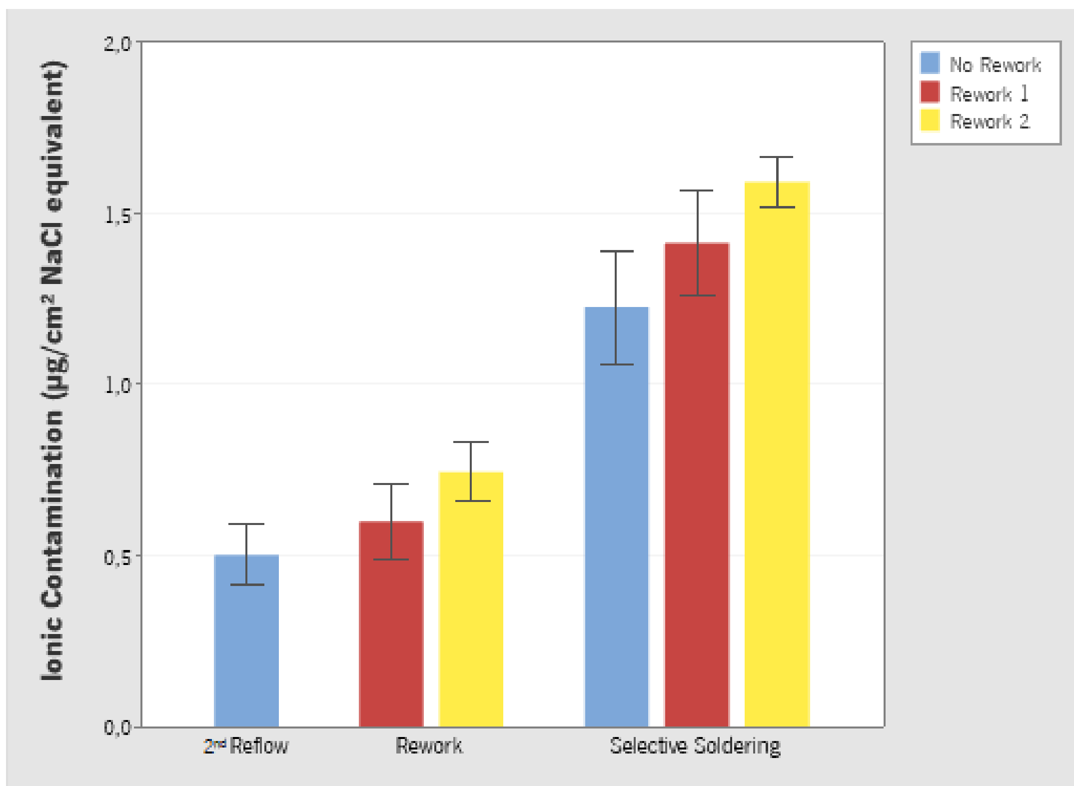

Figure 47 – Column graph of the mean ionic contamination (in µg/cm² NaCl eq.) of Bombardier Compact samples in the reflow, rework and selective soldering stages. Some of the boards were subjected to two different procedures during rework stage (red and yellow columns) while others did not endure rework (blue column). Six samples were analyzed for each condition. The confidence intervals were calculated for a significance level of 0.01 and n-1 degrees of liberty.

The Cobar 94-QMB flux used for rework is the same used in the selective soldering stage. BCM has been looking to replace it with a less contaminant flux with the same performance in selective soldering. However, possible alternatives seem to be less efficient and consequently it was important to assess how much contamination it adds to the board.

Figure 47 shows a noticeable increase in contamination not only from samples collected after reflowing and samples that went through an offline stage to rework their components but also between samples from different rework practices. A 20 % rise in ionic content happens from 2nd reflow to rework 1 stage and almost 50 % between 2nd reflow and rework with Cobar flux. Rework was conducted to 5 small components per board, so the solder and flux added were very minimal. The boards were cleaned with alcohol after this operation. So, even if cleaned and with very minimal interference, the rework stage does affect considerably the cleanliness of a PCB and adding the extra Cobar flux does add a significant amount of ionic content, surpassing the contamination present in sample reworked with only cored solder.

Parallel to this work a comparative study of clean and non-cleaned boards as rework was carried out. Normally right after rework, solder joints are cleaned with an alcohol-based solution in order to remove excess flux. In BCM, it is used a 90/10 % IPA/ethylene glycol solution. In order to evaluate the necessity of cleaning, one of the boards submitted to rework was not cleaned. The results of this study are presented in Figure 48.

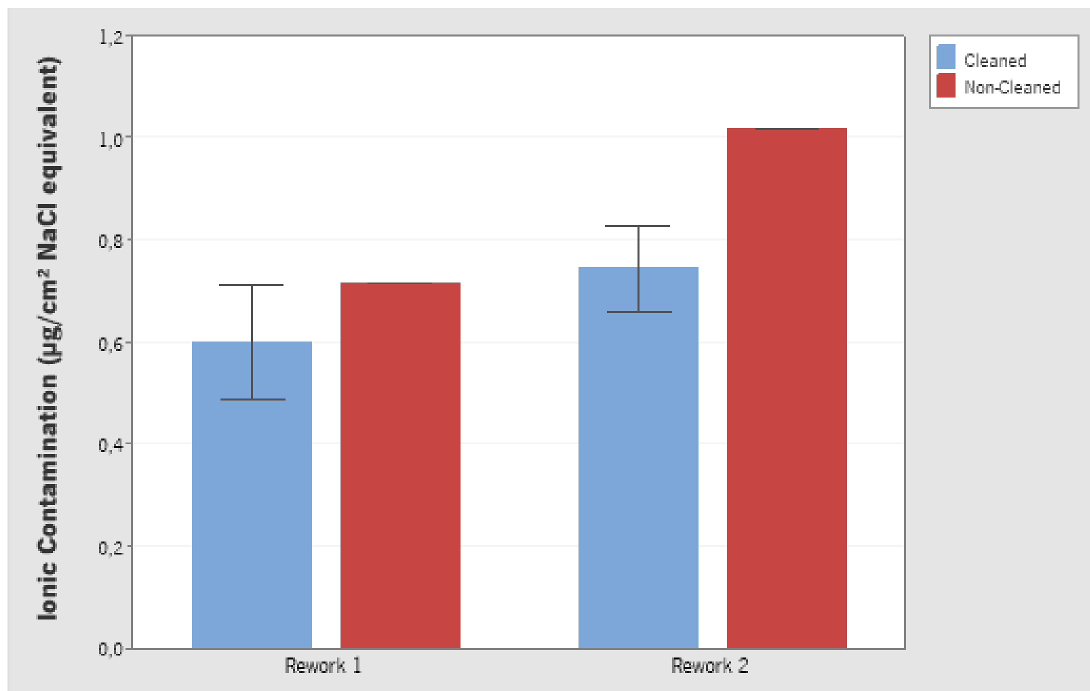

Figure 48 – Columm graph of the mean ionic contamination (in µg/cm² NaCl eq.) of Bombardier Compact samples subjected to different conditions on the rework stage, analyzed by the ROSE method. Columns in blue represent the samples cleaned after rework using a 90/10 % IPA/ethylene glycol solution (already presented in Figure 47) while columns in red represent samples who were not subjected to cleaning after rework. The confidence intervals were calculated for a significance level of 0.01 and n-1 degrees of liberty; the non-cleaned samples don't have a confidence interval as it was only analyzed one uncleaned panel for each rework.

As expected, a simple act of cleaning the board has a major impact on the surface contamination. There is a difference of more than 0.100 μg/cm² NaCl eq. between the cleaned and non-cleaned samples subjected to rework 1, which represents a 20 % decrease. This is especially visible in the rework 2 samples, where a 37 % decrease in contamination occurs, a difference of almost 0.3 μg/cm² NaCl eq. between samples. It seems that the alcohol solution cleans most of the Cobar flux remaining on the surface of the board. Given that it only one unclean sample was analyzed, it cannot be regarded as an absolute value, but it is sufficient to get a sense of the contamination left on the PCB if it is not cleaned with an alcohol solution.

Finally, the last stage studied was the TH soldering. In this step of the production, only one component was attached to the board, a THT connector. Contrary to reflow where the flux was mixed in the form of a paste with the solder, in wave soldering, the Cobar 94-QMB flux was sprayed before applying solder. The solder was then applied using a molten solder wave on the place where the component leads were. The selective soldering stage for the Bombardier Compact product is preceded by the milling stage. Therefore, the boards were analyzed in the contaminometer without a frame involving them.

As can be seen in Figure 47, this stage was where a large part of the ionic contamination was introduced on the assembly. From the reflow to selective soldering stage, sample contamination increased 145 %. Samples subjected to rework add an even more noticeable increase in contamination of 182 % (for samples also subjected to rework 1) and 233 % (for samples subjected to rework 2). In this product, it represents more than double of the value corresponding to the second reflow, and even triple the considering the contamination level of the last samples mentioned. From the samples subjected to selective soldering, the one that obtained through the second method of rework is the only one in which the surface contamination surpassed the reference value of 1.56 μg/cm² NaCl equivalent.

The important conclusion to this study is that the flux used for rework and selective soldering greatly increases surface contamination, especially on the later stage. Since these values of contamination do not mean the board will suffer ECM, these could only be confirmed by an SIR test. But as we observed in this study, the stage which contributes most to the surface contamination was the selective soldering, so it is very misleading to do ionic contamination tests only after reflow stage.

In conclusion, solder paste application, component insertion and reflow steps do not introduce much ionic residues on the Bombardier board surface. In fact, the ROSE level of the PCB obtained from the

supplier decreases during the SMT process. In the specific case of the Bombardier Compact, the ROSE of the PCB is even higher than that obtained for the PCBA after the 2nd reflow.

Furthermore, rework of components increases considerably the ionic content on the board and the flux used in this step does alter considerably the ionic content on the board. The most important step for the ionic contamination in PCB assembly is however the THT soldering. This stage alone causes a twofold increase of the ionic content present on the surface of the board after the 2nd reflow.

Compared with other products made at BCM and analysed in the stage of this thesis (in point 4.1.1), this product is not populated by a high density of components and is relatively small in area. The behaviour of the contamination may alter according to the type of PCB and components used in the assembly process. For ths reason, it is important to analyse similarly other products assembled at BCM.

CHAPTER 5 CONCLUSIONS AND FUTURE WORK

5.1 CONCLUSIONS

The crucial point of this thesis was to study the ionic content added from different stages of the PCBA production. For this, an ionic contamination method was employed, the ROSE test. The project was divided in two distinctive studies. The first part was the evaluation and validation of the response of the ROSE machine, the CM22 contaminometer. The final part was the characterization of the effect of the different assembly phases on the ionic surface contamination of the finished PCBA.

For the first part of this dissertation, several studies were conducted using the ROSE contaminometer. It was important to study this because, even though this technique was already explored in other Bosch units, this is not an established method for cleanliness assessment at BCM. Initially, defective boards from the SMT assembly line were collected and analyzed. Differences in ionic contamination between PCBs were observed depending on the density of components and the phase of assembly where the boards were collected. A standard addition method with NaCl solution allowed us to conclude the response of the contaminometer is perfectly linear in board contaminations in between 0.28 and 4.00 μg/cm^2 NaCl equivalent.

Two factors were identified as possible influencers of the machine response. These factors were the temperature and regeneration time of the 50/50 vol% IPA/deionized water extraction bath. A DOE was developed in order to study these two factors. At high contamination levels (around 6 μg/cm^2 NaCl equivalent), the regeneration time influences the machine response. The more time we give the machine to renew its solution, the less contamination is reported. The interaction between the temperature and the regeneration time also seems to affect contamination readings.

Further tests were done in order to study the effect of the regeneration time. At lower contamination levels (around 1 μg/cm^2 NaCl equivalent), the time of renewal of the extraction solution does not have the same impact. The variance, however, is clearly lower for samples subjected to at least 8 minutes of regeneration compared to those corresponding to shorter period of time. Considering all important aspects, 5-minute regeneration time was kept as established by the Bosch internal procedure.

For the second part of this thesis the assembly of Bombardier Compact boards at BCM was monitored and the boards were collected at 5 different stages. The chosen stages include the initial bare board, first and second reflow, rework and, finally, selective soldering.

For the first stages of assembly, it can be observed that solder paste application, component insertion and reflow steps do not introduce high levels of ionic residue, at least for this specific product. It was observed that the density of ionic contaminants on the boards following paste printing and reflow processes is inferior to its density on the initial unpopulated board. This may mean that high temperatures of the reflow process cause compound volatilization and decomposition. Alternatively, the ionic residues could be absorbed by the flux and/ or covered by solder paste or components after the reflow process.

Additionally, a rework was done using two distinct procedures. Some of the boards were reworked using just solder wire with flux on its core. The second rework practice was done by adding extra flux before applying the cored solder wire to the space in between the component lead and the copper pad. It can be concluded that the rework of components increases the ionic content on the board and the flux used in this step does alter substantially the ionic content on the board.

The most important step for the ionic contamination in PCB assembly is the THT soldering. This stage alone doubles the ionic content present on the surface of the board after the 2nd reflow. It seems that the main contribution for this is due to the flux used, as all processes that can lead to excess flux like rework or THT soldering contribute immensely to surface ionic contamination.

In conclusion, the CM22 ROSE tester is suitable for monitoring processes in assembly plants. It can be used as a process control tool as it can identify contamination trends in assembly processes. This machine is not a precise chemical analyzer but is sufficiently reliable in order to detect major changes at a process line. For this reason, ionic contamination evaluations should be carried in different stages of PCBA production since it can be very misleading to do them only after SMT insertion.

Bosch's PCB assembly lines have a no-clean philosophy, so boards are not subjected to any cleaning processes in order to remove excess substances on the PCBs surface. No-clean flux residues are specifically designed to remain benign even without cleaning, but there is not much research indicating how much flux residues are needed for them to became prejudicial to the PCBAs functioning. This study proves that these fluxes add a significant amount of ionic residue to the final PCBA, so assembly stages involving flux addition should be continuously monitored.

5.2 Future Work

This project revealed that ionic contamination on PCBs has a lot of variables that need to be understood and investigated. For this, in depth studies should be carried out so that we can endorse these results. Some suggestions of analysis and methodologies to be carried out in order to support the conclusions and complement this work are:

- Study of the compounds introduced in each assembly phase using ion chromatography.
- Analysis of the influence of area of the board and the density of components on the response of the CM22 contaminometer.
- Study of the extraction performance with different IPA/H_20 (%v/v) solutions such as 25/75 and a fully aqueous extraction and comparison between them and presently used 50/50 solution in order to verify what is the most efficient.
- Assessment of the assembly run of a variety of other PCBAs manufactured at BCM to understand how ionic contamination differs from product to product and establish internal restrictions of ionic content.
- Study of the applicability of this method to the development of new products (used in the various "sample phases" of development) or to the qualification of new materials (where normally only SIR is used).

REFERENCES

1. K. Fastnacht, "Robert Bosch: his life and achievements," *Bosch*. Bosch Internal Document, Stuttgart, 2016, doi: 10.5860/choice.32-1111.
2. C. Siegel, "The armature in a circle - The creation of the Bosch logo," *Bosch*, 2018. https://www.bosch.com/stories/creation-of-the-bosch-logo/ (accessed Jan. 15, 2020).
3. Bosch, "Bosch Inside Portal," *Bosch*. https://inside.bosch.com/irj/portal (accessed Jan. 15, 2020).
4. Bosch, "Bosch em Portugal," *Bosch*. https://www.bosch.pt/a-nossa-empresa/bosch-em-portugal/ (accessed Jan. 15, 2020).
5. New World Encyclopedia, "Printed circuit board," *New World Encyclopedia*, 2019. https://www.newworldencyclopedia.org/entry/Printed_circuit_board (accessed Nov. 07, 2019).
6. R. Strauss, *SMT Soldering Handbook*, 2nd ed. Manchester: Elsevier Science, 1998.
7. S. Sattel, "The History of PCBs," *Autodesk*, 2017. https://www.autodesk.com/products/eagle/blog/history-of-pcbs/ (accessed Nov. 07, 2019).
8. E. J. Kelley, "Introduction to Base Materials," in *Printed Circuits Handbook*, 6th ed., C. F. Coombs Jr, Ed. New York: McGraw-Hill Education, 2008, pp. 6.1–6.24.
9. M. Judd and K. Brindley, *Soldering in Electronics Assembly*, 2nd ed. Elsevier, 1999.
10. M. Hughes, "Which Via Should I Choose? A Guide to Vias in PCB Design," *All About Circuits*, 2018. https://www.allaboutcircuits.com/technical-articles/which-via-should-i-choose-a-guide-to-vias-in-pcb-design/ (accessed Nov. 11, 2019).
11. P. Wilson, Ed., "Printed circuits," in *The Circuit Designer's Companion*, 3rd ed., Oxford: Newnes, 2012, pp. 59–91.
12. Roettinger, "An Introduction to the Types of Printed Circuit Boards," *StreamlineCircuits*, 2016. http://streamlinecircuits.com/2016/06/introduction-types-printed-circuit-boards/ (accessed Nov. 11, 2019).
13. R. Kansagara, "Basics of PCB," *Circuit Digest*, 2018. https://circuitdigest.com/tutorial/basics-of-pcb (accessed Nov. 11, 2019).
14. PCBCart, "Printed Circuit Boards Assembly (PCBA) Process," *PCBCart*, 2019. https://web.archive.org/web/*/https://www.pcbcart.com/article/content/pcb-assembly-process.html (accessed Nov. 29, 2019).
15. D. Cullen, "Printed Circuit Board Surface Finishes," in *Printed Circuits Handbook*, 6th ed., C. F. Coombs Jr, Ed. New York: McGraw-Hill Education, 2008, pp. 32.1–32.23.

16. T. Henninger, "Solutions without Boundaries PCB Surface Finishes," Viasystems, 2006.

17. W. Paw *et al.*, "Key Characteristics Of A Pb-Free OSP Process," *OnBoard Technol.*, pp. 10–13, 2007.

18. A. Wright, "Printed Circuit Board Surface Finishes - Advantages and Disadvantages." Epec Engineered Tecnologies, New Bedford, 2015, [Online]. Available: https://www.epectec.com/articles/pcb-surface-finish-advantages-and-disadvantages.html.

19. NCAB Group, "PCB Surface Finishes," *NCAB Group*, 2012. https://www.ncabgroup.com/surface-finishes-2/ (accessed Nov. 12, 2019).

20. C. Perry, "Urban Legends of PCB Processes: ENIG Black Pad," *Epec*, 2018. https://blog.epectec.com/urban-legends-of-pcb-processes-enig-black-pad (accessed Nov. 21, 2019).

21. NEPP, "Basic Information Regarding Tin Whiskers," *NASA Electronic Parts and Packaging*, 2019. https://nepp.nasa.gov/whisker/background/ (accessed Nov. 21, 2019).

22. R. J. Hanson, "Electronics Surface Finish Overview," in *SMTA Upper Midwest Expo*, 2015, pp. 1–56.

23. ElProCus, "Here's A Quick Way to Know About Major Electronic Components," *ElProCus*, 2014. https://www.elprocus.com/major-electronic-components/ (accessed Jul. 30, 2020).

24. Lanka Micro, "Portal Homepage," *Lanka Micro*. https://www.lankamicro.com/ (accessed Jul. 30, 2020).

25. N.-C. Lee, *Reflow Soldering Processes and Troubleshooting: SMT, BGA, CSP and Flip Chip Technologies*. Woburn: Elsevier Science, 2002.

26. P. T. Vianco, "Assembly Processes," in *Printed Circuits Handbook*, 6th ed., C. F. Coombs Jr, Ed. New York: McGraw-Hill Education, 2008, pp. 40.3–40.66.

27. P. Swanson, *PCB Rework and Repair Guide*. Haverhill: Circuit Technology Center, Inc., 1996.

28. N. Ahlhelm, *An Introduction to High Reliability Soldering and Circuit Board Repair*, 4th ed. CreateSpace Independent Publishing Platform, 2013.

29. W. J. Plumbridge, R. J. Matela, and A. Westwater, *Structural integrity and reliability in electronics: enhancing performance in a lead-free environment*, 1st ed. Dordrecht: Springer Netherlands, 2003.

30. G. M. Freedman, "Soldering Techniques," in *Printed Circuits Handbook*, 6th ed., C. F. Coombs Jr, Ed. New York: McGraw-Hill Education, 2008, pp. 47.1–47.62.

31. I. Delgado, "N2 in reflow soldering." Bosch Internal Document, Braga, 2010.

32. G. Takyi and P. K. Bernasko, "Optimisation of Reflow Profile of Surface Mount Assembly Using

Taguchi Design of Experiments," *Sci. Res.*, vol. 3, no. 4, pp. 150–169, 2015, doi: 10.11648/j.sr.20150304.13.

33. K. Guan, J. Yin, and A. Zhang, "Overview of PCB Assembly Process." Bosch Internal Document, Suzhou, 2018.

34. Surface Mount Process, "Welcome to Surface Mount Process," *Surface Mount Process*, 2015. http://www.surfacemountprocess.com/ (accessed Nov. 25, 2019).

35. VCTA, "Solder Paste Inspection, SPI systems," *ZhenHuaXing*, 2019. https://aoi-spi.com/solder-paste-inspection-systems/ (accessed Jan. 17, 2020).

36. Electronics Notes, "Automatic optical inspection, AOI systems," *Electronics Notes*, 2017. https://www.electronics-notes.com/articles/test-methods/automatic-automated-test-ate/aoi-optical-inspection.php (accessed Jan. 21, 2020).

37. Electronics Notes, "Automated X-Ray Inspection AXI for PCB & BGA," *Electronics Notes*. https://www.electronics-notes.com/articles/test-methods/automatic-automated-test-ate/axi-x-ray-inspection.php (accessed Jan. 21, 2020).

38. A. Buckroyd, *In-Circuit Testing*. Oxford: Butterwirth-Heinemann, 1994.

39. T. Ziemer, "Designing for Manufacturability," *All About Circuits*, 2015. https://www.allaboutcircuits.com/technical-articles/designing-for-manufacturability/ (accessed Sep. 20, 2020).

40. G. Costa, "Selective Soldering - Lead Free." Bosch Internal Rules, Braga, 2017.

41. T. Lauer *et al.*, *Rework of Electronic Assemblies*. Frankfurt: Zentralverband Elektrotechnikund Elektronikindustrie e. V., 2017.

42. R. S. Khandpur, "Soldering, Assembly and Re-working Techniques," in *Printed circuit boards: design, fabrication, assembly and testing*, McGraw-Hill, 2006, pp. 453–560.

43. W. Li, M. Breier, and T. Aach, "Vision-Based Auto-Teaching for Automated PCB Depaneling," in *IEEE International Conference on Industrial Informatics (INDIN)*, 2012, pp. 910–915, doi: 10.1109/INDIN.2012.6300919.

44. M. H. B. M. Darus *et al.*, "PCBA depaneling stress minimization study," in *Electronic and Green Materials International Conference*, 2017, vol. 1885, doi: 10.1063/1.5002490.

45. R. S. Khandpur, "Mechanical Operations," in *Printed circuit boards: design, fabrication, assembly and testing*, McGraw-Hill, 2006, pp. 384–413.

46. G. M. Freedman, "Soldering Fundamentals," in *Printed Circuits Handbook*, 6th ed., C. F. Coombs Jr, Ed. New York: McGraw-Hill Education, 2008, pp. 44.3–44.9.

47. R. do Carmo *et al.*, "Lead-free soldering processes in the electronic industry: industrial implementation at SMES," *Ciência Tecnol. dos Mater.*, vol. 19, no. 3/4, pp. 15–29, 2007,

[Online]. Available: http://www.scielo.mec.pt/pdf/ctm/v19n3-4/19n3-4a04.pdf.

48. Research International, "Solder Reflow Basics," *Technology & Chemical*. https://www.tch.es/wp-content/uploads//RI_Section_1.pdf (accessed May 15, 2020).

49. M. Tarr, "Solder Paste Basics," University of Bolton, 2007.

50. Safavi, "Everything about PCB: Solder paste," *ETAG Co.*, 2012. http://www.etagco.com/en/everything-about-pcb/63-everything-about-pcb-solder-paste (accessed Jan. 08, 2020).

51. H. Black, "Getting the Lead Out of Electronics," *Environ. Health Perspect.*, vol. 113, no. 10, pp. A682–A685, 2005, doi: 10.1289/ehp.113-a682.

52. *Directive 2011/65/EU of the European Parliament and of the Council on the restriction of the use of certain hazardous substances in electrical and electronic equipment*. Official Journal of the European Union, 2011, pp. 88–110.

53. *Commission Delegated Directive (EU) 2015/863 amending Annex II to Directive 2011/65/EU of the European Parliament and of the Council as regards the list of restricted substances*. Official Journal of the European Union, 2015, pp. 10–12.

54. D. A. Shnawah, M. F. M. Sabri, and I. A. Badruddin, "A review on thermal cycling and drop impact reliability of SAC solder joint in portable electronic products," *Microelectron. Reliab.*, vol. 52, no. 1, pp. 90–99, 2012, doi: 10.1016/j.microrel.2011.07.093.

55. K. N. Subramanian, *Lead-Free Electronic Solders*, 1st ed. New York: Springer US, 2007.

56. G. C. Munie and L. J. Turbini, "Fluxes and Cleaning," in *Printed Circuits Handbook*, 6th ed., C. F. Coombs Jr, Ed. New York: McGraw-Hill Education, 2008, pp. 43.1–43.13.

57. G. M. Freedman, "Solder Fluxes," in *Printed Circuits Handbook*, 6th ed., C. F. Coombs Jr, Ed. New York: McGraw-Hill Education, 2008, pp. 46.1–46.16.

58. B. B. Bauer and R. Lathrop, "An Introduction to Solder Materials," *SMT*, pp. 1–9, 1998.

59. H. Conseil, M. S. Jellesen, and R. Ambat, "Contamination profile on typical printed circuit board assemblies vs soldering process," in *European Corrosion Congress*, 2014, vol. 26, no. 4, pp. 194–202, doi: 10.1108/SSMT-03-2014-0007.

60. V. Verdingovas, M. S. Jellesen, and R. Ambat, "Impact of NaCl contamination and climatic conditions on the reliability of printed circuit board assemblies," in *IEEE Transactions on Device and Materials Reliability*, 2014, vol. 14, no. 1, pp. 42–51, doi: 10.1109/TDMR.2013.2293792.

61. PCB Articles, "PCB Ionic Contamination," *Millennium Circuits Limited*, 2018. https://www.mclpcb.com/pcb-ionic-contamination/ (accessed Feb. 25, 2020).

62. L. Henneken, "Meaning of Electrochemical Migration (ECM), Surface Insulations Resistance (SIR), and Ionic Contamination (IC) on electrochemical reliability of PCBAs." Bosch Internal Report,

Schwieberdingen, pp. 1–20, 2015.

63. M. T. T. Nguyen, “Reliability Assessment of Ion Contamination Residues on Printed Circuit Board,” University of South Florida, 2013.

64. H. S. Villanueva, M. G. Mena, and P. C. Naval, “Estimation of Ionic Contamination in Printed Circuit Boards from Shape and Color Features of Dendritic Patterns,” in *IEEE Conference on Cybernetics and Intelligent Systems (CIS)*, 2013, pp. 48–53, doi: 10.1109/ICCIS.2013.6751577.

65. L. T. F. Mendes, “Estudo experimental da migração eletroquímica em soldagem eletrônica Sn/Ag/Cu ‘Lead Free,’” University of Sao Paulo, 2009.

66. H. Schweigart, “Electrochemical Migration - Emergence and Prevention of Field Failures.” ZESTRON Europe, Ingolstadt.

67. P. Eckold *et al.*, “Process Control of Ionic Contamination Achieving 6-Sigma Criteria in The Assembly of Electronic Circuits,” *Global SMT & Packaging*, 2017. https://globalsmt.net/articles_&_papers/process-control-of-ionic-contamination-achieving-6-sigma-criteria-in-the-assembly-of-electronic-circuits/ (accessed Jul. 16, 2020).

68. D. Q. Yu, W. Jillek, and E. Schmitt, “Electrochemical migration of Sn-Pb and lead free solder alloys under distilled water,” *J. Mater. Sci. Mater. Electron.*, vol. 17, no. 3, pp. 219–227, 2006, doi: 10.1007/s10854-006-6764-0.

69. B. I. Noh and S. B. Jung, “Characteristics of environmental factor for electrochemical migration on printed circuit board,” *J. Mater. Sci. Mater. Electron.*, vol. 19, no. 10, pp. 952–956, 2008, doi: 10.1007/s10854-007-9421-3.

70. S. Zhan, “Surface insulation resistance degradation and electrochemical migration on printed circuit boards,” University of Maryland, 2007.

71. P.-E. Tegehall and B. D. Dunn, *Evaluation of Cleanliness Test Methods for Spacecraft PCB Assemblies*. Noordwijk: ESA Publications Division, 2006.

72. R. Kohli and K. L. Mittal, Eds., “Methods for Assessing Surface Cleanliness,” in *Developments in Surface Contamination and Cleaning*, 1st ed., vol. 12, Cambridge: Elsevier, 2019, pp. 23–105.

73. B. Boyd, “Advances in Ionic Testing,” *SMT Mag.*, 2007.

74. *Detection and Measurement of Ionizable Surface Contaminants by Resistivity of Solvent Extract (ROSE)*. IPC-TM-650-2.3.25, 2012.

75. Gen3 Systems Limited, “Contaminometer CM22 - Ionic Contamination Test System for Electronic Circuit Boards and Components,” *Stannol*, 2011. https://www.stannol.de/fileadmin/user_upload/GEN3/Contaminometer/DE/CM22_Manual_V1.11_de.pdf (accessed Jul. 20, 2020).

76. T. Rountree and S. Stach, “Problems with rose testing using today’s fluxes,” 2018, doi:

10.23919/PanPacific.2018.8319003.

77. B. Natalie, “Guideline Surface cleanliness in electronics,” Bosch Internal Norm, 2019.

78. L. Henneken, “Meaning and Evaluation of Ionic Contamination Measurements on PCBs and PCBAs.” Bosch Internal Report, Schwieberdingen, 2017.

79. *An Overview on Global Change in Ionic Cleanliness Requirements*. IPC-WP-019A, 2018.

80. *Surface Insulation Resistance*. IPC-TM-650-2.6.3.7, 2007.

81. K. H. Lee *et al.*, “Comparison of ROSE, C3/IC, and SIR as an effective cleanliness verification test for post soldered PCBA,” *Solder. Surf. Mt. Technol.*, vol. 23, no. 2, pp. 85–90, 2011, doi: 10.1108/09540911111120159.

82. A. Rahner-Zwerner, “AnP-WI 0050: Operation of Contaminometer CM22.” Bosch Internal Report, Ansbach, 2016.

Annex – Ionic Contamination Plots

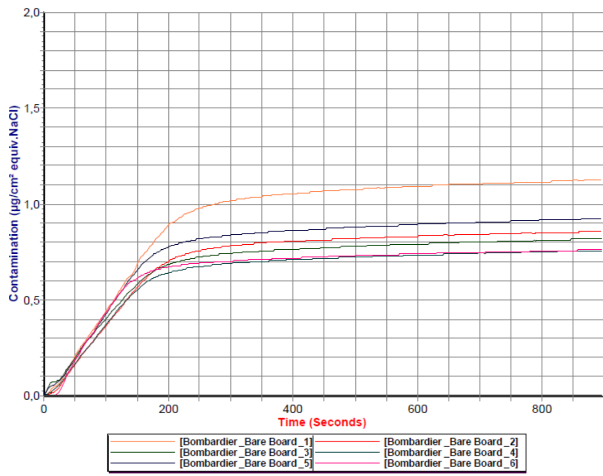

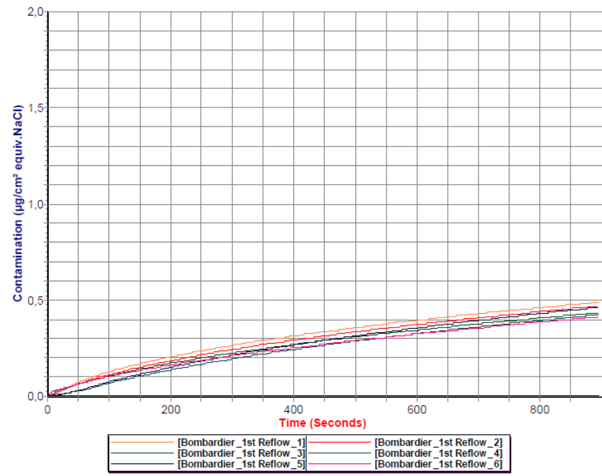

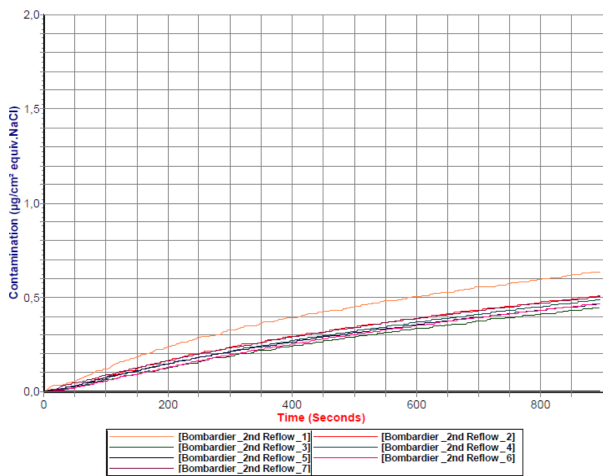

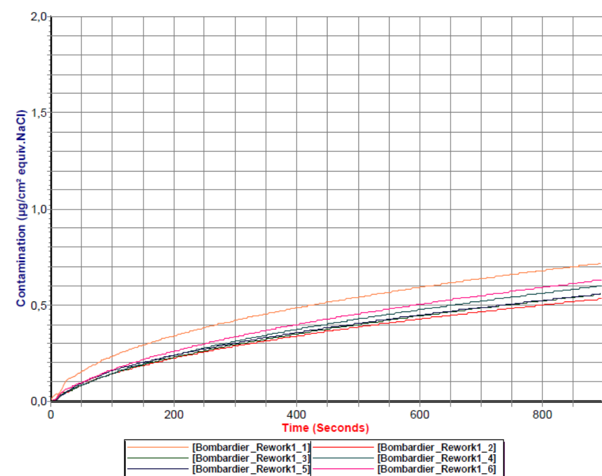

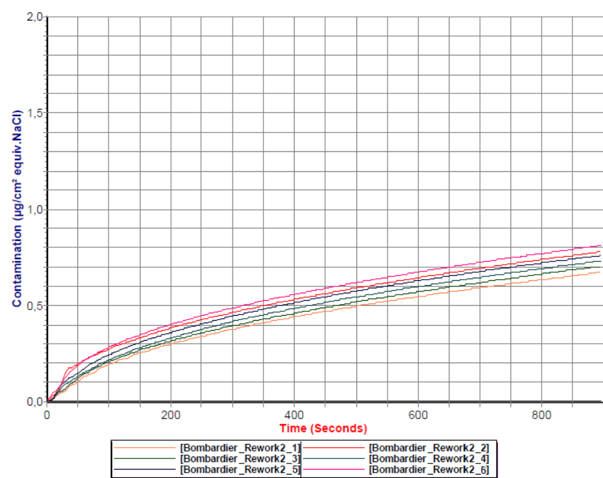

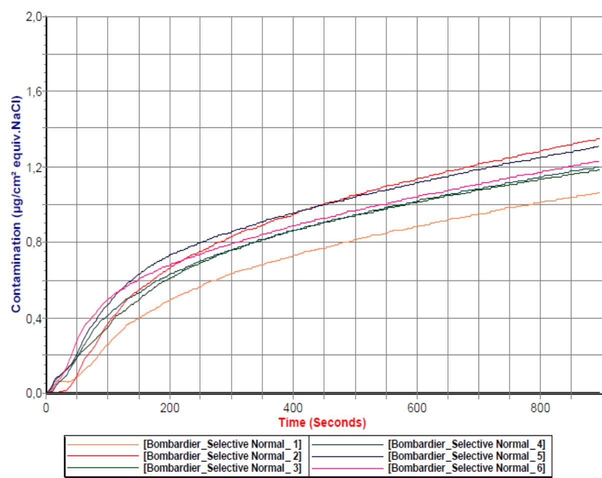

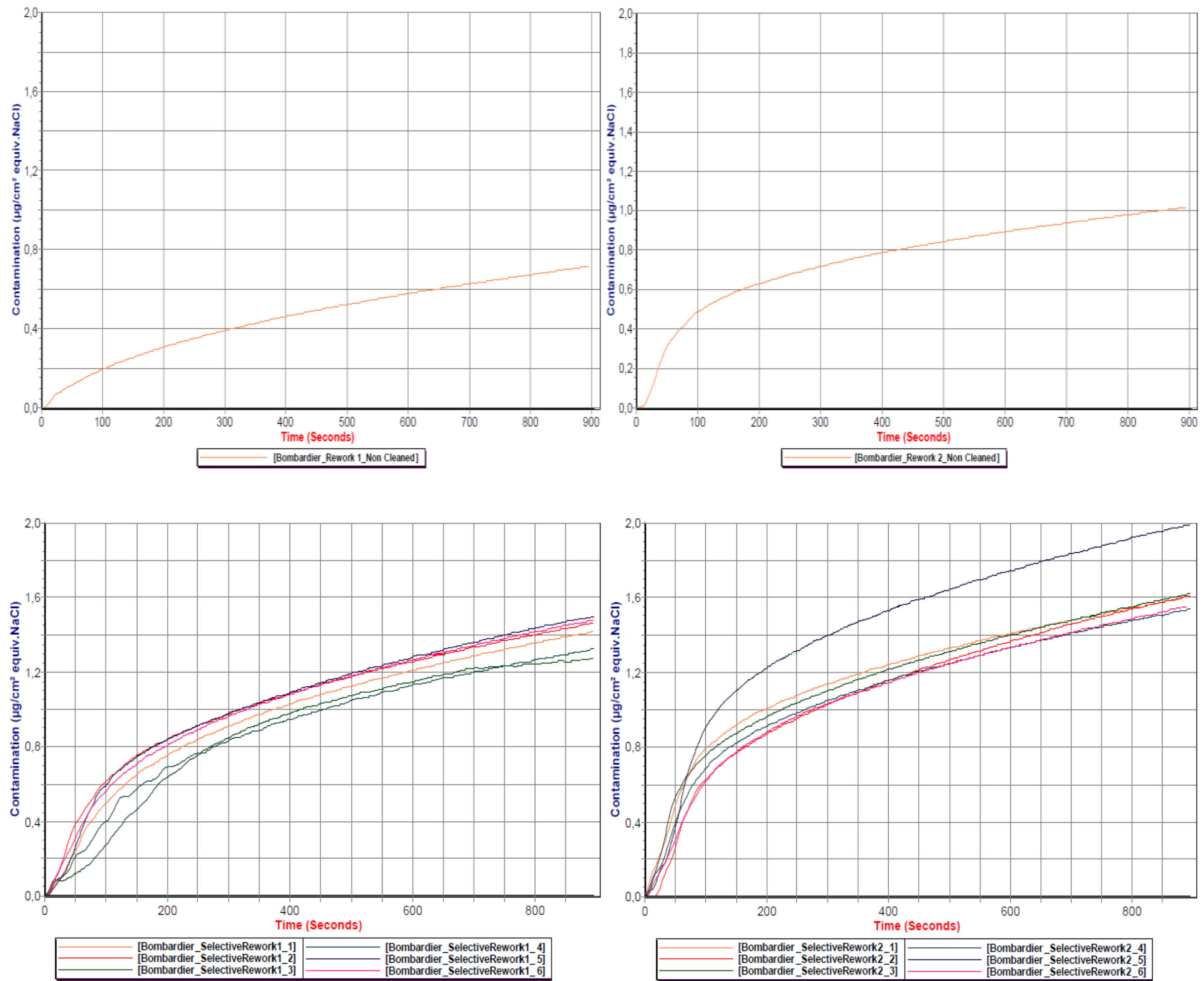

Figure 49 – Graphs of ionic contamination (in µg/cm² NaCl eq.) measured along a 15-minute time on the ROSE contaminometer for Bombardier Compact samples at different stages of the manufactoring process.